

Copyright

by

Shiva Niazi

2000

**Sensitivity Analysis of Time-Step in Modeling River and Aquifer  
Interaction**

**by**

**Shiva Niazi, B.S.**

**Thesis**

Presented to the Faculty of the Graduate School of

The University of Texas at Austin

in Partial Fulfillment

of the Requirements

for the Degree of

**Master of Science in Engineering**

**The University of Texas at Austin**

**August 2000**

**Sensitivity Analysis of Time-Step in Modeling River and Aquifer  
Interaction**

**Approved by  
Supervising Committee:  
Randall J. Charbeneau**

---

**David R. Maidment**

---

to Mom and Dad

## **Acknowledgements**

I would like to express my gratitude to the many people who helped me during my time at the University of Texas at Austin. First, I would like to thank my advisors, Dr. Maidment and Dr. Charbeneau, for their guidance and encouragement during these past two years. I would also like to thank Dr. Maidment's research group, as well as Dan Opdyke, for patiently answering my technical questions and sharing their time with me. To the EWRE gang (Julie, Dave, Misti, Steph, Craig, Ann and Christine), you will be my favorite memory of my time here - thank you for your generosity, spirit and sense of humor. A heartfelt thanks goes to John, Shilpa and Ben for providing me a family away from home. I also would like to show my appreciation for Dr. Lawler and those in the *Water Treatment in Developing Countries* class (Katherine, Pablo, Caroline, Todd, Terri, Mary, Dave F., Dave A. and Andrea) for reminding me of why I wanted to become an engineer. Most importantly, I would like to thank my family for their support and for inspiring me to pursue higher education.

August 10, 2000

# **Sensitivity Analysis of Time-Step in Modeling Aquifer and River Interaction**

Shiva Niazi, M.S.E.

The University of Texas at Austin, 2000

Co-Supervisors: Randall J. Charbeneau and David R. Maidment

## **ABSTRACT**

In modeling groundwater and surface water systems simultaneously, the issue of time-step length is important because of the difference in residence times of water in rivers and aquifers. To determine the effect of time-step length in modeling river and aquifer systems, a MODFLOW groundwater model of Milam, Lee and Bastrop counties Texas was dynamically linked to a surface flow routing model of the Colorado River. In the dynamic link between separate surface water and groundwater models, the output of one model is used to update the input of the other model in a cyclic fashion. Time-step length is defined as the length of time each model is allowed to run before updating the other model. A series of 32-day flood wave simulations was performed to determine the effect of averaging a highly fluctuating river discharge over 2, 4, 8 and 16-day time-steps. The results of this study suggest that time-step affects the quantity of water that the model predicts is exchanged between the river and aquifer.

## Table of Contents

List of Tables .....	x
List of Figures .....	xi
Chapter 1: Introduction.....	1
1.1 Background.....	1
1.1.1 Observational Data .....	2
1.1.2 Dynamically-Linking Models .....	2
1.1.3 Time Terminology.....	4
1.2 Research Objectives .....	6
1.3 Study Area .....	6
1.4 Summary.....	7
Chapter 2: Literature Review .....	9
2.1 Introduction .....	9
2.2 Water Regulation.....	9
2.2.1 Texas Water Law.....	10
2.3 Existing Models .....	12
2.3.1 MIKE-SHE .....	13
2.3.2 MODFLOW-SURFACT .....	15
2.3.3 Approximations of the Saint Venant's Equations .....	17
2.4 Time-step Analysis .....	19
Chapter 3: MODFLOW Groundwater Model.....	21
3.1 Introduction .....	21
3.2 MODFLOW .....	22
3.2.1 Organization of MODFLOW Program .....	23
3.3 River Package .....	27
3.4 Bureau of Economic Geology Model.....	30

3.4.1	Changes to the River Package Cells .....	33
3.4.2	Software Incompatibility .....	35
Chapter 4:	Surface Water Model .....	37
4.1	Introduction .....	37
4.2	Observational Data .....	37
4.3	Manning's Equation.....	44
4.4	Kinematic Wave Theory.....	46
4.5	Explicit Solution to the Kinematic Wave Equation .....	50
4.5.1	Courant Condition.....	52
4.6	Determining Initial Flowrate in the Colorado River .....	54
4.6.1	Data.....	54
4.6.2	GIS Processing of Data .....	55
4.6.3	Upstream Flowrate .....	60
4.6.4	Runoff and River Reach Lengths .....	62
4.6.5	Surface Water Model Calibration.....	63
4.7	Excel-Based Surface Water Model .....	65
4.7.1	Surface Water Simulation.....	65
4.7.2	Surface Water Model.....	69
Chapter 5:	Visual Basic Interface .....	76
5.1	Introduction .....	76
5.2	Overview .....	77
5.2.1	Input.....	77
5.2.2	Dynamic Linkage .....	79
5.2.3	Output .....	80
5.3	Structure .....	81
5.4	Formatting of MODFLOW Files.....	84
5.5	Interface Enhancement .....	84
5.5.1	Automation of MODFLOW Run .....	84



5.5.2 Efficiency .....	85
Chapter 6: Results.....	87
6.1 Introduction .....	87
6.2 Spatial Variation in River Reaches.....	88
6.3 Aquifer Head in Layer 1 .....	91
6.3.1 Effect of Time-Step .....	93
6.3.2 Effect of Distance from River .....	94
6.4 Aquifer Head in Layer 2 .....	96
6.5 River Leakage Rates .....	98
6.6 Approximation of Saint-Venant Equations .....	105
Chapter 7: Conclusions .....	108
7.1 Introduction .....	108
7.2 Objectives .....	108
7.3 Software.....	110
7.3.1 The Role of GIS.....	110
7.3.2 FORTRAN Compiler .....	111
7.4 Preliminary Results .....	111
7.5 Recommendations .....	112
Appendix A: Surface Water Model Data .....	116
Appendix B: Interface Visual Basic Code.....	122
Appendix C: Simulation Results .....	136
References .....	177
Vita .....	178

## List of Tables

Table 2.1 A Description of the MIKE-SHE Modules Excluding the Overland and River Module .....	14
Table 3.1 MODFLOW Packages and Their Purpose .....	24
Table 4.1 GIS Data and Their Sources .....	55
Table 4.2 Data from USGS Gages Located Upstream of the Subject Area.....	61
Table 5.1 The Nine Sub-Procedures of the "cmdOK_click" Procedure .....	82
Table 6.1 Volume of Groundwater Flow Entering in the Colorado River of the 32-Day Total Simulation Time .....	103
Table 6.2 Volume of Water Leaked from River During the First 8, 16, 24 and 32 Days of Simulation .....	104

## List of Figures

Figure 1.1 Schematic of the Dynamically Linked Groundwater and Surface Water Models .....	3
Figure 1.2 Schematic of Model Timelines .....	5
Figure 1.3 Location of Study Area.....	7
Figure 3.1 Schematic of MODFLOW River Package .....	30
Figure 3.2 Layer 1 of the BEG Model and Revised BEG Model.....	32
Figure 3.3 Layer 1 of BEG Model in GMS Software .....	32
Figure 3.4 River Package Cells Used in the BEG Study.....	34
Figure 3.5 River Package Cell Used in the Revised BEG Model .....	34
Figure 4.1 Location of the USGS Stream Gage and the Three Groundwater Wells .....	38
Figure 4.2 Location of USGS Gage 8159200 with Respect to Layer 1 of Revised BEG Model.....	39
Figure 4.3 Comparison of the Aquifer Head Deviation from the Average Head and the River Discharge at USGS Gage 8159200 .....	40
Figure 4.4 Head Deviation in Well 584706 as a Function of River Discharge Deviation .....	41
Figure 4.5 Comparison of Daily River Discharge at USGS Gage 8159200 and Aquifer Heads at Three Nearby Wells .....	43
Figure 4.6 Schematic of the 8-Direction Pour Point Model.....	58
Figure 4.7 The Flow Direction Grid for the Subwatersheds Underlying Milam, Lee and Bastrop Counties.....	59
Figure 4.8 Location of the Three USGS Gages Used in Determining the Upstream Flowrate in the Colorado River .....	61
Figure 4.9 Finite Difference Nodes Along the Colorado River .....	63
Figure 4.10 Location of USGS Gage 8160400 with Respect to the Finite Difference Nodes .....	64
Figure 4.11 Time-Step Averaged River Discharge at the Inlet.....	67
Figure 4.12 Aquifer Cross Sections 1 and 2 in Layer 1 of the Revised BEG Model .....	69
Figure 4.13 A Section of the <i>inlet2</i> Worksheet .....	72
Figure 4.14 A Section of the <i>Par</i> Worksheet .....	73
Figure 4.15 A Section of the <i>Q</i> Worksheet .....	75
Figure 5.1 Schematic of the Three Main Functions of the Interface .....	77
Figure 5.2 "frmInput" Form.....	79
Figure 5.3 Flowchart of the "cmdOK_click" Procedure.....	83
Figure 6.1 River Discharge Along the Colorado River During Three 2-Day Time-Steps .....	89

Figure 6.2 River Discharge as Function of Simulation Time at Three Locations Along the River. ....	91
Figure 6.3 Location of Selected Cells in Cross Section 1 .....	92
Figure 6.4 3-Dimensional View of the Selected Cells in Each Layer of Cross Section 1 .....	92
Figure 6.5 Changes in Aquifer Head in the Cell Containing Reach 14 .....	94
Figure 6.6 Aquifer Heads in Layer 1 of Cross Section 1 Using a 2-Day Time-Step .....	95
Figure 6.7 Aquifer Heads in Layer 2 of Cross Section 1 Using a 2-Day Time-Step .....	97
Figure 6.8 River Leakage Rate in Reach 14 Using Three Different Time-Steps ..	99
Figure 6.9 Sum of River Leakage Rates for All 35 Reaches Using Three Different Time-steps .....	99
Figure 6.10 Aquifer Heads in Layer 1 of Cross Section 1 .....	101

# **CHAPTER 1: INTRODUCTION**

## **1.1 Background**

The successful management of water resources involves managing the two main components of a region's water resources, namely groundwater and surface water. Surface water and groundwater are often managed separately (Lusk 1998), the fact that they are known to exchange water creates a strong incentive for the conjunctive management of these two resources. However, before the conjunctive management of surface water and groundwater can occur, it is imperative to determine how these two systems interact.

One of the challenges in understanding the interaction of surface and ground water systems lies in their different time scales. Rivers, as a subset of surface water systems, have a much shorter residence time for water than do aquifers. Aquifers have much slower flow velocities and consequently may show slower changes in hydraulic head over time. Therefore, questions arise regarding the time-scale with which river and aquifers interact. Do the relatively fleeting river discharge fluctuations make an impact on the aquifer heads? If so, how are these changes distributed in time and space within the aquifer?

### **1.1.1 OBSERVATIONAL DATA**

To determine whether observational data could provide insight into comprehending a river and aquifer's effect on one another, a study was performed using data provided by a USGS stream gage and three nearby groundwater wells.

The wells and stream gage are located in Bastrop County, inside the study area shown in Figure 1.3. The study demonstrated the difficulty in using sparsely gathered observational data to determine the dynamic nature of aquifer and river interaction. Only a minimal level of correlation was observed between the aquifer and river hydraulic heads as a function of time. Furthermore, the spatial distribution of the river's impact on the aquifer was difficult to examine due to a lack of groundwater data. The details of this study are presented in Section 4.2, however from this analysis it was learned that a physically distributed model may provide a better understanding of an aquifer and river's interaction, as compared to relying on observational data alone.

### **1.1.2 DYNAMICALLY-LINKING MODELS**

In modeling the river and aquifer flow systems, the inherent difference in their time scale makes choosing an appropriate time-step difficult. A long time-step, which would be appropriate for modeling a groundwater system alone, might cause a loss of accuracy by over-averaging the river stage values. A short time-step, while good for modeling river systems, would substantially increase the computation time, and render the process inefficient for projecting water availability in the distant future. Therefore, it is hypothesized that an optimum time-step exists which would balance the need for accuracy and an efficient modeling system.

In this project, a dynamic link was created between a surface water and groundwater model to help assess the role of time-step in the modeling of the two systems. In the dynamic link between separate surface water and groundwater

models, the output of one model is used to update the input of the other model in a cyclic fashion, as shown in Figure 1.1. A physically distributed model of a river was created specifically for this study in Microsoft Excel. A calibrated MODFLOW groundwater model that was developed by the University of Texas Bureau of Economic Geology was used in this research. As seen in Figure 1.1, the parameters that are exchanged between the two models are the river hydraulic head,  $H_R$  and the lateral aquifer inflow into the river,  $q_a$ .

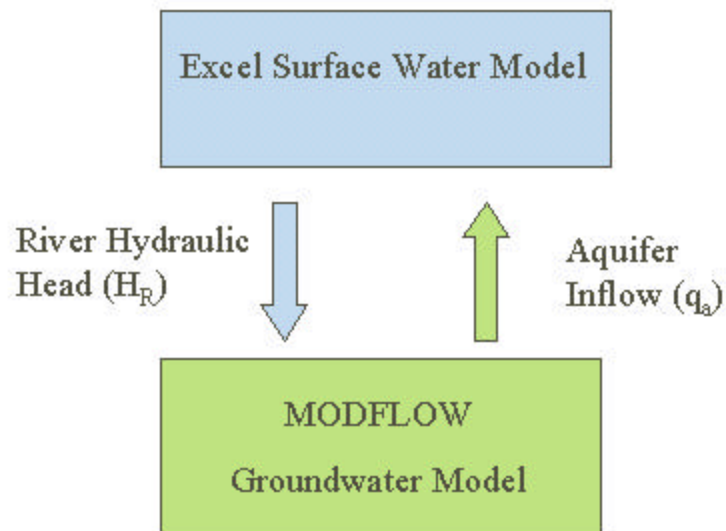


**Figure 1.1 Schematic of the Dynamically Linked Groundwater and Surface Water Models**

### **1.1.3 TIME TERMINOLOGY**

Figure 1.2 shows a schematic of the time terminology that is used in this thesis. For the purpose of this study, the time-step of interest is the Visual Basic Interface time-step shown in Figure 1.2. In a dynamic linkage of two models, the *interface time-step* length corresponds to the length of time each model is allowed

to run before updating the other model. Therefore, the *run-time* of a model (i.e. the length of time each model is run) is equivalent to the *interface time-step*. However, there are also separate time-steps intrinsic to the surface water and groundwater models. When discussing these time-steps the words *groundwater* or *surface water* will precede *time-step* to indicate its limited applicability to the scope of that one model. As shown in Figure 1.2, the surface water model consists of multiple surface water time-steps. However, due to the implicit finite difference scheme used by MODFLOW, the relatively short run-time of the MODFLOW model consists of only one groundwater time-step. Typical MODFLOW models that are used to model groundwater movement alone, however, often require multiple time-steps. The *total simulation time* is defined as length of time for which the dynamically linked models have been run. Therefore, the *total simulation time* is the summation of all of the *interface time-steps*.



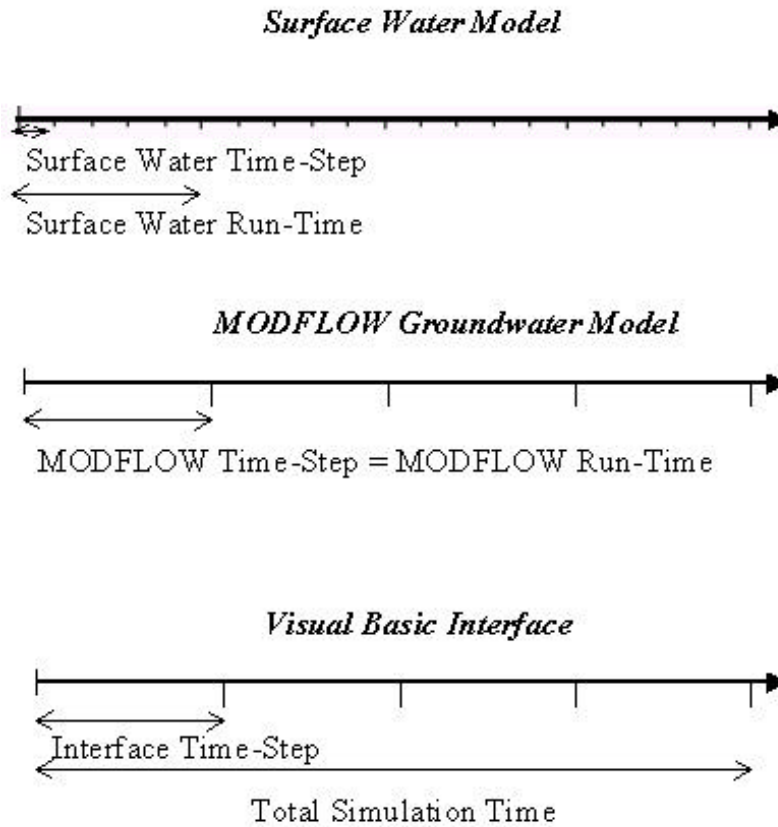


**Figure 1.2 Schematic of Model Timelines**

## **1.2 Research Objectives**

There are three primary objectives for this research. The first is to build a simple but appropriate surface water model that may be used to simulate flow in real rivers, such as Colorado River. This model needs to be easily manipulated by the interface that is facilitating the dynamic linkage. The second objective is to design the code for the interface that dynamically links the models. In this project, the interface was written in the Visual Basic Language. The interface needs to be able to run each model in an alternating fashion and transfer the

necessary information between the models. Lastly, the effect of time-step in modeling the interaction between the groundwater and surface water systems is analyzed. To do so, a highly time-varying river discharge caused by a flood wave is routed through the domain using the kinematic wave equation. The river discharge is averaged over varying time-steps to determine if a relationship exists between the interface time-step and the river and aquifer interaction.

### **1.3 Study Area**

The study area chosen is located in Milam, Lee and Bastrop counties in Texas and is shown in Figure 1.3. The two main rivers in this area are the Colorado River in the west and the Brazos River in the east. The main aquifer analyzed in this region is the Carrizo-Wilcox aquifer. This area has recently undergone a groundwater availability investigation by the Bureau of Economic Geology (Dutton 1999). The groundwater model was therefore available from the Bureau of Economic Geology for use in this study.

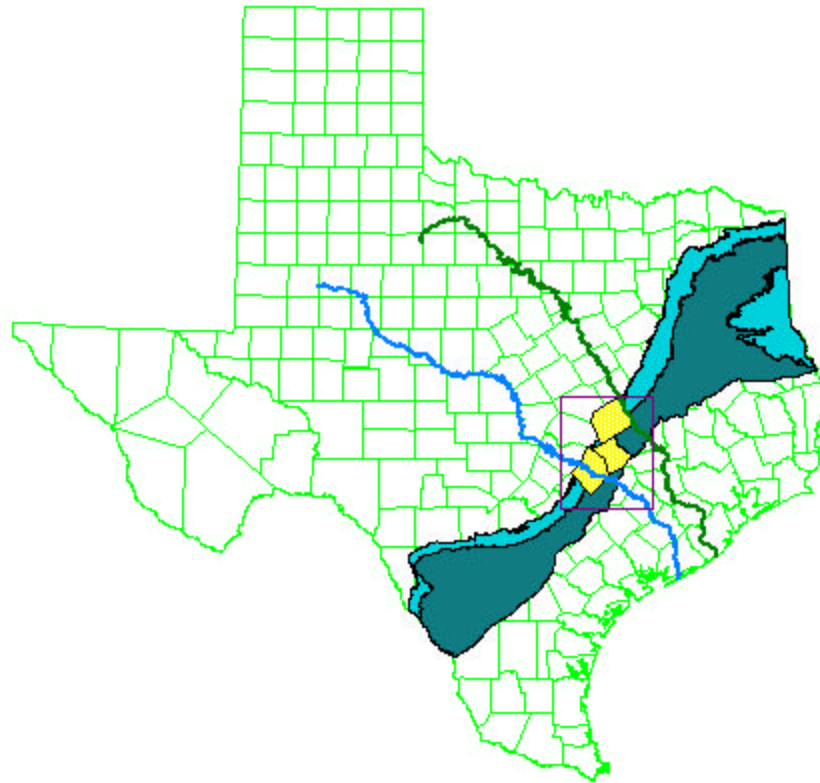


**Figure 1.3** Location of Study Area

## **1.4 Summary**

This research attempts to determine the interface time-step appropriate for modeling groundwater and surface water interaction. The case study considers a specific site in Texas. In this research a groundwater and surface water model are dynamically linked. In Chapter 2, the literature review for this research is presented. The groundwater and surface water models are described in Chapters 3 and 4, respectively. The description of the Visual Basic interface is left to Chapter 5. Lastly, in Chapter 6, the results of the different simulations with

varying time-step are reported and conclusions and recommendations are addressed in Chapter 7.

## **CHAPTER 2: LITERATURE REVIEW**

### **2.1 Introduction**

This chapter discusses the available literature in the field of surface and subsurface water modeling. In Section 2.2 the current state of water regulations, as it pertains to both surface and subsurface systems in Texas, is examined. Next, Section 2.3 explains the different types of models used for water management purposes, with a detailed look at the MIKE-SHE and MODFLOW-SURFACT models. Lastly, previous parameter sensitivity analyses are examined and the possible contributions of this research are considered.

### **2.2 Water Regulation**

As water demand continues to increase with population growth, water management practices that promote water conservation become increasingly necessary. Unlike the Clean Water Act that sets federal limits on the contamination of all “navigable” waters in the U.S., no such federal law exists for the withdrawal of water (Vance 1996). Instead, individual States are given the right to protect their own water resources as they see fit. This lack of federal regulations creates a varied approach to State resource management practices, with the result that some States are better at passing laws to conserve their resources than others (Vance 1996).

### **2.2.1 TEXAS WATER LAW**

As compared with other state codes, Texas Water Law has been slow to keep up with more advanced water management practices. Before the passing of Senate Bill 1, the extensive water management bill, in 1997, Texas was one of three western states without a state drought plan (Hubert 1999). Furthermore, Texas is the only western state that still abides by the rule of capture with respect to groundwater pumping (Vance 1996). The rule of capture states that landowners have property rights to the water below their land, and therefore can withdraw groundwater at their discretion<sup>1</sup> (Lusk 1998). As a result, there is no motivation for landowners to conserve groundwater under this rule, leading to the overuse of groundwater resources (Lusk 1998).

Unlike groundwater, surface water withdrawals are governed by the State of Texas under the system of prior appropriation. Under prior appropriation, priority is given to surface water rights based on the dates the permits were issued under the doctrine of “first in time...first in right.” (Lusk 1998) In a conflict between two water rights during a water shortage, the senior water right, namely the one that was issued first, can exercise its full water rights before the junior water right can use the water. Under this system, the power to decrease water usage during droughts is left within the hands of the State (Lusk 1998).

Paradoxically, Texas does not regulate the pumping of groundwater wells that could be robbing baseflow to a nearby river. Pumping of such groundwater would lead to a decrease in the river’s flowrate, as would a surface water

---

<sup>1</sup> In Texas, the rule of capture has been modified; groundwater pumping can be curtailed if it is proven 1.) to be malicious or 2.) to constitute willful waste. (Vance 1996)

withdrawal. However, under the rule of capture, this pumping could not be regulated by the State (Lusk, 1998). Therefore, this system of regulation can create inequities between groundwater and surface water users.

With the passing of Senate Bill 1, Texas Water Law has taken large strides towards managing its scarce water resources (Hubert 1999). Although there is still no state regulation on groundwater pumping, Senate Bill 1 did give more power to local communities to alter the rule of capture, through revising its legislation toward groundwater conservation districts (Hubert 1999). Should they choose, groundwater conservation districts have the power to deny groundwater well permits based on numerous criteria, including if the “proposed use of water unreasonably affects existing ...surface water resources” (Texas Water Code 36.113).

Also due to Senate Bill 1 (Texas Water Code 16.012), an effort has begun to assess the extent of the state’s surface water and groundwater resources through the Water Availability Modeling (WAM) and the proposed MODFLOW-based Groundwater Availability Modeling (GAM) projects (Mace and Mullican 2000). A complete water resources management plan requires an understanding of how the groundwater and surface water systems affect one another. Texas water resource planning and management stands, therefore, to gain from models that can predict the dynamics of groundwater and surface water interaction.

## **2.3 Existing Models**

Since the 1980's, various states have been making use of joint surface/subsurface modeling systems to help create legislation that would equitably manage their water resources (Sophocleous 1995; Mueller 1993). Models can provide information where data is not available, for example to project water availability in the future. Models typically fall under two categories: lumped conceptual and physically based distributed (Refsgaard 1997). Physically based distributed models can represent spatially varying parameters that are based on physical characteristics of the system. Lumped conceptual models treat complex physical systems, such as a watershed, as an integrated unit (Refsgaard and Knudsen 1996). The advantage of using a physically based distributed model is that localized changes, such as changes in land-use, can be modeled more effectively. Furthermore, in theory, physically based distributed models require less time-series data for calibration (Abbott 1986).

In recent years, there has been an emphasis on linking physically distributed models to a Geographic Information Systems (GIS). GIS, as a powerful graphical tool, has helped in the visualization of model output (Orzol 1993). Furthermore, models that were previously created in arbitrary coordinates can now, with a GIS, be geographically referenced. This ability to view and manipulate disparate data sets within one integrated system increases the ease and efficiency with which physically based data can be gathered and formatted for input into the model (Hinaman 1993; Richards 1993).



Computer advances have also created increasingly sophisticated models that are able to integrate complicated physical processes such as runoff, river flow, subsurface flow, evapotranspiration and contaminant transport. Two such models will be discussed below: MIKE-SHE and MODFLOW-SURFACT.

### **2.3.1 MIKE-SHE**

MIKE-SHE is the most recent development of the Systeme Hydrologique Europeen hydrological model created in a joint project by the Danish Hydrological Institute, the British Institute of Hydrology and the French consulting company SORGEAH (Abbott 1986). Like MODFLOW, MIKE-SHE consists of separate modules that model different aspects of the hydrological cycle (Danish Hydraulic Institute 2000b). The basic modules include the following: Overland and River Module, Evapotranspiration Module, Unsaturated Zone Module, Saturated Zone Module and the Irrigation Module. Note that there are additional modules that can be purchased separately. The basic modules, excluding the Overland and River Module, which will be discussed in more detail in the following paragraph, are described in Table 2.1.

**Table 2.1 A Description of the MIKE-SHE Modules Excluding the Overland and River Module**

MODULE	DESCRIPTION
Evapotranspiration (ET)	Models rain interception and evapotranspiration by either: i. Rutter model (interception) and Penman-Monteith Equation (evapotranspiration) ii. Kristensen-Jensen model
Unsaturated Zone Module (UZ)	Models vertical flow in unsaturated zone of surface by either: i. Richard's Equation ii. Gravity flow
Saturate Zone (SZ) <sup>2</sup>	Models saturated flow in subsurface. Solver methods: i. Pre-conditioned Conjugate Gradients (PCG) ii. Modified Gauss-Seidel
Irrigation (IR)	Models irrigation management: Highly flexible, can place priority on water source

The Overland and River Module models the overland runoff and river flows in tandem. The two-dimensional diffusive wave approximation of the Saint-Venant equations and Manning equation are used for modeling the overland flow. The river can be modeled in two levels of complexity, using 1) a one-

---

<sup>2</sup> It should be noted that the river/aquifer interaction is specified in the SZ Module. The river/aquifer interaction can be modeled assuming: 1.) the river is in full contact with the aquifer or 2.) a low permeability layer separates the river and aquifer.

dimensional diffusive wave approximation for the Saint-Venant equations or 2) MIKE-11, a one-dimensional river hydraulic model distributed by the Danish Hydraulic Institute. MIKE-11 is also structured in a modular fashion, with modules that describe river flow (Hydrodynamic Module), contaminant transport (Advection-Dispersion Module) and biological processes (Water Quality Module). The Hydrodynamic Module solves the Saint-Venant equations for open channel flow for fully dynamic, diffusive, kinematic and quasi-steady state waves. Furthermore, this module can model flows around a variety of structures including broadcrested weirs and culverts (Danish Hydraulic Institute 2000a).

### **2.3.2 MODFLOW-SURFACT**

The MODFLOW-SURFACT modeling system is a product of HydroGeologic, Inc. MODFLOW is a modular 3-Dimensional finite difference modeling system of saturated subsurface flow that was created by the United States Geologic Survey (USGS). MODFLOW-SURFACT integrates an enhanced version of MODFLOW-96 with packages that model overland flow, channel flow and contaminant transport. Open-channel flow and overland flow are modeled using the 1-D Channel Flow (CHF1) and 2-D Areal Overland Flow (OLF1) Packages, respectively. The OLF1 Package uses the two-dimensional diffusive wave approximation to model overland flow. The package provides an extra layer of nodes that are located above the aquifer layers that are modeled by MODFLOW. These overland flow nodes are able to exchange water with the first active layer of groundwater nodes directly below them via leakage through the soil surface. The CHF1 Package uses the one-dimensional diffusive wave

approximation to model flow in an open channel. Two types of channel cross sections are supported in the CHF1 Package: a wide rectangular channel and a trapezoidal channel. The aquifer and river interaction is modeled using Darcy's Law, which is described in more detail in Chapter 3 of this thesis (HydroGeologic 1999). Both packages provide the following five types of boundary conditions:

- First type
- Areal recharge
- Sources and Sinks
- Evaporation
- Zero-depth gradient and critical depth gradient

The following is a brief explanation of the five boundary conditions listed above. The First Type boundary condition is equivalent to the constant head boundary option that is offered by MODFLOW, in which the heads at the boundary are kept at the initial head value throughout the simulation. The second boundary condition (Areal Recharge) applies a recharge rate to a horizontal area in the OLF1 Package and the channel surface area in the CHF1 Package. This boundary condition contains a maximum depth constraint that can limit the recharge rate. The Sources and Sinks boundary condition and the Evaporation boundary condition provide net fluxes and an areal sink to the boundary node, respectively. The Sink and Evaporation conditions are subject to a non-negative depth constraint and, therefore, cannot cause the hydraulic head at the node to

drop below the bed elevation. The last boundary condition, the Zero-Depth Gradient and Critical Depth Gradient, simulates the condition at the bottom of a hill or at the downstream end of a river reach. The Zero-Depth Gradient condition causes the slope of the water surface to equal the riverbed slope, while the Critical Depth Gradient condition forces the water depth at the boundary to be equivalent to the critical depth.

Both the overland and channel flow algorithms are fully integrated into an implicit system of matrix equations and are solved during each time-step. The overland and open channel nodes modeled separately by the two packages, exchange water via equations for a free-flowing weir and submerged weir. The free-flowing weir equation is used under the condition that the hydraulic head within the channel is lower than the elevation of the channel bank. Alternatively, a submerged weir condition occurs when the hydraulic head within the channel is higher than the channel bank elevation (HydroGeologic 1999).

Other features of the enhanced MODFLOW modeling system include a 3-dimensional vadose zone transport addition to the Block-Centered-Flow Package and an advanced time-stepping mechanism in the ATO4 package. The advanced time-stepping package can modify the groundwater model time-step depending on the computer's available memory so as to have the solver algorithm more easily converge to a solution (HydroGeologic 1999).

### **2.3.3 APPROXIMATIONS OF SAINT VENANT'S EQUATIONS**

Although both the MIKE-SHE and MODFLOW-SURFACT modeling systems use the diffusive wave approximation of the Saint-Venant equations,

Lighthill and Whitham (1955) showed that the main part of a natural flood wave approximates a kinematic wave (a simplified version of the diffusive wave). Because of the flood wave simulations investigated in this study, the kinematic wave approximation is believed to be suitable. However, in instances where changes in river discharge are based solely on lateral inflow and not influenced by a flood wave, Vieira (1983) investigated the accuracy of different approximations of the Saint-Venant equations based on two parameters: the kinematic wave number,  $\mathbf{k}$ , and the Froude number,  $\mathbf{F}_0$ . Equations 2.3.1 and 2.3.2 define the two parameters. The approximations were solved under two lower boundary conditions: the zero-depth-gradient and critical-flow. These two conditions are identical to the zero-depth gradient and critical-depth gradient boundary conditions used in the MODFLOW-SURFACT modeling system. In the study, Vieira compared the implicit finite difference solutions to the kinematic, diffusive and gravity wave equations to those of the full Saint-Venant equations. The results of the study showed that for values of  $\mathbf{k}$  much greater than 50, the kinematic wave approximation can be used with either boundary condition. However, for  $\mathbf{k}$  values between 5 and 20, the kinematic and diffusive wave approximations are applicable depending on the Froude number. For example, a flow regime with the parameters  $\mathbf{k} = 20$  and  $\mathbf{F}_0 < 0.5$  would require the diffusive wave approximation as opposed to the more simplistic kinematic wave approximation. The boundary conditions become significant only when  $\mathbf{k} < 5$ .

$$k = \left( \frac{g^3 L \sin \boldsymbol{q}}{C^4 q^2} \right)^{1/3} \quad (2.3.1)$$

$$F_o = C \left( \frac{\tan \boldsymbol{q}}{g} \right)^{1/2} \quad (2.3.2)$$

where,

k= kinematic wave number

F<sub>o</sub> = Froude number

g = gravitational acceleration [L<sup>2</sup>/T]

L = length of river reach [L]

θ = constant angle of the slope

R = hydraulic radius [L]

q = lateral runoff [L/T]

## 2.4 Time-Step Analysis

The hydrologic modeling systems discussed above are powerful in their ability to model complex physical processes, such as river and aquifer interaction, simultaneously. However, to use these modeling systems effectively it is important to choose spatial and time variables that model the system of interest to the desired degree of accuracy. There have been studies done on the changes that various physical and structural parameters of the coupled surface water and groundwater models can make on the river and aquifer hydraulic heads

(Refsgaard 1996; Bathurst 1986; Perkins 1999). However, attempts to look at the effect of time-step have been, at best, brief.

This research, therefore, aims to continue the work of previous sensitivity analyses of surface and groundwater models with an emphasis on examining the effects of changing the time-step. Furthermore, the linking of the models is done in a GIS context. In this way, the benefits that GIS can provide in linking two separate physically distributed models are examined.



## **CHAPTER 3: MODFLOW GROUNDWATER MODEL**

### **3.1 Introduction**

The groundwater model, MODFLOW, was chosen to model the groundwater system in this project for two reasons. Firstly, MODFLOW is well established and widely used in the United States in the fields of civil and geotechnical engineering, and in hydrogeology, making this research directly relevant to the work of many industries modeling subsurface flow. Secondly, the model contains a module known as the River Package that is able to model the interaction between the river and aquifer, albeit in a non-dynamic fashion. Therefore, MODFLOW has the means to dynamically link the surface and subsurface models embedded in its program.

The following section of this chapter describes the general capabilities of MODFLOW and its organization. In Section 3.3, the River Package and the underlying theory of its code are described in more detail. Finally, the specific parameters that describe the University of Texas Bureau of Economic Geology (BEG) MODFLOW model of the area within the Milam, Lee and Bastrop counties are discussed in Section 3.4.

### **3.2 MODFLOW**

The Three-Dimensional Modular Ground-Water Flow Model (MODFLOW) was created by the United States Geological Survey (USGS) in

1983 and since then has been updated numerous times, the latest version being MODFLOW-96. Since its inception, MODFLOW has become one of the most frequently used groundwater models in both academia and industry. MODFLOW is written in FORTRAN and uses a block-centered finite difference technique to solve the mass conservation equation that describes subsurface flow (Equation 3.2.1). In many "real-life" systems, complexities such as irregular model geometry, heterogeneous parameters, complex boundary conditions or some combination thereof, often make analytical solutions impossible. In such cases, MODFLOW and other models can provide numerical solutions. MODFLOW solves Equation 3.2.1 by employing the finite-difference method in a time-iterative fashion. In the most general sense, MODFLOW determines the aquifer hydraulic heads as a function of time based on boundary and initial conditions and stresses on the aquifer being modeled. Aquifer stresses include well pumping, interaction with rivers, and area recharge as well as others.

$$S_s \frac{\partial h}{\partial t} = \frac{\partial}{\partial x} \left( K_{xx} \frac{\partial h}{\partial x} \right) + \frac{\partial}{\partial y} \left( K_{yy} \frac{\partial h}{\partial y} \right) + \frac{\partial}{\partial z} \left( K_{zz} \frac{\partial h}{\partial z} \right) + W' \quad (3.2.1)$$

where,

$S_s$  = specific storage [ $L^{-1}$ ]

$K_{ii}$  = principal components of the hydraulic conductivity tensor [ $L/T$ ]

$h$  = hydraulic aquifer head [ $L$ ]

$W'$  = source strength [Volume/(VolumeT)]

### **3.2.1 ORGANIZATION OF MODFLOW PROGRAM**

The MODFLOW model is organized into a main program and several independent modules called packages. Some of the packages are described in Table 3.1. The modular organization of the model allows the user to choose the packages that are needed to describe the system being modeled. For instance, depending on whether wells are located in the domain, the Well Package can be turned on or off. Therefore, unnecessary packages are ignored and do not increase the run time of the model.

**Table 3.1 MODFLOW Packages and Their Purpose (Charbeneau 2000)**

<b>Package</b>	<b>Purpose</b>
Basic Package	Handles tasks that are required for each simulation. Including specification of boundaries, determination of time-step length, establishment of initial conditions, and printing of results.
Block-Centered Flow Package	Calculates hydraulic conductance and external source terms of finite-difference equations that represent flow from cell to cell and storage.
River Package	Stress package. Adds terms representing flow to rivers to the finite-difference equations.
Recharge Package	Stress package. Adds terms representing diffuse recharge to the finite-difference equations.
Well Package	Stress package. Adds terms representing flow to wells to the finite-difference equations.
Drain Package	Stress package. Adds terms representing flow to drains to the finite-difference equations.
Evapotranspiration Package	Stress package. Adds terms representing evapotranspiration to the finite difference equations.
General-Head Boundary Package	Stress package. Adds terms representing general-head boundaries to the finite-difference equations.
Solution Procedure Package	MODFLOW (1996) supports preconditioned-conjugate gradient, strongly-implicit, slice-successive over relaxation, and direct solver using diagonal ordering procedures.

In MODFLOW-96, the main program receives the Name file or the file consisting of the names and unit numbers of the different packages being used for

the simulation. Table 3.1 describes the different contents of the packages in MODFLOW-96. The most basic model (i.e. with no aquifer stresses) needs a minimum of the Basic, Block-Centered-Flow (BCF), Solution Procedure, and Output Control Packages to be defined by the user. The following paragraphs provide a brief description of the different packages in MODFLOW required for a basic model.

In the Basic Package, the number of rows, columns and layers are specified. The initial hydraulic heads as well as the groundwater stress period and time-step are also specified in the Basic Package. Stress periods coincide with periods where parameters specifying the aquifer stresses (such as pumping rate, river stage, etc.) and boundary conditions must be held constant. Stress periods are further broken down into groundwater time-steps. The finite difference equations are solved iteratively for each of these groundwater time-steps. Typical MODFLOW groundwater stress periods can range from months to years, depending on the objectives of the model. As discussed before, the duration of groundwater time-steps are very much dependent on the solver algorithm and are therefore difficult to generalize.

The BCF Package contains parameters, such as the hydraulic conductivity, aquifer types and row and column spacing, which describe the cell-to-cell flow. The spacing does not need to be uniform across the grid, and often to decrease the computation time, a modeler will have large grid cell sizes near the boundaries of the study area where accuracy is less important.

Thirdly, the Solution Procedure Package contains the information on what kind of solution method will be applied to solve the finite difference equations. Examples of two different solution methods are the Strongly Implicit Procedure (SIP) and Slice-Successive Over Relaxation (SSOR) algorithms. Certain solution methods could fail to solve the finite difference equations because the model will be unable to converge to a solution. Convergence, however, is not only dependent on the solution method but also relies on other parameters such as MODFLOW's time-step length. Therefore, by having different solution methods, the modeler is given more freedom in choosing values for parameters, such as the groundwater time-step length and various iteration parameters, which also influence the possibility of a solution.

Finally, the Output Control Package specifies the format and content of the output files. There are two formats for the output of a MODFLOW simulation: a text file and a binary file. The text file, known as the listing file, lists each computational process performed by MODFLOW as it occurs during the simulation. The listing file also may contain, among other things, the aquifer heads and drawdowns at any groundwater time-step specified by the user. Through the Output Control Package, the user can also save the river leakage rates for each River Package cell to the listing file. This last capability is important in facilitating the dynamic linkage of the MODFLOW and surface water models.

Unlike text files, binary files can't be opened in word processing software, and require a GUI to display their contents. Common binary file outputs include

the aquifer head file (\*.hed), the drawdown file (\*.dm) and the cell-to-cell flow file (\*.ccf). The cell-to-cell flow contains a water budget for each grid cell by recording the amount of water that flows through a cell during a specified groundwater time-step. MODFLOW uses binary files as a means of saving output as well as a means of entering input. Therefore, the output of one MODFLOW simulation can be used as the input for another simulation via binary files. For this research, aquifer heads contained in the \*.hed file resulting from a MODFLOW run in one interface time-step are used as the starting aquifer heads in the following interface time-step. In this way, the \*.hed file creates continuity between the disparate MODFLOW runs in each interface time-step. To summarize, the modeler can designate whether a specific output, such as aquifer heads, is “printed” to a text file and/or “saved” to a binary file by changing the contents of the Output Control Package.

### **3.3 River Package**

MODFLOW consists of a River Package that models the water influx into or drainage out of the aquifer from overlying rivers. Figure 3.1 depicts how MODFLOW models the river-aquifer interaction. This interaction is based on Darcy's Law where the flowrate of water between the river and aquifer is directly proportional to the hydraulic head difference between the two. The exact form of Darcy's Law used by MODFLOW, which describes the river/aquifer interaction is:

$$\begin{aligned}
W_{i,j,k} &= C_{i,j,k} (H_{RIV} - h_{i,j,k}) && \text{for } h_{i,j,k} > H_{BOT} \\
W_{i,j,k} &= C_{i,j,k} (H_{RIV} - H_{BOT}) && \text{for } h_{i,j,k} < H_{BOT}
\end{aligned}
\tag{3.3.1}$$

where,

$W_{i,j,k}$  = aquifer recharge rate [ $L^3/T$ ]

$C_{i,j,k}$  = riverbed conductance [ $L^2/T$ ]

$H_{RIV}$  = hydraulic head in river [L]

$H_{BOT}$  = elevation of the riverbed bottom [L]

$h_{i,j,k}$  = hydraulic head in aquifer [L]

$i,j,k$  refers to the parameter value in row  $i$ , column  $j$  and layer  $k$

Note that the Darcy Law equation is defined with respect to two conditions. Under the first condition, the hydraulic head in the aquifer is greater than the bottom of the riverbed, causing the flowrate to be partially controlled by the head in the aquifer. However, once the hydraulic head in the aquifer falls below the riverbed elevation, the aquifer recharge rate is independent of the hydraulic head in the aquifer. Under this second condition, the recharge rate is constant and at its maximum value. In this research, the second condition was never met.

The conductance term,  $C_{i,j,k}$ , is a function of the physical parameters of the river and is defined in Equation (3.3.2). In addition, Figure 3.1 shows a schematic describing the river/aquifer interaction as modeled by the River Package.



$$C_{i,j,k} = \frac{wLK}{M} \quad (3.3.2)$$

where,

w = width of river [L]

L = length of river in cell i,j,k [L]

M = riverbed thickness [L]

K = hydraulic conductivity of the riverbed [L/T]

In general, conductance values are very difficult to measure or assess with certainty. Although topographic maps or GIS coverages can lend some assistance in assigning the length and width of a river, the two riverbed parameters are difficult to ascertain. Often, to attain some estimate of the hydraulic conductivity, assumptions must be made about the texture of the riverbed material. Hydraulic conductivities of clays and silt soils are sometimes used for lack of better information. Overall, little riverbed data exist because soil samples are not typically taken from the riverbed for the purpose of determining the riverbed conductivity.

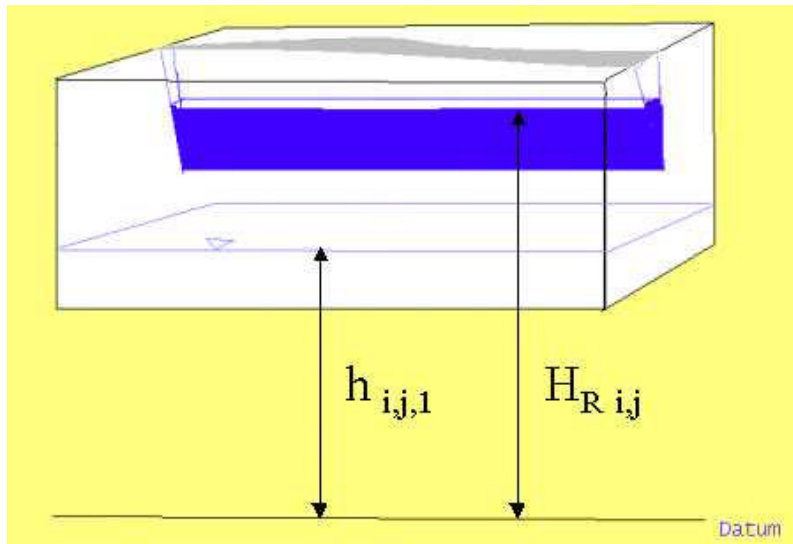
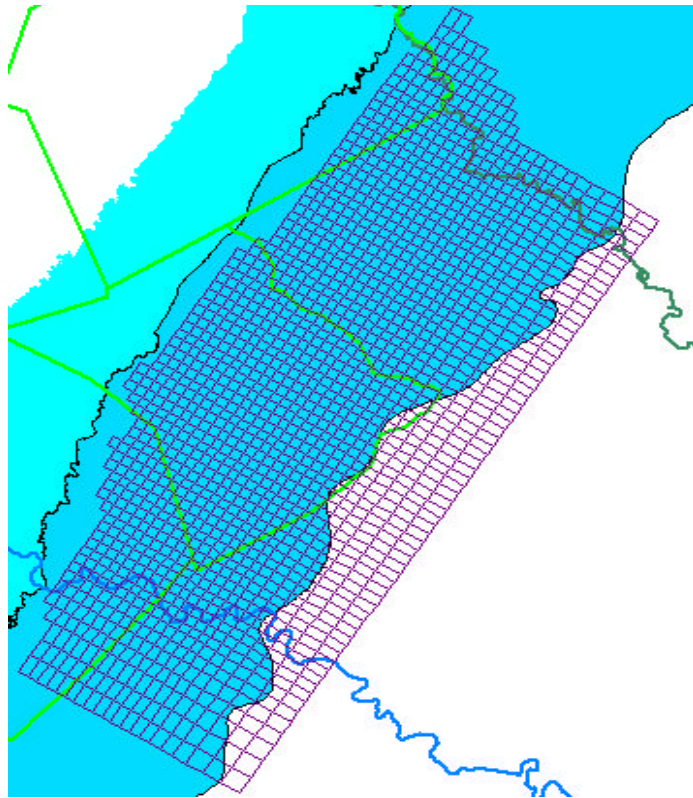


Figure 3.1 Schematic of MODFLOW River Package

### 3.4 Bureau of Economic Geology Model

The MODFLOW groundwater model that was used in this project was developed by the University of Texas Bureau of Economic Geology (BEG). The objective of the BEG project was to determine the potential hydrologic impact of the purchase of groundwater from Milam, Lee and Bastrop counties by San Antonio on wells of private users in the vicinity. The groundwater model provided by the BEG is referred to as the "BEG model," while the altered version of the BEG model used in this study will be referred to as the "revised BEG model." This section will describe only the BEG model parameters that are relevant to the scope of this study. A more complete description of the BEG model is presented by Dutton (1999).

Like the BEG model, the revised BEG model consists of one confined aquifer layer (Layer 1) and four confined/unconfined aquifer layers. A confined/unconfined layer includes both the outcrop and downdip areas of an aquifer. Layer 1 of the groundwater model area is shown in Figure 3.2. The River Package module was used to describe the influence of the Colorado, Brazos and Yegua Creek Rivers on the Carrizo-Wilcox aquifer. Figure 3.2 delineates the grid cells that were designated as River Package cells in Layer 1 of the BEG model. As discussed in the following subsection, the revised BEG model altered the location of some of the Colorado River Package cells. The remaining four layers of the groundwater model also contain River Package cells. These cells occur where one of the three rivers cross the outcrop area of the lower layer. These River Package cells were neither altered nor included in the dynamic linkage.



**Figure 3.2** Layer 1 of the BEG (and revised BEG) model. The turquoise and light blue areas signify the Carrizo-Wilcox aquifer's outcrop and downdip areas, respectively. The Colorado and Brazos Rivers are shown in dark blue and green. The bright green lines coincide with the boundaries of Milam, Lee and Bastrop counties.

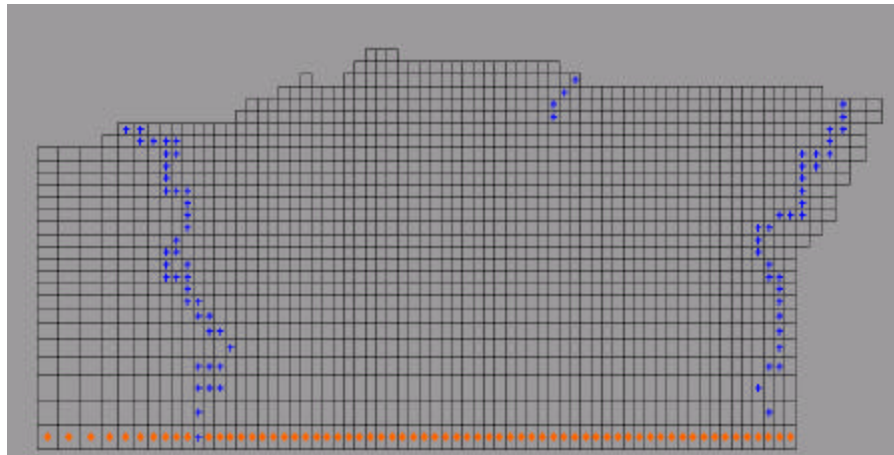


**Figure 3.3** Layer 1, as used in the BEG study, seen in the GMS software. The blue crosses indicate the River Package cells. The constant head cells are displayed with orange dots.

### **3.4.1 CHANGES TO THE RIVER PACKAGE CELLS**

For the purpose of this study, only the grid cells underlying the Colorado River in Layer 1 were linked to the surface water model. Furthermore, these cells were rearranged from locations shown in Figure 3.4 to those in Figure 3.5. As can be seen from Figure 3.4, the Rf1 file of the Colorado River did not directly overlie many of the original River Package cells, making the river length in each cell impossible to assess. Even after this alteration, two cells in a winding section of the Colorado River posed hydrologic problems when modeled separately. Because each River Package cell in MODFLOW can have only one river head value, the two separate river reaches that cross grid cell 32 were forced to have identical head values. Therefore, for the sake of continuity, the river segment in cell 31, which joins the two segments in cell 32, also has the same river head.

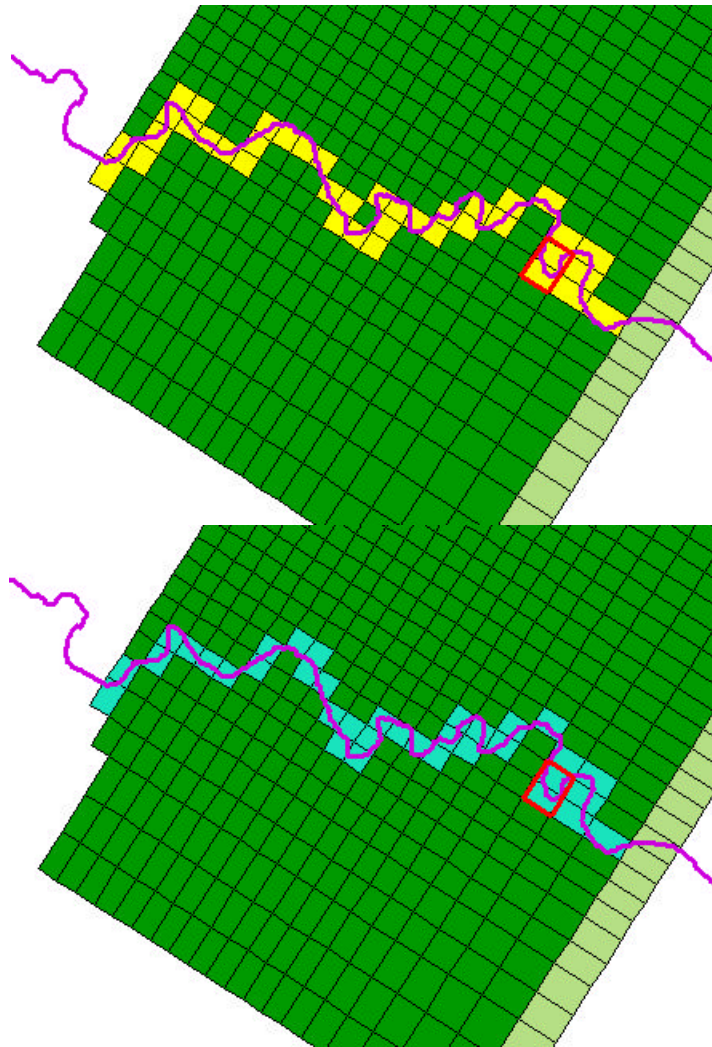


**Figure 3.4 (top)** shows the River Package cells representing the Colorado River that were used in the BEG study. The cells were modified to those shown in Figure 3.5 (bottom) to better fit the Colorado River. The red lines indicate cells 31 and 32 that were modeled as one reach in the surface water model.

To stay consistent with the BEG model, the BEG riverbed elevations were primarily adopted for this study. Cells that were designated as River Package cells in both the BEG and revised BEG models, kept their assigned BEG riverbed elevations. However, cells that were newly designated as River Package cells in

the revised BEG model were assigned elevations that were interpolated from the BEG riverbed elevations.

River conductance terms ( $C_R$ ) for the Colorado River Package cells were designated as 48,000 ft<sup>2</sup>/d (0.052 m<sup>2</sup>/s) by the BEG. To confirm that these values were still reasonable after the alterations to the River Package cells, the hydraulic conductivities of the riverbed were back - calculated using Equation 3.3.2. The river reach lengths were determined using a Geographic Information System, while the river width was taken from the BEG study to be 76.2 meters. Lastly, the riverbed thickness was assumed to be 10 cm. The resulting riverbed conductivities were found to range between 1E-06 and 1E-07 cm/s. This range of hydraulic conductivities is characteristic of silt or loess (Charbeneau 2000), a soil type that is often deposited on riverbeds. Therefore, the conductance terms of the BEG model were determined to be suitable for this study.

### **3.4.2 SOFTWARE INCOMPATIBILITY**

It should be noted that some packages supported in MODFLOW-based software such as Visual MODFLOW and Groundwater Modeling System (GMS) are not supported by MODFLOW-96 as provided by the USGS. The BEG model was created using Visual MODFLOW. However, to simplify the interaction between the Visual Basic interface and MODFLOW, the original MODFLOW-96 executable as downloaded from the USGS website was used for this study. Therefore, three packages, the Horizontal Flow Barrier Package (HFB), Constant Head (CH) and the WHB Solver Package created for the BEG model could not be

used during the simulations presented in this study. However, this loss in modeling capability is not expected to affect the results of this study.



## **CHAPTER 4: SURFACE WATER MODEL**

### **4.1 Introduction**

For this study, a surface water model was created with the use of a Geographic Information System (GIS) and Microsoft Excel (Excel). The model is based on Manning's equation and kinematic wave theory, and serves to quantify the change in river stage as a function of the groundwater recharge rate. Although surface water models abound, a simple model in Excel has the advantage of being easily manipulated by the Visual Basic interface.

As mentioned in Chapter 1, the possible relationship between observational river and groundwater data was investigated in a brief study. The study's results and limitations are presented in Section 4.2. Next, the assumptions and theory of both Manning's equation and kinematic wave theory are presented in Section 4.3 and 4.4, respectively. Section 4.5 describes the numerical solution to the kinematic wave equation used in this study. The methodology employed in determining the initial flowrate in the Colorado River will be discussed in Section 4.6. Lastly, Section 4.7 discusses the structure of the Excel surface water model.

### **4.2 Observational Data**

To determine whether observational data could provide insight into comprehending a river and aquifer's effect on one another, a USGS gage measuring streamflow in the Colorado River at Bastrop and three aquifer

observation wells near the river were chosen for analysis. Figure 4.1 shows the relative locations of the USGS stream gage 8159200 and of the three groundwater wells (5854801, 5854706, 5862603) used in this study. The USGS stream gage is located directly upstream of the BEG MODFLOW modeling domain, as shown in Figure 4.2. The USGS streamflow data was downloaded from the USGS web site (<http://waterdata.usgs.gov/nwis-w/TX/>). Similarly, the hydraulic head values for the aquifer were provided by the Texas Water Development Board web page ([http://www.twdb.state.tx.us/data/groundwater/groundwater\\_toc.htm](http://www.twdb.state.tx.us/data/groundwater/groundwater_toc.htm)).

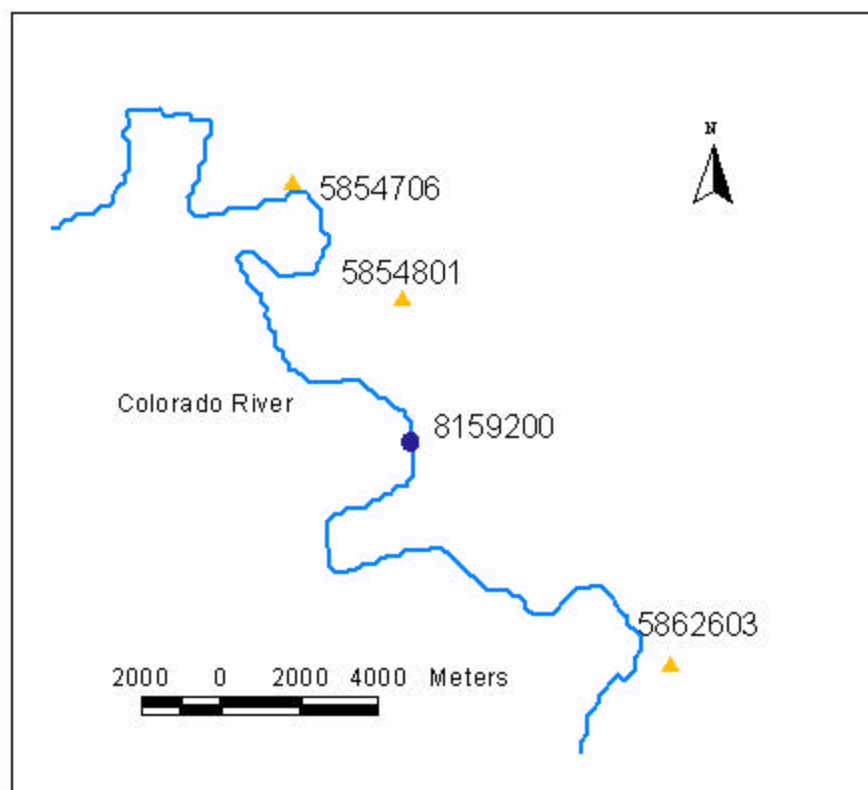


**Figure 4.1 Location of the USGS Stream Gage and the Three Groundwater Wells**

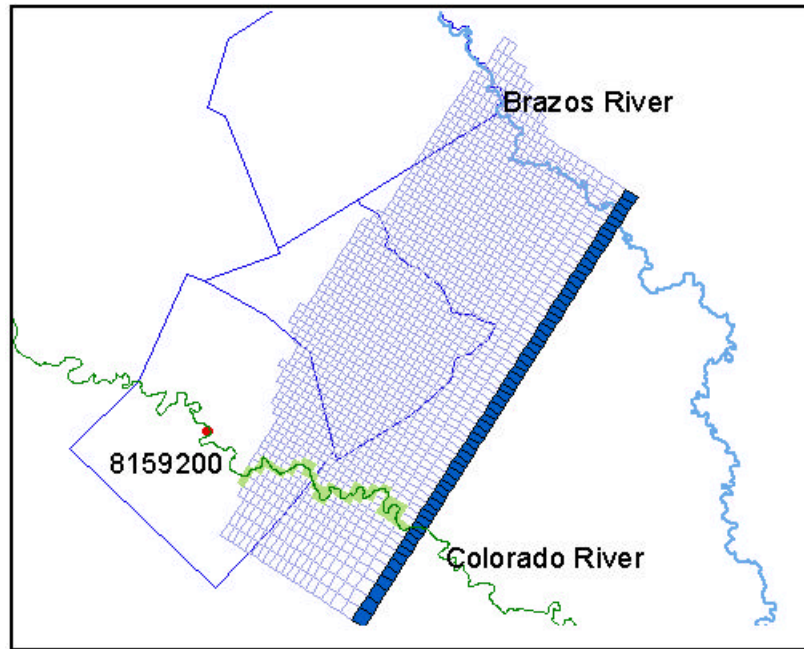


**Figure 4.2 Location of USGS Gage 8159200 with Respect to Layer 1 of Revised BEG Model**

Aquifer hydraulic head and river discharge data were analyzed between the months of April, 1981 and June, 1985. This period was chosen because it contained data that had been recorded consistently at least once every two or three months. Figure 4.3 shows a graph of the aquifer hydraulic head deviation in the three wells and the river discharge at the stream gage as a function of time. In this study, the head deviation ( $\Delta h$ ) corresponds to the difference between the instantaneous aquifer head and the time averaged aquifer head. In Figure 4.3, the aquifer head deviation is plotted on the primary axis on the left, while the river's flowrate as measured by the USGS gage, is plotted on the secondary axis on the right. Based on visual analysis, there appears to be some correlation between the river discharge and aquifer head deviation.

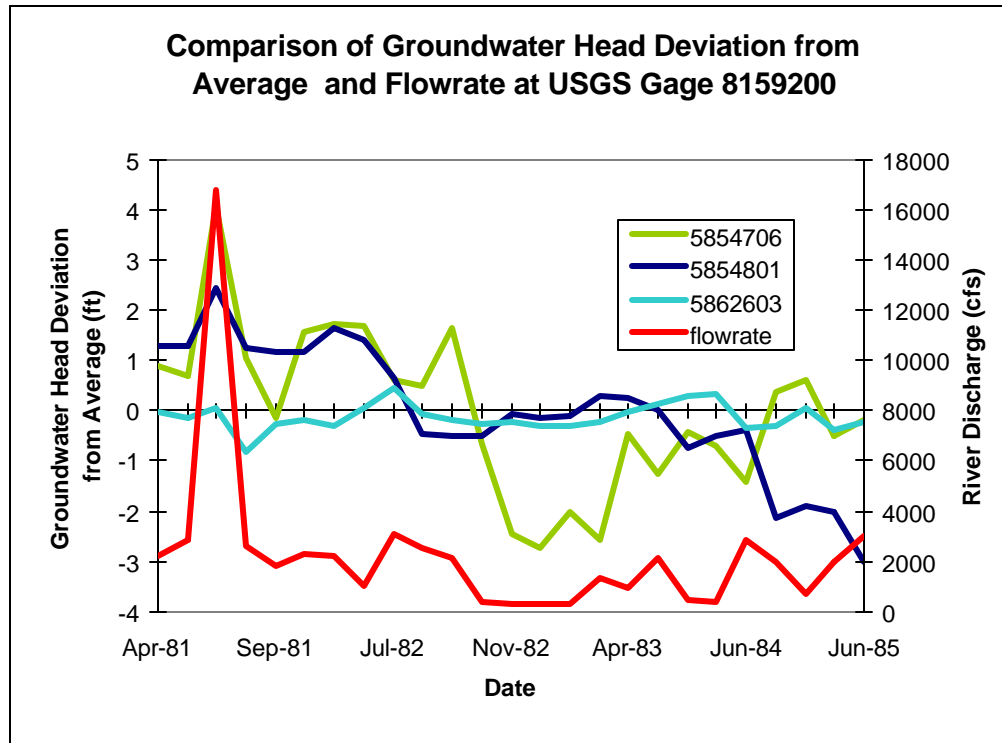


**Figure 4.3 Comparison of the Aquifer Head Deviation from the Average Head and the River Discharge at USGS Gage 8159200**

To quantify the level of correlation between the aquifer and river fluctuations, the head deviation ( $\Delta h$ ) from the average was plotted against the river discharge deviation from the average ( $\Delta Q$ ). Similarly, the river deviation from average ( $\Delta Q$ ) is defined as the difference between the instantaneous river discharge and the time averaged river discharge. Figure 4.4 presents these values for well 5854706. A linear regression of this data produced an  $R^2$  value of 0.4088. A similar analysis of wells 5854801 and 5862603 yielded  $R^2$  values of 0.1564 and 0.0085, respectively. Overall, the  $R^2$  values seemed to indicate that

there was moderate to no correlation between the changes in river flowrate and aquifer head near the river.

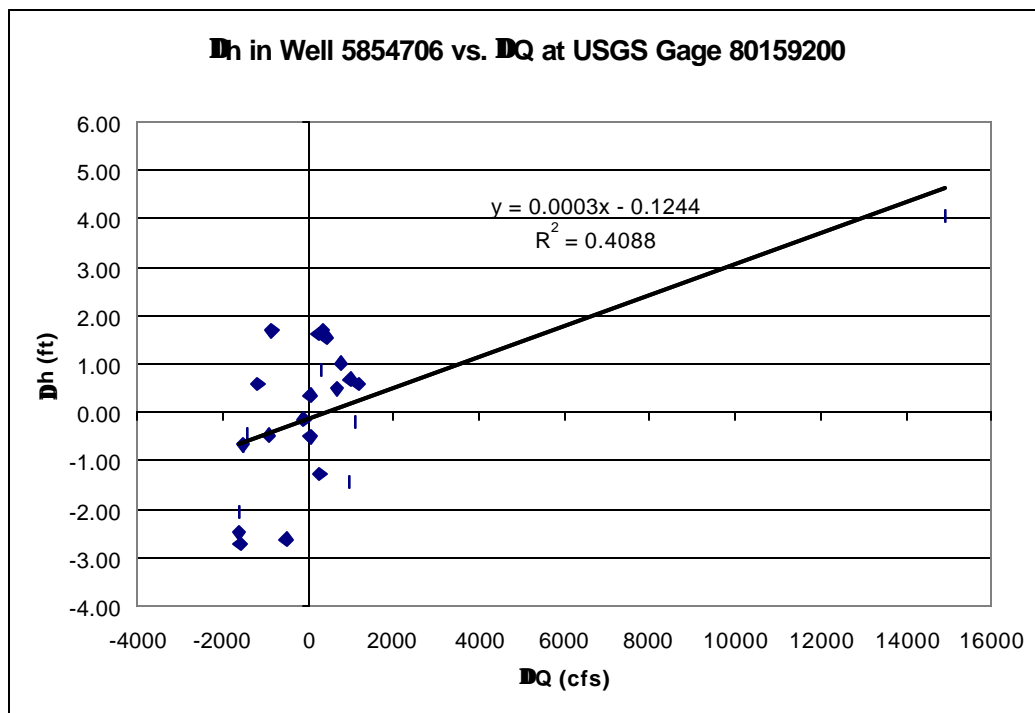
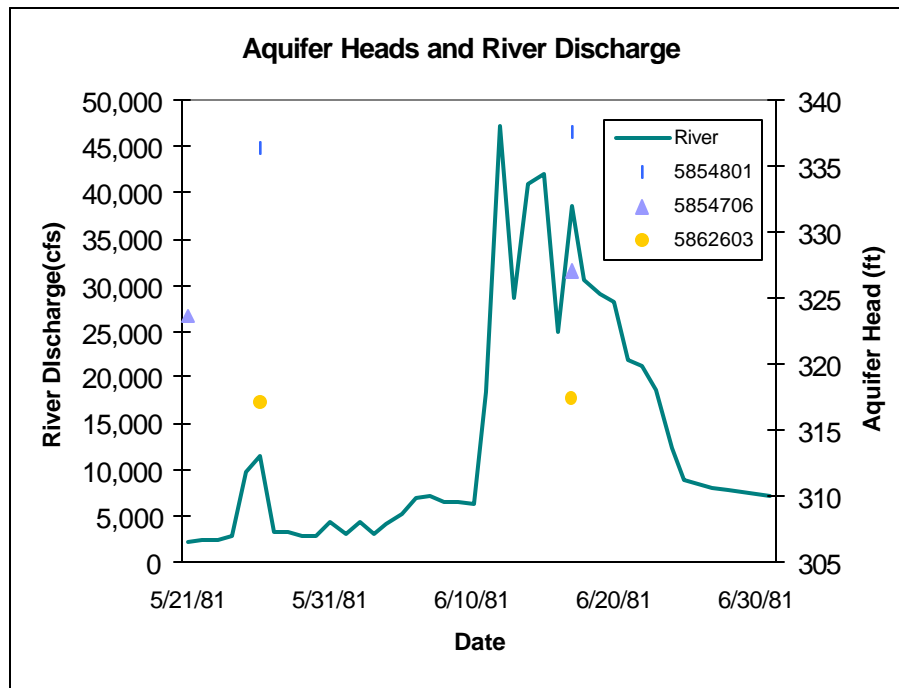


Figure 4.4 Head Deviation in Well 584706 as a Function of River Discharge Deviation

From Figure 4.3, there appears to be a similar pattern in hydraulic heads in all three wells in response to a flood wave occurring between the months of May and June of the year 1981. Figure 4.5 presents daily river discharges and aquifer heads during the flood wave period. As displayed in the figure, the hydraulic heads in all three wells increased in accordance with the higher river discharge rates. Not surprisingly, well 5854706, which has the highest correlation of the three wells, also displays the highest change in head of nearly 3 ft. Similarly, the

smallest increase in hydraulic head (approximately 0.5 ft.) occurs in well 5862603, which also has the lowest  $R^2$  value. Therefore, in response to the flood wave, the head change observed in the wells ranged from 0.5 ft. to 3 ft. over a period of one month.

However, due to the lack of data, the lateral distance from the river and the well screening intervals do not appear to provide insight to the spatial distribution of the river and aquifer interaction. Well 5854706 has the highest  $R^2$  value of the three wells and is the closest well to the river, however its screening interval is the lowest of the three wells at 400-440 ft. below the top of the casing. Well 5854801 shows a medium range of correlation, however it is the farthest from the river. The screening interval for this well is in the middle range at a depth of 300-360 ft. Finally, the well with the lowest correlation (well 5862603) has the most shallow screening interval at 100-152 ft. below the top of the casing and is the second closest well to the river.



**Figure 4.5 Comparison of Daily River Discharge at USGS Gage 8159200 and Aquifer Heads at Three Nearby Wells**

This analysis reveals the difficulty in using sparsely recorded observational aquifer data to assess the interaction between the river and aquifer systems. Despite, the appearance of some correlation between the river and aquifer in observation well 5854706, with the lack of data taken at smaller time intervals, it was difficult to determine the response time of the aquifer to the changes in river discharge. Furthermore, the spatial variation in the aquifer's response could not be assessed with the given data, because of the few number of wells available. There is also the matter of arbitrarily choosing a monthly average

of the daily streamflow values, which may have affected the correlation between the surface and groundwater fluctuations.

As a result of this study, the direction of the research changed to include two linked physically distributed models of the river and aquifer systems. Unlike the observational data, a physically distributed model provides information in locations where groundwater data is not available. Furthermore, although a model may require additional field data, it inherently reduces the dependence on time series data such as the aquifer heads, which were not available.

### **4.3 Manning's Equation**

The physically distributed model of the Colorado River is based on Manning's equation and kinematic wave theory. In this study, Manning's equation, along with additional assumptions, was used to convert the river's flowrate, as determined by kinematic wave theory, into river stages. The stage was then added to the riverbed elevations to result in the river hydraulic heads,  $H_R$ , for input into MODFLOW's River Package.

The Manning equation describes open channel flow based on three different parameters: hydraulic radius,  $\mathbf{R}$ ; friction slope,  $\mathbf{S}_f$ ; and  $\mathbf{n}$ , the Manning roughness coefficient. The hydraulic radius  $\mathbf{R}$  is defined as the cross-sectional area  $\mathbf{A}$  of the channel divided by  $\mathbf{P}$ , the wetted perimeter. The wetted perimeter is defined as the perimeter length of the channel that is in contact with the water, and thus "wetted."  $\mathbf{S}_f$  is equivalent to the head loss along the channel, divided by the length of the channel.



In SI units, Manning's equation takes the following form:

$$V = \frac{R^{2/3} S_f^{1/2}}{n} \quad (4.3.1)$$

where,

V = velocity [L/T]

R = hydraulic radius [L]

S<sub>f</sub> = friction slope

n = Manning roughness coefficient

In English units the above equation is multiplied by a factor of 1.49. SI units were used in constructing the surface water model. The Manning equation is only valid if the flow is turbulent. The criterion for turbulent flow is the following (Chow et al. 1988):

$$n^6 \sqrt{RS_f} \geq 1.1 \times 10^{-13} \quad \text{with R in meters} \quad (4.3.2)$$

The four additional assumptions used in this study are the following:

- Channel is a rectangular conduit

- Width of the rectangular conduit is much larger than the depth of the water; wetted perimeter,  $P$  equals width of channel,  $w^3$
- Manning roughness coefficient,  $n = 0.04$  for clean, winding rivers (Chow et al. 1988)

Solving Manning's equation for the river's water depth ( $y$ ), with the aforesaid assumptions yields:

$$y = \left( \frac{Qn}{wS_f^{1/2}} \right)^{3/5} \quad (4.3.3)$$

where,

$Q$  = river flowrate ( $m^3/s$ )

$w$  = width of the river (m)

$S_f$  = friction slope

#### 4.4 Kinematic Wave Theory

Kinematic wave theory describes the change in river flowrates, both in time and distance along the channel, based on lateral inflow into the river. In this study, the output of MODFLOW, namely the river leakage rates, is one component of the lateral inflow that is modeled. Therefore, the surface water

---

<sup>3</sup> Future research may wish to eliminate this assumption by using the Newton-Raphson method to solve for  $R$ , the hydraulic radius. The Newton-Raphson method solves linear non-algebraic equations in an iterative fashion.

model uses kinematic wave theory and Manning's equation in succession to determine the change in river hydraulic heads based on the aquifer lateral inflow.

The kinematic wave model is a simplified version of the Saint-Venant equations that describe unsteady non-uniform flow in a channel. The entire set of the conservation form of the Saint-Venant equations is as follows (Chow et al. 1988):

Continuity Equation

$$\frac{\partial Q}{\partial x} + \frac{\partial A}{\partial t} = q \quad (4.4.1)$$

Momentum Equation

$$\frac{1}{A} \frac{\partial Q}{\partial t} + \frac{1}{A} \frac{\partial}{\partial x} \left( \frac{Q^2}{A} \right) + g \frac{\partial y}{\partial x} - g(S_o - S_f) = 0 \quad (4.4.2)$$

where,

A = cross-sectional area of channel [L<sup>2</sup>]

Q = flowrate of water in channel [L<sup>3</sup>/T]

x = length along the river centerline [L]

g = gravitational constant = [L/T<sup>2</sup>]

t = time [T]

y = water depth in river [L]

q = lateral inflow into the river [L<sup>2</sup>/T]

The following are the assumptions of the Saint-Venant Equations<sup>1</sup> as reported by Chow, et al. in 1988:

- The flow is one-dimensional; depth and velocity vary only in the longitudinal direction of the channel. This implies that the velocity is constant and the water surface is horizontal across any section perpendicular to the longitudinal axis.
- Flow is assumed to vary gradually along the channel so that the hydrostatic pressure prevails and vertical accelerations can be neglected.
- The longitudinal axis of the channel is approximated as a straight line.
- The bottom slope of the channel is small and the channel bed is fixed; that is, the effects of scour and deposition are negligible.
- Resistance coefficients for steady uniform turbulent flow are applicable so that relationships such as the Manning's equation can be used to describe resistance effects.
- The fluid is incompressible and of constant density throughout the flow.

In the kinematic wave model, inertial and pressure forces are assumed to be negligible. With these assumptions, the kinematic wave equations are the following:

---

<sup>1</sup> Neglecting the effects of wind shear, lateral inflow, and eddy losses and assuming the momentum correction factor,  $\beta = 1$

Continuity Equation

$$\frac{\partial Q}{\partial x} + \frac{\partial A}{\partial t} = q \quad (4.4.3)$$

Momentum Equation

$$S_o = S_f \quad (4.4.4)$$

By setting the pressure and inertial terms of the momentum equation (Eq. 4.4.2) to zero and solving for **A** in terms of **Q**, Equation 4.4.4 could also be written as the following:

$$A = \alpha Q^\beta \quad (4.4.5)$$

where,

$\alpha, \beta$  = general coefficients

Although this is a general solution, Manning's equation can be shown to be a specific solution of the momentum equation. Manning's equation (Eq. 4.3.1) along with the momentum equation (Eq. 4.4.4), yield the following relationships for **a** and **b**:

$$\mathbf{a} = \left[ \frac{nP^{2/3}}{\sqrt{S_o}} \right] \quad (4.4.6a)$$

$$\beta = 0.6 \quad (4.4.6b)$$

Substituting Equation 4.4.5 for  $\mathbf{A}$  into Equation 4.4.3 yields the kinematic wave equation:

$$\frac{\partial Q}{\partial x} + \mathbf{a}bQ^{b-1} \frac{\partial Q}{\partial t} = q \quad (4.4.7)$$

In this study there are two components of lateral inflow. These are  $\mathbf{q}_a$  and  $\mathbf{q}_r$ , representing the aquifer inflow and local surface inflow, respectively. Therefore, the form of Equation 4.4.7 that is used in the surface water model is shown in Equation 4.4.8.

$$\frac{\partial Q}{\partial x} + \mathbf{a}bQ^{b-1} \frac{\partial Q}{\partial t} = q_a + q_r \quad (4.4.8)$$

## 4.5 Explicit Solution to the Kinematic Wave Equation

Due to the complexity of the region being modeled, a finite difference solution was chosen over an analytical solution to the kinematic wave equation. The finite difference method is based on a Taylor series expansion of a differential equation, in this case Equation 4.4.8. The result of the finite difference method as applied to the kinematic wave equation is seen in Equation

4.5.1. This equation has been modified from what was reported by Chow et al. to incorporate both lateral inflow terms. Also note that the aquifer inflow term is held constant throughout the duration of the surface water run-time and therefore does not require time averaging.

$$Q_{i+1}^{j+1} = \frac{\left[ \frac{\Delta t}{\Delta x} Q_i^{j+1} + \mathbf{ba} Q_{i+1}^j \left( \frac{Q_{i+1}^j + Q_i^{j+1}}{2} \right)^{b-1} + \Delta t \left( \frac{q_{ri+1}^{j+1} + q_{ri+1}^j}{2} + q_{ai+1} \right) \right]}{\left[ \frac{\Delta t}{\Delta x} + \mathbf{ab} \left( \frac{Q_{i+1}^j + Q_i^{j+1}}{2} \right)^{b-1} \right]}$$

(4.5.1)

where,

j = time-step index

i = river reach index

$q_r$  = overland runoff [ $L^2/T$ ]

$q_a$  = aquifer recharge [ $L^2/T$ ]

$\Delta t$  = time-step length [T]

$\Delta x$  = river reach length (L)

Two methods of solution for a finite difference equation exist: an implicit scheme and an explicit scheme. The implicit scheme involves solving the unknown values of the equation simultaneously and requires a specially constructed computer program. Alternatively, the explicit scheme solves the unknown values sequentially, in this case, with the help of an Excel spreadsheet. To ensure a stable solution, however, the explicit scheme requires smaller surface

water time-steps (Chow et al. 1988). In the explicit scheme, the length of the surface water time-step is constrained by the Courant condition described in Section 4.5.1. For the purpose of this study, the explicit solution was chosen for ease of implementation.

#### 4.5.1 COURANT CONDITION

A necessary but insufficient condition for stability of the explicit scheme is dictated by the Courant condition. This condition states that the time-step chosen for the surface water model must be smaller than or equal to the time it takes the wave to transverse any given river reach. Mathematically, the Courant condition is equivalent to Equation 4.5.2.

$$\Delta t \leq \frac{\Delta x_i}{c_k} \quad (4.5.2)$$

where,

$\Delta t$  = surface water model time-step [T]

$\Delta x_i$  = reach length i [L]

$c_k$  = kinematic wave celerity [L/T]

The wave celerity,  $c_k$ , can be determined from the Method of Characteristic solution of Equation 4.4.7. The Method of Characteristics produces a set of ordinary differential equations that are mathematically equivalent from a partial differential equation, in this case the kinematic wave equation. The Method of Characteristics solution to the kinematic wave equation



is presented in Equation 4.5.3. The right hand side equation can be rearranged to result in Equation 4.5.4, the wave celerity. By substituting in Manning's equation (Eq. 4.3.3), the wave celerity can be calculated using river parameters as shown in Equation 4.5.5.

$$dx = \frac{dt}{\alpha \beta Q^{b-1}} = \frac{dQ}{q} \quad (4.5.3)$$

$$\frac{dx}{dt} = c_k = \frac{1}{\alpha \beta Q^{b-1}} \quad (4.5.4)$$

$$c_k = \left( \frac{5}{3} \right) \left( \frac{S_o^{1/2} y^{2/3}}{n} \right) = \frac{5}{3} V \quad (4.5.5)$$

where,

$c_k$  = wave celerity (m/s)

$Q$  = river discharge ( $m^3/s$ )

$q$  = lateral inflow ( $m^2/s$ )

$\alpha, \beta$  = general coefficients

$S_o$  = riverbed slope

$y$  = water depth (m)

$n$  = Manning's roughness coefficient

$V$  = velocity (m/s)

## **4.6 Determining Initial Flowrate in the Colorado River**

In order to begin modeling the Colorado River, it was necessary to determine the initial condition of the river for the model. It was decided to use the average discharges in the Colorado as the initial condition. To determine the Colorado River's average discharges, terrain and runoff data were modeled in a Geographic Information System (GIS). Because of the large amount of data involved in analyzing the entire Colorado watershed, a subwatershed in the domain of interest was the only one modeled in GIS. Contributions from the watersheds upstream of the model domain were determined by using average daily flowrate data collected from USGS stream gages. Section 4.6.2 discusses the GIS processing of the domain subwatershed. Section 4.6.3 describes the contribution of the upstream subwatersheds to the average flowrate.

### **4.6.1 DATA**

The data required to perform the average flowrate analysis is shown in Table 4.1. Although some of the data were in files at the Center for Research of Water Resources (CRWR), all files that were needed could just as easily have been downloaded from the Internet. All GIS processing of data for this study was conducted in version 3.2 of ArcView and version 7.1 of Arc/ Info.

A Digital Elevation Model (DEM) is a digitized representation of the landscape and can be imported into ArcView as a grid. The value in each grid cell corresponds to the elevation of the terrain at the center of the grid cell. In this study, the grid cells were approximately 90 meters on each side.

The runoff grid was based on a coverage created by Andrew Romanek (Romanek 1998). The grid was created from data gathered by the USGS between 1951 and 1980.

**Table 4.1 GIS Data and their Sources**

<b>Data</b>	<b>Source</b>	<b>Type of GIS Coverage</b>
90 m. Digital Elevation Model (DEM)	USGS	Grid
8-Digit Hydrologic Unit Code Subwatersheds (HUC8)	CRWR	Polygon
Counties	CRWR	Polygon
River Reach 1 Files (Rf1)	CRWR	Polyline
Runoff Grid	CRWR	Grid
Width of Colorado River	BEG	--
Average daily flowrates upstream of domain watersheds	USGS	--

#### **4.6.2 GIS PROCESSING OF DATA**

To determine the contribution of the domain subwatersheds to the initial flowrate of the section of the Colorado River used in this study, it was necessary to cut the DEM into the shape of the domain subwatersheds. Subsequently, the DEM was taken through the steps of the CRWR-PrePro Project (Olivera 1998). From this process, a flow direction grid was produced. The runoff grid and the flow direction grid were then processed using the Non-Point-Source Project (nonpoint.apr) created in ArcView to produce a weighted flow accumulation grid.

## **Merging and Clipping DEMs**

To clip out the DEMs in the shape of the domain subwatersheds, the following steps were taken:

- Initially, Milam, Lee and Bastrop counties were “intersected” in ArcView with the HUC subwatershed shapefile to determine which subwatersheds were underlying the three counties. Only one HUC8 subwatershed of the Colorado River, the Lower Colorado-Cummins (Cataloging Unit: 12090301), is located within these three counties. However, before the scope of this research was limited to modeling the Colorado River alone, the original GIS analysis was performed on all of the subwatersheds underlying the modeling domain.
- The 90 meter DEM data is available on the USGS web site (<http://edcwww.cr.usgs.gov/doc/edchome/ndcdb/ndcdb.html>). The DEM grid was then clipped out in the shape of the subwatershed basins of interest in Arc/Info.
- The DEMs were converted from their original floating point format to integer format to save disk space and decrease computing time in the subsequent analysis stage.

## **Flow Direction Grid**

The DEM, now in the shape of the domain subwatersheds, was manipulated through the steps offered by CRWR-PrePro to create a flow direction

grid. First, the Rf1 line representing the Colorado and Brazos River were selected and clipped in the shape of the domain subwatersheds using the GeoProcessing Wizard Extension. Although more accurate digital representations of the Colorado and Brazos Rivers exist (in both River Reach 3 files and National Hydrologic Dataset formats), the Rf1 files are sufficient for the purpose of this study. The Rf1 representations of the Colorado and Brazos Rivers were then "burned into" the DEM by using the "Burn-in Stream" command in the CRWR-PrePro menu. This command consists of raising all non-river grid cells by 5000 meters to ensure that water will flow into the location where the river is known to be. Due to inaccuracies in the DEM, depressions (i.e. grid cells bordered by two other grid cells with higher DEM values) can exist in the grid cells below the Rf1 representation of the rivers. To prevent water from stagnating in depressions in the river and disturbing the flow to downstream cells, the DEM was processed using CRWR-PrePro "Fill DEM" function. During this process, depressions along the river were raised to the value of the lowest neighboring cell so as not to act like a sink in the river.

Once the DEM had been filled, the flow direction grid was computed using the "Flow Direction" command in the CRWR-PrePro Project in ArcView. In executing this command, the computer uses the 8-direction pour point model to calculate which direction the water will flow out of a cell. This model compares the DEM values of the 8 cells that surround any given cell and determines the direction of the steepest decline from the center cell. The model then assigns a number (and later a color) to this direction, based on the values shown in Figure

4.6. For example, if the direction of the steepest decline is due east, the number "1" is assigned to the center cell shown in the figure. In the resulting flow direction grid, seen in Figure 4.7, each color designates the direction of steepest descent and thus the direction that water will flow out of the cell. Although the flow direction grid contains data for all of the subwatersheds in the modeling domain, only the Lower Colorado-Cummins subwatershed was used to determine the initial flowrate in the Colorado River.

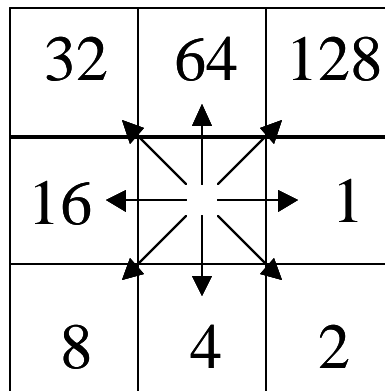


**Figure 4.6 Schematic of the 8-Direction Pour Point Model**

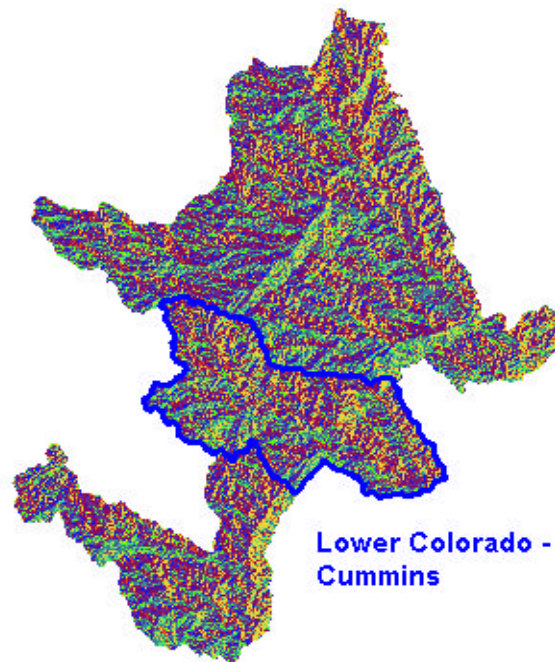


**Figure 4.7 The Flow Direction Grid for the Subwatersheds Underlying Milam, Lee and Bastrop Counties**

### **Weighted Flow Accumulation Grid**

To determine the amount of runoff that gathered into the river cells, it was necessary to enter the flow and runoff grids into the ArcView Non- Point Source Analyst Project and employ the "Flow Accumulation" command. Unlike the flow accumulation command under CRWR-PrePro, which assumes each grid cell has an equal weight (i.e. 1), the Non-Point Source Analyst weighs the upstream cells with the runoff grid values before summing them up. For example, if 3 cells with runoff grid values of 4, 2 and 5 inches flow into a certain cell, the resulting flow accumulation value in the cell would be "11" inches and not "3" cells as reported by CRWR-PrePro. The flow eventually accumulates into the lowest DEM grid

cells, (i.e. the "burned in" river) and in this way calculates the average flow in the river being modeled.

#### **4.6.3 UPSTREAM FLOWRATE**

Because the domain of interest was on the lower portion of the extensive Colorado watershed, it was necessary to consider the contribution of the flow originating from upstream of the domain subwatershed. Upstream flowrates were determined using the average daily flowrate provided by 3 USGS gages located directly upstream of the Lower Colorado - Cummins subwatershed. Figure 4.8 shows the location of the three gages with respect to the Lower Colorado - Cummins subwatershed. All three gages are located in Austin, TX. Gages 818600 and 815900 measure the flowrates of two tributaries of the Colorado River. They are located on Walnut Creek at Webberville Rd. and Onion Creek at U.S. Highway 183, respectively. Gage 815800 measures the river discharge of the main stem of the Colorado River at Austin. Table 4.2 shows the different dates of data used and the resulting flowrate at each gage station. Note that some days of data were missing from the interval stated in the third column of the table, accounting for the variation in the "Numbers of Days of Data" column from what is expected. The flowrate from the upstream watersheds of the Colorado River was determined to be  $58 \text{ m}^3/\text{s}$ .



**Table 4.2 Data from USGS Gages Located Upstream of the Subject Area**

<i>USGS Station ID</i>	<i>River/Tributary</i>	<i>Dates of Data</i>	<i>Number of Days of Data</i>	<i>Avg. Flowrate (m<sup>3</sup>/s)</i>
<b>8158600</b>	Walnut Creek	12/29/74- 12/21/98	8758	0.9
<b>8158000</b>	Colorado River	12/29/74- 12/29/98	8694	54.4
<b>8159000</b>	Onion Creek	3/23/76- 10/17/98	9313	2.6

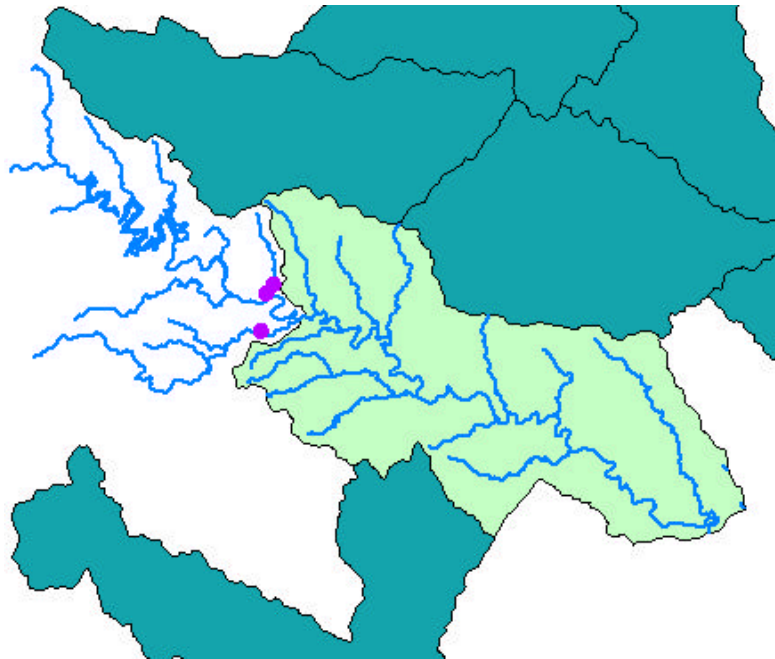


**Figure 4.8 Location of the Three USGS Gages Used in Determining the Upstream Flowrate in the Colorado River**

#### 4.6.4 RUNOFF AND RIVER REACH LENGTHS

In the surface water model, there are 35 reaches that make up the stretch of the Colorado River being modeled. These reaches correspond to the portions of the river overlying the River Package cells of the Colorado River in the 1<sup>st</sup> layer of the revised BEG MODFLOW model. As shown in Figure 4.9, the finite difference nodes defining the surface water model are located at the top and bottom of the river reaches, and at the boundary between the River Package cells, shown in the figure as blue boxes. Consequently, the most upstream MODFLOW River Package cell is located between nodes 0 and 1 of the surface water model. The river reach lengths, corresponding to  $\Delta x$  in Equation 4.5.1, were determined using the measuring tool in ArcView. The river flowrates resulting from the domain subwatershed were determined for each of the nodes 0-35, by querying the weighted flow accumulation grid at the node locations. This value was then added to the upstream flowrate and resulted in the initial flowrates for the Colorado River. Runoff values, corresponding to  $q_r$  in Equation 4.4.8, were calculated based on the initial flowrate and river reach lengths according to Equation 4.6.1. Values of the river reach length and runoff can be viewed in Appendix A.

$$q_{ri} = \left( \frac{Q_i - Q_{i-1}}{\Delta x_i} \right) \quad (4.6.1)$$

where,

$q_{ri}$  = overland inflow at node  $i$  [ $L^2/T$ ]

$Q_i$  = initial flowrate at node  $i$  [ $L^3/T$ ]

$\Delta x_i$  = length of river reach between nodes  $i$  and  $i-1$  [ $L$ ]

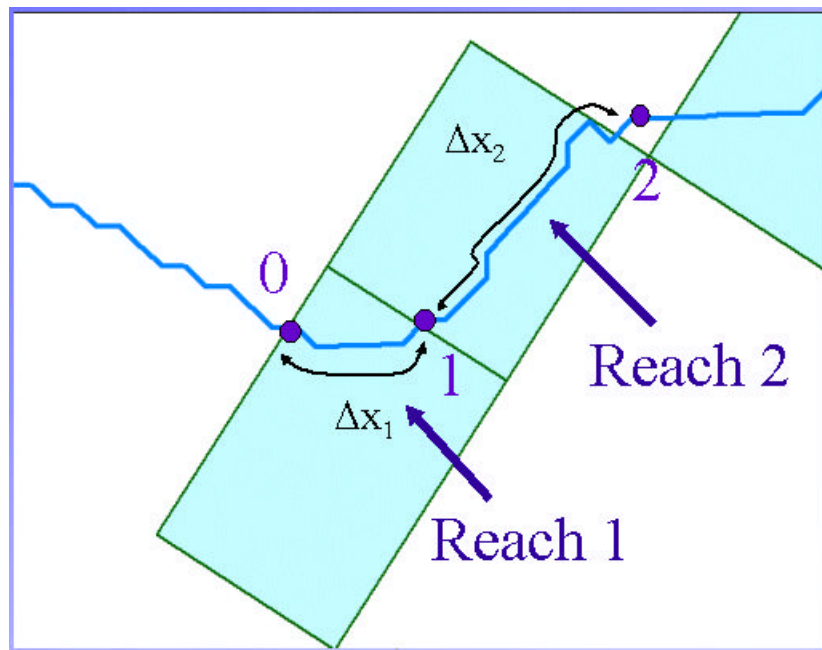


Figure 4.9 Finite Difference Nodes Along the Colorado River

#### 4.6.5 SURFACE WATER MODEL CALIBRATION

The surface water model was calibrated based on the mean daily streamflow data of USGS gage 8160400 located on the Colorado River Above La Grange, TX. As shown in Figure 4.10, USGS gage 8160400 is situated near node 34. Streamflows from this gage were averaged over a span of 10 years starting in January 1, 1988. The 10-year average river discharge ( $81.65 \text{ m}^3/\text{s}$ ) is approximately  $9.4 \text{ m}^3/\text{s}$  more than what was predicted by the GIS analysis to be

the river discharge in node 34. To calibrate the model to match the observed data, the flowrate at node 0 was increased from 65.7 m<sup>3</sup>/s to 77.3 m<sup>3</sup>/s.

New river heads were determined from these newly calibrated river discharge values, which caused a recalibration of the revised BEG model. To remain consistent with the original river heads in the BEG model, the riverbed elevations were adjusted to account for the new river stages, so that the revised BEG model contained approximately the same river heads as the original BEG model.

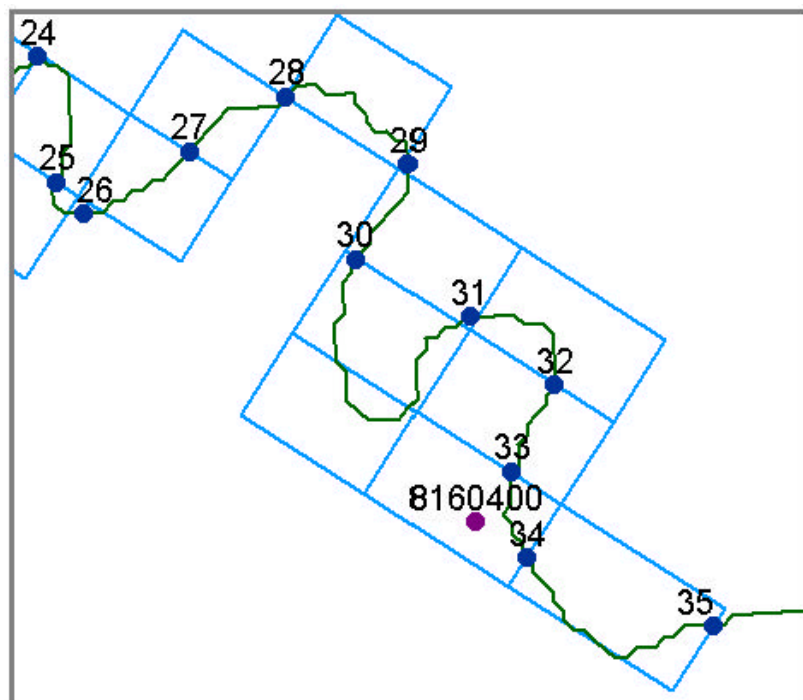


Figure 4.10 Location of USGS Gage 8160400 with Respect to the Finite Difference Nodes

## **4.7 Excel-Based Surface Water Model**

To determine the effect of time-step on the interaction between a river and aquifer, a flood wave was simulated through the Colorado River. The rapid fluctuations in river discharge caused by the flood wave were averaged over various time-steps before being entered into the dynamically linked surface and ground water models. The organization of the surface water model was designed with the flood wave simulation in mind. Therefore, a description of the simulation is provided in Section 4.7.1 before the framework of the surface water model is discussed in the subsequent section.

### **4.7.1 SURFACE WATER SIMULATION**

The surface water model simulations were based on changing the inlet river discharge at node 0 to model the river discharges created by a flood wave. Each simulation occurs over a 32-day period. The inlet river discharge for the 32 days of the simulations were based on average daily streamflow data gathered by the USGS starting on January 8, 1991 from gage 8160400. This stream gage was also used to calibrate the surface water model and its location with respect to the domain can be seen in Figure 4.10. Although the gage is located near node 34, the streamflow data was applied as the boundary condition at the inlet of the domain (i.e. node 0). This was justifiable because the focus of this research is on the effect of time-step in modeling rapidly fluctuating river discharges; a baseline change of  $4 \text{ m}^3/\text{s}$  in the river discharge is not expected to affect the results of this study.

Figure 4.11 presents the original USGS data for the inlet river discharge as 1-day averaged data. The inlet wave has three peaks occurring approximately during day 3, 11 and 28. The three peak discharges are approximately 1033 m<sup>3</sup>/s, 583 m<sup>3</sup>/s, and 427 m<sup>3</sup>/s. The river discharge in the long stretch of time between peaks 2 and 3 varies between 17 and 80 m<sup>3</sup>/s.

To determine the effect of the time-step on modeling the river and aquifer interaction, 4 different time-steps were considered. The time-steps corresponded to averaging the river discharge over a period of 2, 4, 8 and 16 days. Figure 4.11 displays the time-step averaged river discharge at the inlet. As was expected, the smallest time-step was still able to capture the rapid fluctuations in the river discharge while the 16-day time step was not able to do so.

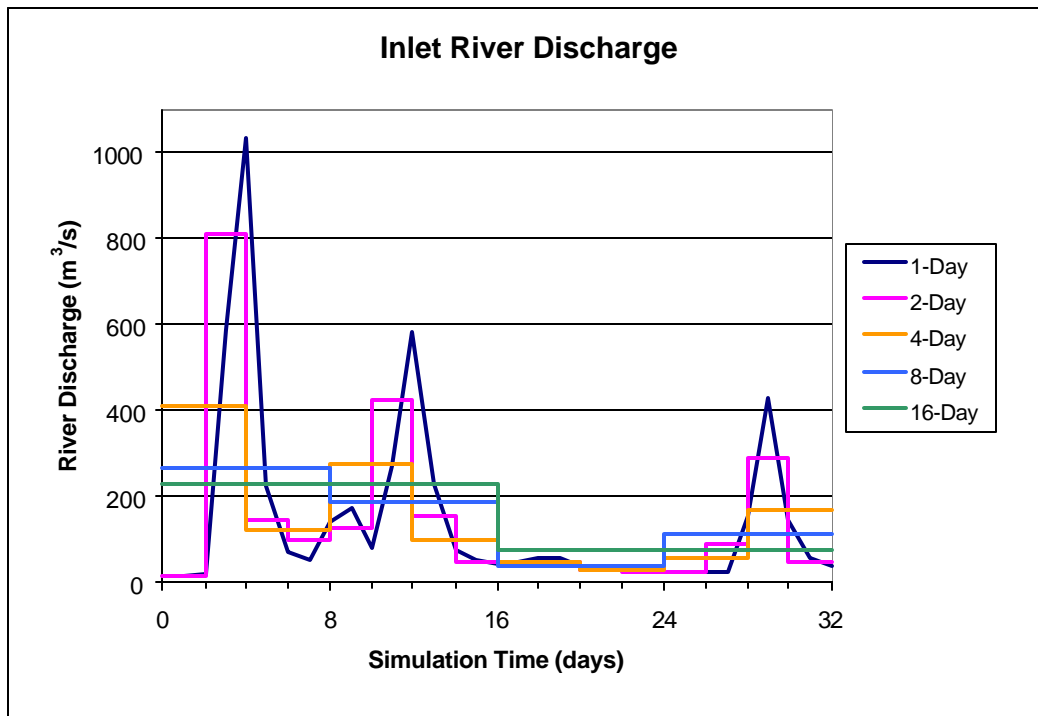


**Figure 4.11 Time-Step Averaged River Discharge at the Inlet**

To ensure that any changes in the groundwater system were due to the inlet wave and not due to the new average river heads resulting from the surface water calibration, the groundwater and surface water systems were allowed to come into equilibrium. The dynamically linked models were run for 1280 days (or approximately 3.5 years) using 64-day time-steps. Although heads in the aquifer were still changing slowly with time, most of the changes occurred over a period that was longer than 32 days. The dynamically linked models were believed to be in pseudo-equilibrium for the purposes of this study. The new river and aquifer heads, now in pseudo-equilibrium, were used as the initial conditions for the 32-day simulations

There are three main components to the output of the simulations: river discharge, river hydraulic head and aquifer hydraulic heads. The output of the surface water model is comprised of the river discharge and hydraulic head in the 35 reaches. In order to assess the spatial variability in the aquifer's response to the flood wave, aquifer heads in two cross sections of the aquifer were recorded in the output. Figure 4.12 displays the location of the two cross sections in Layer 1. The first cross section includes nine cells in row 40, between columns 5 and 11. These cells include the aquifer cell directly below River Reach 14, shown as the light blue cell in Cross Section 1, and the four cells adjacent to it on both sides. The aquifer heads in Layer 2 of the same 9 cells were also recorded, so as to facilitate an understanding of the aquifer's vertical response to the flood wave. Cross Section 2 includes the ten aquifer cells located in row 37, between columns 8 and 17. These cells include River Reaches 27 and 28 along with the 8 cells in the same row straddling those reaches. Similarly, Cross Section 2 also extends to Layer 2.



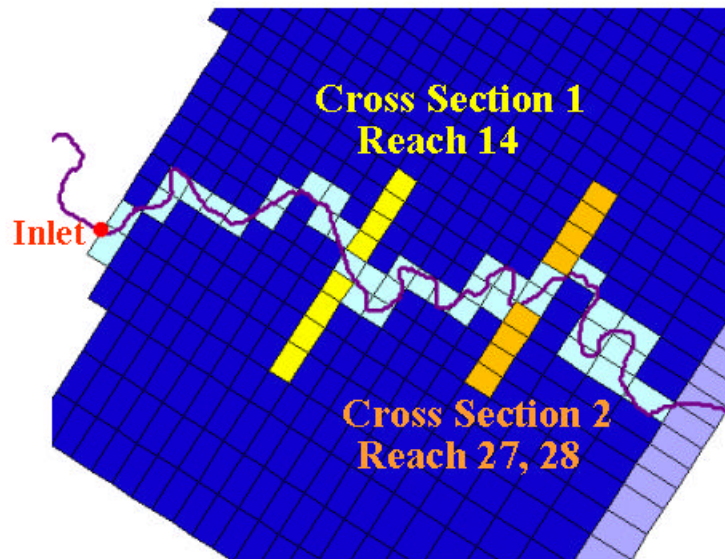


**Figure 4.12 Aquifer Cross Sections 1 and 2 in Layer 1 of the Revised BEG Model**

#### **4.7.2 SURFACE WATER MODEL**

The surface water model is an Excel file, “kinematic8.xls”, which consists of 13 different worksheets. Four of the worksheets (*inlet2*, *inlet4*, *inlet8*, and *inlet16*) contain the time-averaged inlet river discharges for the four different time-steps. The kinematic wave and Manning's equations calculations are performed using six worksheets (*Q*, *h*, *qa*, *qr*, *Par* and *qa,h\_fix*). The remaining three worksheets (*flowrate*, *riv\_head*, and *aq\_head*) are used to store the output of the dynamically linked models. The following sections provide a description of the methodology used in determining the surface water time-step as well as the worksheets in "kinematic8.xls."

## Surface Water Time-Step

To ensure that the Courant condition was met throughout the surface water simulation, a critical time-step was determined that was applied to the entire simulation. By examining the Courant condition equation (Equation 4.5.2) the critical time-step results from minimizing the value on the right hand side of the equation or the river reach length divided by the wave celerity. The critical time-step would need to satisfy the Courant condition in the smallest river reach and during the time of the greatest wave celerity. From Manning's equation, it is evident that wave celerity increases with increasing river discharge. Therefore, the first peak discharge of  $1033 \text{ m}^3/\text{s}$  produces the highest wave celerity during the 32-day simulation. During that peak discharge, the time-step is also limited by the smallest reach, in this case Reach 15. A steady-state simulation in worksheet *Q* using  $1033 \text{ m}^3/\text{s}$  as the inlet river discharge provided a critical time-step in Reach 15 of 197 seconds. A safety factor of 17 seconds was used in case the lateral inflow caused a significant increase in flowrate in any downstream reaches. Therefore, the critical surface water time-step used throughout each simulation is 180 seconds.

## Inlet Discharge Worksheets

The time-step averaged inlet discharges are held in four different worksheets. The worksheets *inlet2*, *inlet4*, *inlet8* and *inlet16* contain the inlet river flowrates averaged over a time-step of 2, 4, 8 and 16 days, respectively. Although Figure 4.13 shows only a portion of *inlet2*, the other three inlet river discharge worksheets are organized in a similar fashion.

Starting from the far left, columns A-C contain different time variables used in the simulation. Column B of the worksheet contains the surface water time-step (180 seconds) and can be altered should other flood wave simulations be considered in the future. The inlet river discharge for each day of the simulation is located in each column, starting in column D. Therefore, in worksheet *inlet2*, columns D and E contain the 2-day average inlet flowrates for the first two days of the simulation. Similarly, the 2-day averaged inlet flowrates between days 2 and 4 are stored in columns F and G.

The rows in the worksheet, starting at row 3, correspond to different surface water time-steps. There are 480 rows of flowrates in the worksheets, which correspond to the 480 surface water time-steps that comprise a day of the simulation. Although the inlet river discharge values did not change with each surface water time-step, the worksheets are set up to facilitate any kind of surface water data. Real-time data for instance, should it become available, could make better use of the 480 rows available in the inlet discharge worksheets.

1	A	B	C	D	E	F	G
2	<b>Time index</b>	<b>(Sec)</b>	<b>(Days)</b>	<b>0</b>	<b>1</b>	<b>2</b>	<b>3</b>
3	0	180.00	0.00	47.07992	47.07992	809.8542	809.8542
4	1	180.00	0.002	47.07992	47.07992	809.8542	809.8542
5	2	180.00	0.004	47.07992	47.07992	809.8542	809.8542
6	3	180.00	0.006	47.07992	47.07992	809.8542	809.8542
7	4	180.00	0.008	47.07992	47.07992	809.8542	809.8542
8	5	180.00	0.010	47.07992	47.07992	809.8542	809.8542
9	6	180.00	0.013	47.07992	47.07992	809.8542	809.8542
10	7	180.00	0.015	47.07992	47.07992	809.8542	809.8542
11	8	180.00	0.017	47.07992	47.07992	809.8542	809.8542
12	9	180.00	0.019	47.07992	47.07992	809.8542	809.8542

Figure 4.13 A Section of the *inlet2* Worksheet

### Kinematic Wave Worksheets

The river parameters, such as riverbed slope, river width (or P, the wetted perimeter), and river segment length ( $\Delta x$ ), are contained in worksheet *Par* shown in Figure 4.14. RECNO corresponds to the record number given to the cell polygons in the GIS representation of the MODFLOW grid. Unlike, the inlet river discharge worksheets, the bold numbers along the top of the 4<sup>th</sup> row correspond to each of the 35 river nodes. The most important parameter on this worksheet is the lumped parameter  $\alpha$ , one of the main parameters in Equation 4.4.8. The Manning coefficient factor used throughout the simulation is 0.04, for clean winding rivers, and can be seen in cell B2. In addition, the *Par* worksheet contains the river leakage rates and the river discharge in the 35 reaches that resulted from the calibration of the dynamically linked models. These values are

used to produce consistent initial conditions in the surface water model for each simulation.

	A	B	C	D	E	F	G
1							
2		n= 0.040					
3							
4		<b>Units</b>	<b>0</b>	<b>1</b>	<b>2</b>	<b>3</b>	<b>4</b>
5	<b>RECNO</b>			2800	2764	2746	2713
6	<b>Δx</b>	(m)	0.0	1120.0	2665.0	2445.0	3280.0
7	<b>X (distance)</b>	(m)	0	1120.0	3785.0	6230.0	9510.0
8	<b>slope</b>		2.36E-04	2.36E-04	2.36E-04	4.25E-04	1.54E-04
9	<b>Width / P</b>	(m)	76.2	76.2	76.2	76.2	76.2
10	<b>α</b>		10.04	10.04	10.04	8.42	11.42
11							
12							

Figure 4.14 A Section of the *Par* Worksheet

Like the *Par* worksheet, *qa* and *qr* provide input values for the surface water model. Worksheets *qa* and *qr* contain values of aquifer recharge and runoff, respectively. In the *qa* worksheet, because the river recharge by the aquifer is assumed to stay constant for the entire surface water simulation, there is only one row of aquifer recharge values. The  $q_a$  values are based on the output of MODFLOW, but have been modified in the *qa.h\_fix* worksheet to stay consistent with the units used in the surface water model. The *qr* worksheet, on the other hand, contains a row of runoff data per surface water time-step. It was believed at the beginning of the project that precipitation events might also be considered when modeling the surface water system. These events would give rise to time-dependent runoff, and the worksheet was set up to accommodate this aspect of the

analysis. However, due to the added complexity posed by simulating precipitation, simulations that were conducted in this study were limited to the steady-state average runoff values that were calculated in Section 4.6.4. The *qr* worksheet, however, is equipped to handle the analysis of time-dependent runoff, should further analysis of the region be desired.

The *qa,h\_fix* worksheet exists to modify and reorder the two parameters,  $\mathbf{H}_R$  and  $\mathbf{q}_a$ , that are being transferred between the two models. The parameters in the surface water model are ordered from upstream to downstream. The revised BEG MODFLOW model, however, is organized by increasing row number, which at times does not correspond to the direction of river flow. The sequence of the  $\mathbf{q}_a$  and  $\mathbf{H}_R$  vectors are therefore shuffled in *qa,h\_fix* to suit the organization of the model that is being updated. In addition, *qa,h\_fix* worksheet converts MODFLOW's output (i.e. river leakage rates in units of  $\text{ft}^3/\text{d}$ ) to suit the units of  $\mathbf{q}_a$  ( $\text{m}^2/\text{s}$ ) in the surface water model. Lastly, in *qa,h\_fix* the riverbed elevations are added to the river stage values to result in river hydraulic head before MODFLOW's River Package was updated.

Worksheets *Q* and *h* are set up very similarly to each other and contain what can be considered the output of the surface water model. The *Q* worksheet contains the river discharge at the 36 finite difference nodes, which are calculated using the linear explicit scheme described in Section 4.5. Similar to the *Par* worksheet, the columns of worksheet *Q* contain the river discharge by each river node shown in row 4. The inlet (or node 0) river discharge is stored in column D. During each day of the simulation, depending on the time-step specified by the

user, a column from one of the four inlet river discharges worksheets is copied into column D of the *Q* worksheet to provide the new boundary condition for that day of the simulation. Changes in the new inlet discharge create a wave that is propagated through the rest of the reaches via the kinematic wave equation. The *h* worksheet is directly linked to the *Q* and *Par* worksheets and calculates the river stages based on Manning's equation.

	A	B	C	D	E	F	G
1	<b>Time index</b>	<b>delt</b>	<b>time</b>				
2		<b>(s)</b>	<b>(days)</b>	<b>0</b>	<b>1</b>	<b>2</b>	<b>3</b>
3	0	180.00	0.000	47.71	47.66	47.66	47.57
4	1	180.00	0.002	47.71	47.69	47.67	47.58
5	2	180.00	0.004	47.71	47.71	47.68	47.60
6	3	180.00	0.006	47.71	47.73	47.69	47.62
7	4	180.00	0.008	47.71	47.75	47.70	47.64
8	5	180.00	0.010	47.71	47.76	47.71	47.65
9	6	180.00	0.013	47.71	47.78	47.72	47.67
10	7	180.00	0.015	47.71	47.79	47.73	47.69
11	8	180.00	0.017	47.71	47.80	47.74	47.70
12	9	180.00	0.019	47.71	47.81	47.76	47.72

Figure 4.15 A Section of the *Q* Worksheet

### Output Worksheets

Three worksheets contain the output of the dynamically linked surface and groundwater models. The river discharge and river hydraulic head are recorded in the *riv\_head* and *flowrate* worksheets, respectively. The *aq\_heads* worksheet contains the aquifer heads from in Cross Sections 1 and 2, as well as the river leakage rates for Reaches 14, 27 and 28 and the total river leakage for all 35 reaches being modeled.

## **CHAPTER 5: VISUAL BASIC INTERFACE**

### **5.1 Introduction**

The Visual Basic interface (called the “Interface” for the remainder of this document) was created inside the Visual Basic editor of Excel. The purpose of the Interface is to act as the dynamic link between the MODFLOW model and the Excel-based surface water model. More specifically, the Interface elicits input from the user, transfers data between the two models and executes each model in a cyclic fashion. The Interface also writes the river hydraulic heads, the aquifer hydraulic heads in the two cross sections of the aquifer, and the river discharge to three output worksheets in the “Kinematic8.xls” Excel file. Visual Basic was chosen as the programming language of the interface because of its compatibility with Excel; Excel uses Visual Basic to perform many of its commands.

Section 5.2 gives an overview of the capabilities of the Interface. In Section 5.3, the basic structure of the Interface’s programming code is described. Section 5.4 discusses some of the format requirements for the MODFLOW packages. In conclusion, possible methods to improve the interface performance are discussed in Section 5.5.



## 5.2 Overview

On a very general level, the function of the Interface can be broken down into three main objectives, as depicted in Figure 5.1: reading input, dynamically linking the models and writing output.

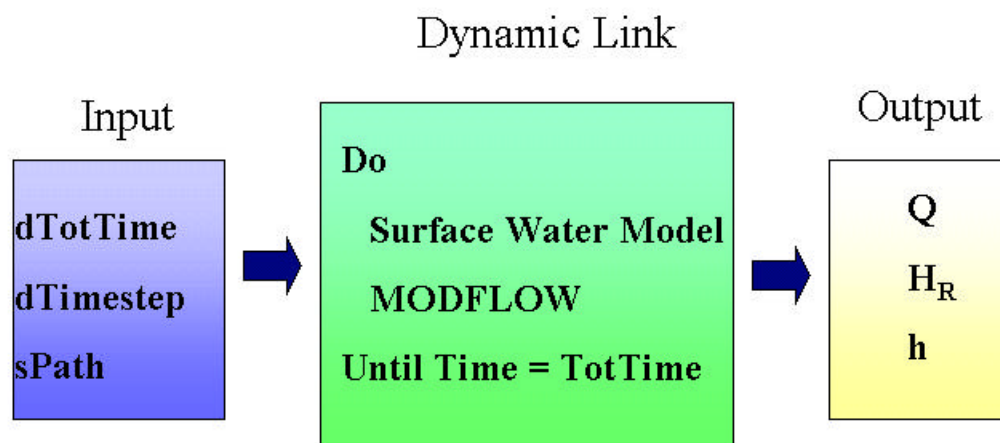


Figure 5.1 Schematic of the Three Main Functions of the Interface

### 5.2.1 INPUT

The input to the Interface is entered by way of a Visual Basic form called "frmInput", shown in Figure 5.2. The variable names, shown in the Input box of Figure 5.1, store the user-defined values that are entered through "frmInput". In order to stay within programming conventions, single letters (such as the "d" in **dTotTime**) were used as prefixes to variable names to indicate the variable type

of each variable. The letter "d" and "s" designate double precision and string variable types, respectively.

The first of the three user-specified variables is **dTotTime**, the total simulation time of the dynamically linked models. Although, river discharge data exists for 32 days of simulations, the length of the simulation is still kept as a user-defined variable for added flexibility. Should any simulations that involve more or less days of data be investigated, the user would be able to change this variable without having to change the Interface code. This feature was also extremely helpful during the debugging of the Interface code, when a number of shorter simulations were run to determine if certain portions of the model were working correctly.

Next, "frmInput" asks for the user to designate a time-step for the simulation via the variable **dTimestep**. Since the surface water model only contains values for four time-step averaged inlet discharge worksheets (*inlet2*, *inlet4*, *inlet8* and *inlet 16*), the Interface only simulates flood waves for **dTimestep** equivalent to 2, 4, 8, and 16 days. All other time-steps result in groundwater/surface water simulations under non-flood wave conditions.

Finally, the input form asks the user for the pathname of a folder "modflow" that contains the following: the surface water model ("Kinematic8.xls"), the MODFLOW-96 executable and the individual MODFLOW packages. The pathname of the folder entered by the user is stored in the variable **sPath**.

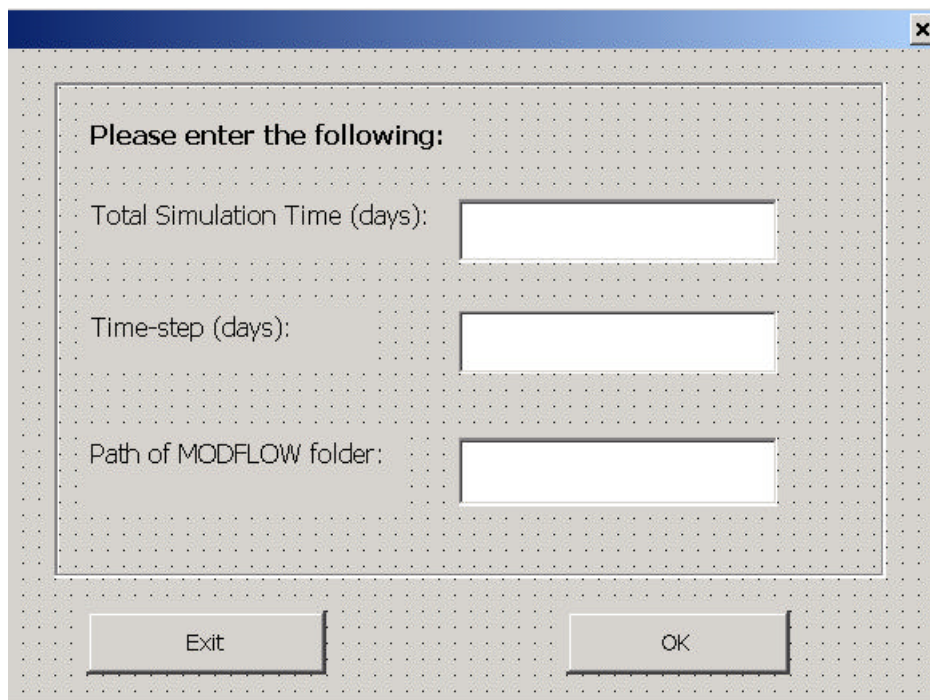


Figure 5.2 "frmInput" Asks the User for Input into the Visual Basic Interface

### 5.2.2 DYNAMIC LINKAGE

The second capability of the interface is its main function, namely, dynamically linking the two models. This subject will be covered in much more detail in the following section, but will be simplified to provide a quick overview here. The dynamic linkage can be thought of as one large loop. The surface water model is run first with its updated aquifer inflow rates and inlet river discharge, followed by MODFLOW with its updated river hydraulic heads. After each time the MODFLOW is run, the output is written to the three output worksheets. The loop is repeated until the total simulation time entered in by the user, or **dTotTime** is reached. At this time the interface ends the Visual Basic program, leaving the output of the models stored in the three output worksheets.

The surface water model isn't run in the conventional sense, but because the cells in the  $Q$  worksheet are linked to the cells in the aquifer lateral inflow ( $qa$ ) worksheet, the updated  $q_a$  and inlet discharge values automatically result in new river flowrates and new hydraulic heads. The MODFLOW program was run conventionally, although attempts to automate this function in the interface were unsuccessful due to compiler incompatibility. This topic is discussed in more detail in Section 5.5.

### 5.2.3 OUTPUT

The last capability of the interface is the writing of the output of the MODFLOW and surface water models to the three output worksheets. The output worksheets are updated after each model is run. The river's discharge and hydraulic heads are fairly easily copied from the  $Q$  and  $qa, h_{fix}$  worksheets, and pasted into the *flowrate* and *riv\_head* sheets, respectively. The MODFLOW output, however, is more difficult to extract. Manipulating MODFLOW's listing file, where all printed output is written, has two challenges. As described in Chapter 3, depending on what was indicated in the Output Control package, the length of MODFLOW's text output or listing file can vary. For instance, the Output Control Package can determine whether the starting aquifer heads are printed or not printed to the listing file, thus changing the location of the aquifer heads that are to be extracted within the file. To allow for flexibility in the listing file format, the "Find" capabilities of Excel were employed to locate key words in the listing file, which would indicate the location of the aquifer heads of interest.

The aquifer heads cells were then referenced from the row containing the key words.

The second challenge in extracting the MODFLOW aquifer heads of the Colorado River Package cells, lay in the format of the output file, known as the listing file. MODFLOW -96 formats the listing file so that each row in the domain would fit onto an 8 1/2" by 11" paper when printed. Therefore, though River Package cells were next to each other in the domain, they were rows apart in the listing file. To overcome this problem, a sub-procedure named "makegrid" was written to convert the output file back into the domain grid format. This sub-procedure, along with others, is described in the following section.

### **5.3 Structure**

The Interface contains two main procedures and nine sub-procedures. The two main procedures result from clicking either the OK or Exit buttons located on bottom of the "frmInput" form. If the Exit button is clicked, the "cmdExit\_click" procedure is called, which ends the Visual Basic program. Alternatively, clicking the OK button calls the "cmdOK\_click" procedure that proceeds to run the dynamic link.

To modularize the dynamic linking process, nine sub-procedures were created to perform the separate tasks within the "cmdOK\_click" procedure. These sub-procedures are described in Table 5.1. Figure 5.3 provides a flow-chart to show how the sub-procedures are organized to perform the dynamic linkage.

**Table 5.1 The Nine Sub-Procedures That Constitute the "cmdOK\_Click" Procedure**

<b>Sub-procedure</b>	<b>Function</b>
Initialize	Clears output sheets and initializes the river leakage rates and river discharges
Surface_Run	Sets new inlet river discharges as the upper boundary condition for one day simulation
Outputsheet	1. Runs Surface_Run for the number of days in iTimestep 2. Copies the river flowrate and hydraulic heads into the <i>flowrate</i> and <i>riv_head</i> sheets
Rename	Copies the binary file containing the heads at the end of one MODFLOW run to the binary file containing the initial heads for the next MODFLOW run
Open_Bas	Enters the new time-step of the MODFLOW run into Basic Package
Open_Riv	Updates river hydraulic heads in River Package
Run_MODFLOW	Runs MODFLOW-96 executable
Output_qa	1. Extracts aquifer heads from MODFLOW's listing file and pastes into the <i>aq_head</i> worksheet using "Makegrid" and "Outputhead" sub-procedures 2. Extracts river leakage rates for each of the 35 River package cells from MODFLOW's listing file
Makegrid	Reformats aquifer heads in the MODFLOW listing file to resemble the domain grid
Outputhead	Extracts aquifer heads underlying Colorado River from the MODFLOW listing file

The Visual Basic code corresponding to each sub-procedure can be viewed in Appendix B.

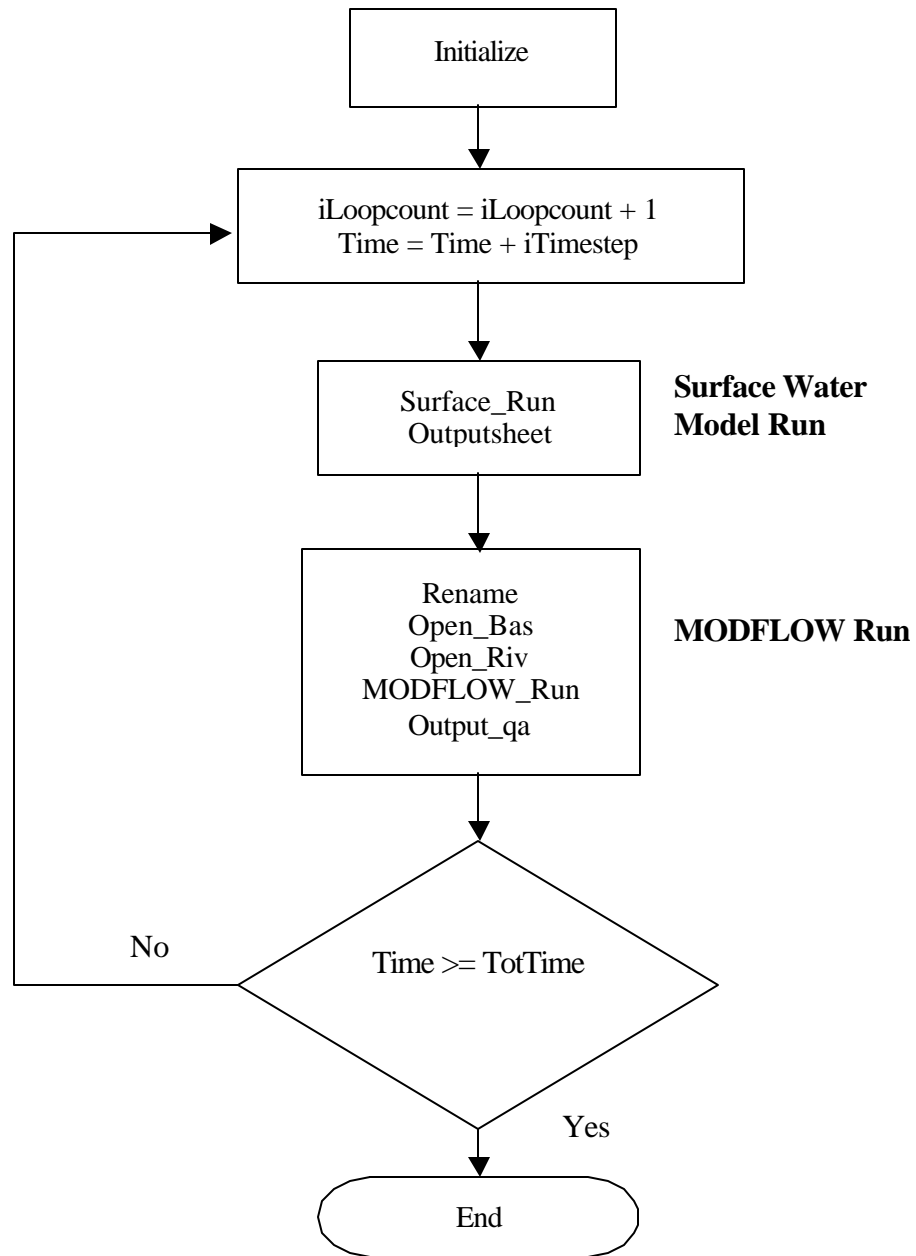


Figure 5.3 Flowchart of the "cmdOK\_click" Procedure

## **5.4 Formatting of MODFLOW Files**

The formatting of the MODFLOW input files is crucial to the performance of the interface. Even with the free format option offered in the Basic Package, MODFLOW-96 can only read space and comma delimited files. The two files that are opened and saved in Excel during the coupled-model run are the Basic and River packages. Due to its large array of numbers, the Basic Package would not save properly with the space-delimited format and therefore was saved using the comma-delimited format. To stay consistent with the Basic Package formatting, the River Package was also saved as a comma-delimited file. The format of the MODFLOW files must be strictly adhered to because the Interface opens the file in Excel with these two formats incorporated in the code.

## **5.5 Interface Enhancement**

There are several changes that would enhance the performance of the Interface. These changes are described in the following sections.

### **5.5.1 AUTOMATION OF MODFLOW RUN**

The interface was unable to automate the process of running the MODFLOW executable. This limitation is in part due to the structure of MODFLOW's source code. Once MODFLOW is run by the Interface, a window emerges asking the user to enter in the name of the Name file of the model of interest. As described in Chapter 3, the Name file contains a list of the names of



the different packages that are used during the simulation. Attempts to automate the process of typing in the name of the revised BEG model's Name file (cw409\_s2.nam) were unsuccessful. Therefore, the user is required to manually enter in the name of the Name file into MODFLOW after each time MODFLOW is run.

One way of overcoming this problem would be to change MODFLOW's source code to automatically search for the Name file and recompile. This approach was not taken because of the compiler-related errors that were anticipated to occur. The format of the files had been adjusted to be compatible with the Lahey compiler used by the USGS in its downloadable executable. However, the only FORTRAN compiler available for this work was the Microsoft Power Station FORTRAN compiler, which most likely would have been incompatible with some of the input files and function calls.

### **5.5.2 EFFICIENCY**

The surface water model portion of the dynamic linkage was significantly longer in execution time than the MODFLOW model. Two processes contributed to the relatively long computation time of the coupled programs. The first was the Excel-based explicit solution. Due to the Courant condition, the explicit solution requires smaller surface water time-steps than what is required by the implicit solution. These smaller time-steps, in turn, result in a longer surface water model run-time.

The "makegrid" sub-procedure also hindered the efficiency of the Interface. This procedure changes the format of MODFLOW's output file to a

format resembling the domain grid. Although the procedure made it easier to extract the aquifer heads of interest and to subsequently check if the correct aquifer heads had been extracted, it significantly decreased the efficiency of the model.

## CHAPTER 6: RESULTS

### 6.1 Introduction

As described in Chapter 4, in order to investigate the aquifer's response to changing river heads, a flood wave was simulated to pass through the modeling domain. The influence of time-step on the river and aquifer interaction was explored by averaging the river discharge at the upper boundary of the modeling domain for 2, 4, 8 and 16-day time-steps. The daily streamflow data from USGS gage 8160400 was averaged over the time-step prior to being used as input into the surface water model. The river heads produced at the end of the surface water model run were subsequently used to update MODFLOW's River Package.

The changes in river discharge and aquifer hydraulic heads, as a function of the time-step, are discussed in this chapter. Section 6.2 investigates the spatial variation in flowrate along the length of the river. Next, discussions of the changes in aquifer head in Layer 1 and Layer 2 are presented in Sections 6.3 and 6.4, respectively. Section 6.5 presents the trend observed in river leakage rates as a function of time-step. Finally, Section 6.6 discusses the appropriate approximation of the Saint-Venant equation, should flood waves not be considered in future simulations.

## **6.2 Spatial Variation in River Reaches**

As seen in Figure 6.1, the inlet discharge was the main component in dictating the flowrates throughout the 35 reaches. During each of the three 2-day time-steps shown in the figure, all 36 finite difference nodes experienced approximately the same river discharge. This is not surprising, considering the time it takes any change in inlet flowrate to transverse all 35 reaches ranges between approximately 0.5 and 2.0 days. These values were calculated by summing up the wave travel times for each river reach under the maximum and minimum inlet river discharges of the 2-day time-step simulations, respectively. Therefore, even the 2-day time-steps were often too long to capture any transitions the downstream reaches were experiencing due to the changes in inlet flowrate.

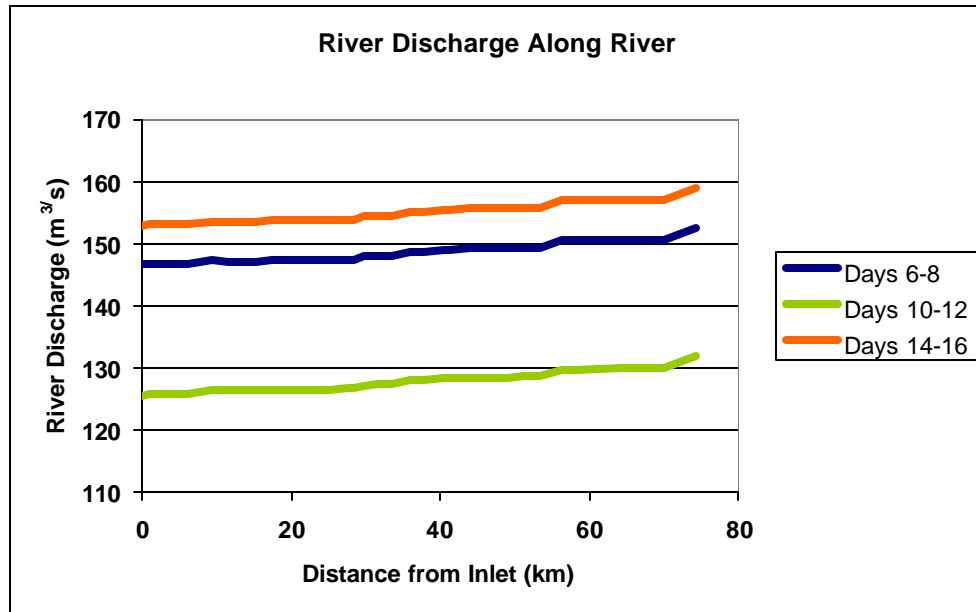


Figure 6.1 River Discharge Along the Colorado River During Three 2-Day Time-Steps

The small increase in the discharge along the river is caused by the lateral inflow terms,  $q_a$  and  $q_r$ . The aquifer lateral inflow ( $q_a$ ) can be either positive or negative depending on the river flowrate, while the runoff lateral inflow ( $q_r$ ) is constant throughout the simulation and remain positive. A comparison of the summation of the  $q_a$  and  $q_r$  terms for the 35 reaches revealed that the range of the lateral aquifer inflow is between two to three magnitudes smaller than the runoff inflow. The runoff flow ( $q_r$ ) of the 74.4 km. stretch of the Colorado River being modeled was held at a constant rate of  $8.3 \text{ E-}5 \text{ m}^2/\text{s}$  for the total simulation time. The absolute average of the aquifer lateral inflow ( $q_a$ ) for that same stretch of river was  $1.3 \text{ E-}6 \text{ m}^2/\text{s}$  and  $2.0 \text{ E-}7$  for the 2-day and 16-day time-steps, respectively. The average aquifer lateral inflow ( $q_a$ ) resulting from the steady-

state analysis conducted prior to the 32-day simulations was calculated to be  $9.3 \times 10^{-8} \text{ m}^2/\text{s}$ . The river head resulting from the  $q_a$  induced changes in the flowrate are therefore significantly smaller when compared to those induced by the  $q_r$ . Furthermore, both lateral inflow terms are significantly less influential than the changing inlet river discharge. Therefore, apart from providing insight to the amount of water that was transferred between the two systems, the aquifer lateral inflow had little effect on the river discharge.

The overlapping graphs presented in Figure 6.2 show a different interpretation of the same results. The different river nodes in Cross Sections 1 and 2 corresponding to Reaches 14 and 27, shown in Figure 4.7, experienced almost identical changes in river discharge as a function of time. Consequently, similar trends were observed in the river heads and the aquifer heads in both cross sections. For the sake of brevity, only the results from the analysis of Cross Section 1 will be discussed in this chapter. However, it can be inferred that all of the trends that pertain to Cross Section 1 were also observed in Cross Section 2. The results of the simulations for Cross Sections 1 and 2, as well as the Colorado River, are presented in Appendix C

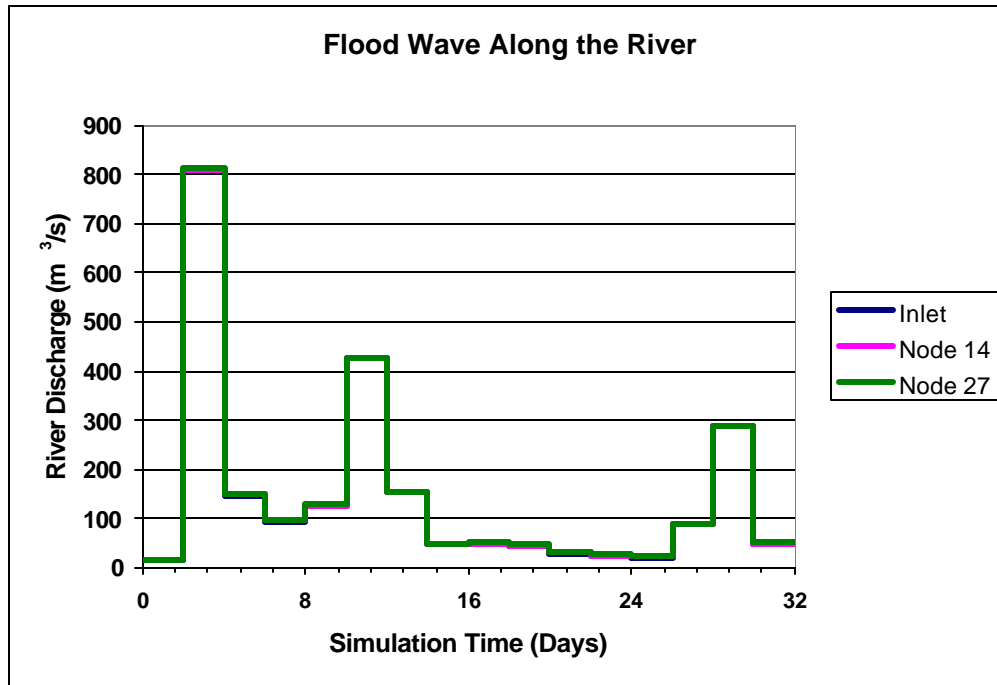


Figure 6.2 River Discharge as Function of Simulation Time at Three Locations Along the River.

### 6.3 Aquifer Head in Layer 1

Although the simulations provided results for the eighteen cells comprising Cross Section 1, the results from six cells, in particular, are presented in this section. Figure 6.3 shows the location of the three cells in Layer 1 of Cross Section 1. The other three cells are located in Layer 2 of the MODFLOW model, as shown in Figure 6.4. All three cells have roughly the same width, ranging from 1 mile for the cell containing Reach 14 and its neighboring cell, to 1.25 miles for the cell two away from Reach 14.

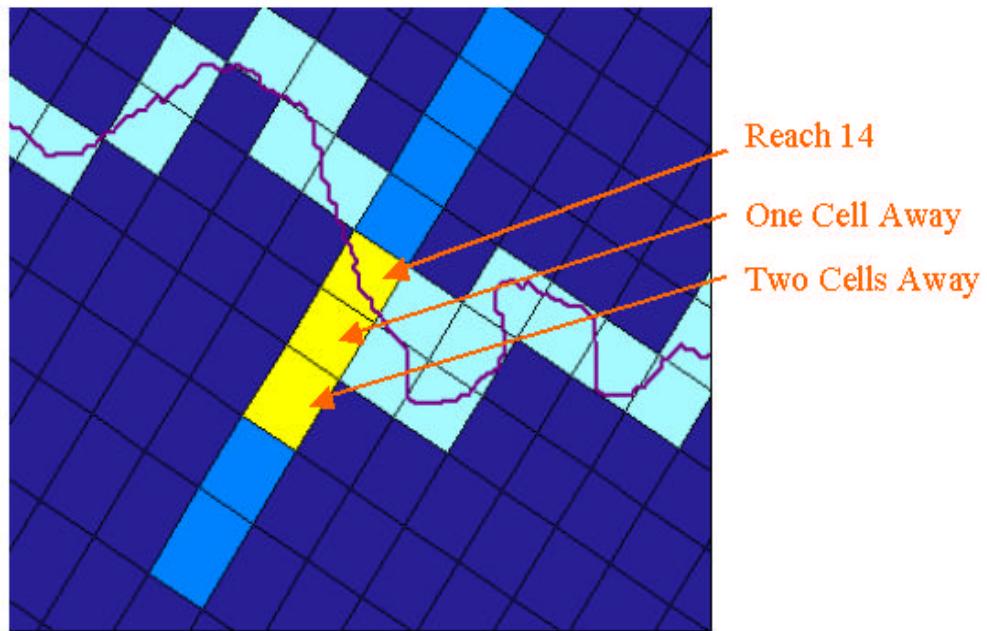


Figure 6.3 Location of Selected Cells in Cross Section 1

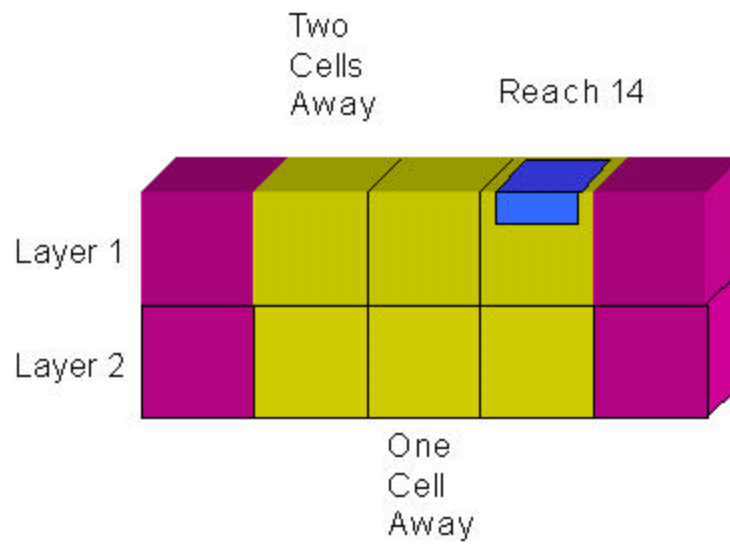


Figure 6.4 3-Dimensional View of the Selected Cells in Each Layer of Cross Section 1



### **6.3.1 EFFECT OF TIME-STEP**

The amplitude of the fluctuations in the river and aquifer head is a function of the time-step used in the simulation. Figure 6.5 presents the changes in the aquifer head in the Reach 14 River Package cell for three of the four time-steps. During the 2-day time-step simulation, the aquifer head below Reach 14 increased to 108 ft. during the first peak discharge in the river. However, the results of the 16-day time-step simulation show that the aquifer in the same cell increased to only 88 ft. during that period. Therefore, fluctuations in both the river and aquifer heads were observed to decrease with an increasing time-step. This result can be attributed to the fact that larger time-steps average over the peak discharges and consequently, by Manning's equation, the river hydraulic heads. Since the river head is the driving force for any changes in the aquifer in the vicinity of the river package cells, reductions in the variability of the river heads as a result of longer time-steps produce smaller head changes in the aquifer.

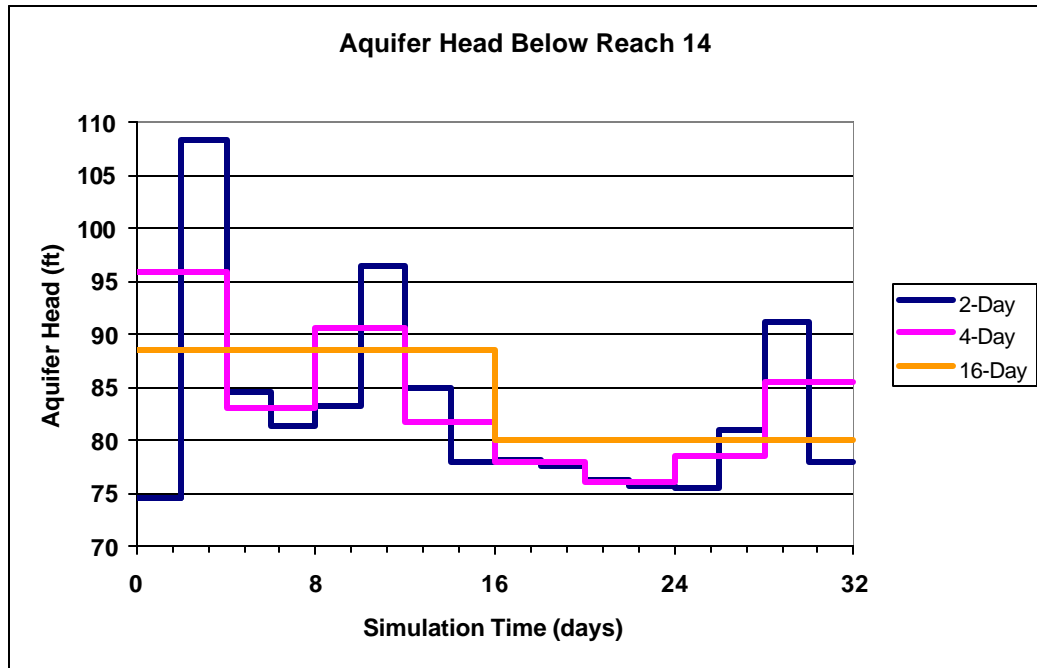


Figure 6.5 Changes in Aquifer Head in the Cell Containing Reach 14

### 6.3.2 EFFECT OF DISTANCE FROM RIVER

The spatial variability in the aquifer's response to the flood wave was examined by analyzing the aquifer heads in Cross Section 1. Figure 6.5 presents the aquifer heads corresponding to the three cells in Layer 1. Although, not shown here, the changes in river head in Reach 14 as calculated by the surface water model, is identical to the aquifer head below Reach 14. Therefore, during each interface time-step, the MODFLOW model allowed the aquifer head in the River Package cell to come into equilibrium with the newly calculated river head. It should be noted that this result is influenced by the hydraulic conductivity of the riverbed. The ease with which water is exchanged between the aquifer and river systems depends on the assumptions made regarding the texture of the

riverbed material. As noted in Chapter 3, the hydraulic conductivity chosen for this study was determined to be characteristic of silt or loess soils and therefore deemed suitable. However, since assumptions were made regarding the hydraulic conductivity and the riverbed thickness, both of which contribute to the riverbed conductance, a sensitivity analysis of the river conductance term is recommended for any future research of this system.

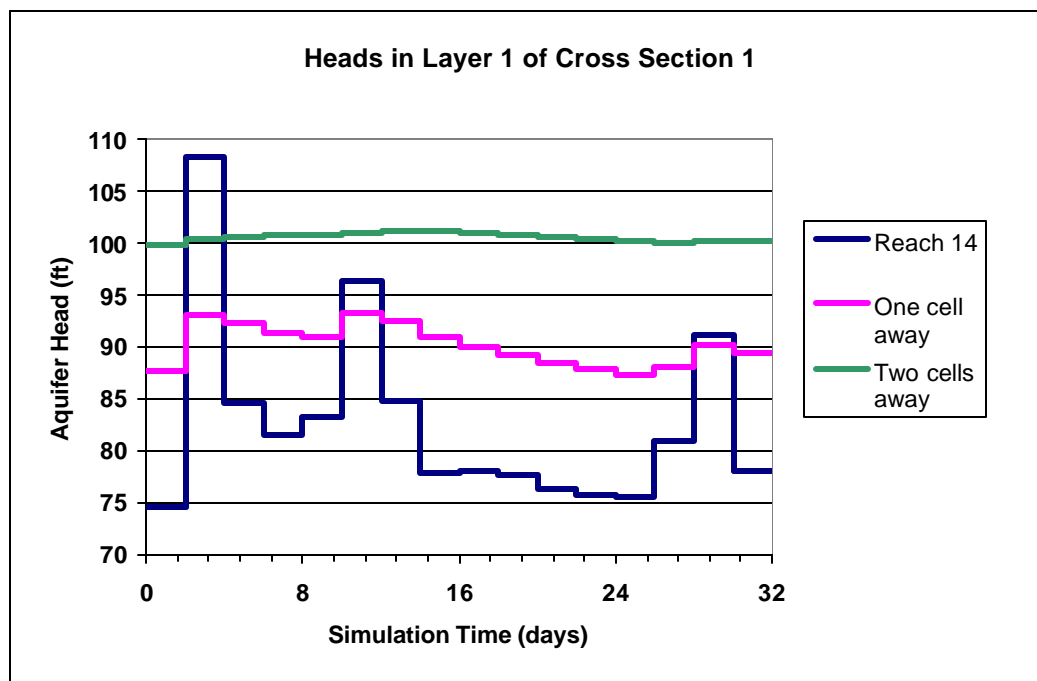


Figure 6.6 Aquifer Heads in Layer 1 of Cross Section 1 Using a 2-Day Time-Step

Two observations can be made regarding the aquifer heads in Cross Section 1 as shown in Figure 6.6. The first is that the fluctuations in aquifer head diminish as the distance from the river increases. The aquifer cells neighboring Reach 14 show less dramatic changes in aquifer head as a result of the flood wave

in the river than those observed in the Reach 14 River Package cell. For the 2-day simulation, the aquifer head fluctuations in the Reach 14 cell and those in one cell and two cells away from Reach 14, show a range of approximately 30 ft., 7 ft., and 1 ft., respectively. Therefore, the wave in Layer 1 of the aquifer appears to dampen or attenuate as it flows away from the river.

The second observation is that cells farther from the river display a lag in response time to the changes occurring in the river. Unlike the immediate response seen in the aquifer head in the cell containing the river reach, the head fluctuations in the neighboring cells were slower to respond to the oscillations in the river. Figure 6.6 shows that there was only one peak in the cell located two cells away from Reach 14, which occurred approximately 8 days after the initial peak in river discharge. The simulation time appears too short to fully capture the cell's response to the two subsequent peak discharges.

In conclusion, aquifer heads situated farther from the river appear to fluctuate less and respond more slowly than those directly below the river.

## **6.4 Aquifer Head in Layer 2**

The aquifer heads in Layer 2 shows a different response pattern than those in Layer 1. Changes in aquifer head in Layer 2 in the three selected cells of Cross Section 1 are presented in Figure 6.7. Due to the barrier imposed by the semi-impermeable layer separating Layers 1 and 2, the range in head fluctuation is considerably smaller than those observed in Layer 1. As shown in the figure, the head changes in Layer 2 are on the order of inches. In addition, unlike the heads

in Layer 1, the Layer 2 heads neighboring Reach 14 do not show any lag time in responding to the flood wave. It should be noted that there is a hint of a lag time seen in Layer 2, in the cells three and four cells away from the river reach. However, this lag time is much less dramatic than what is observed in Layer 1. Furthermore, the heads in Layer 2 display very little wave dampening away from the river. All three cells in Figure 6.7 show a similar range in head fluctuation.

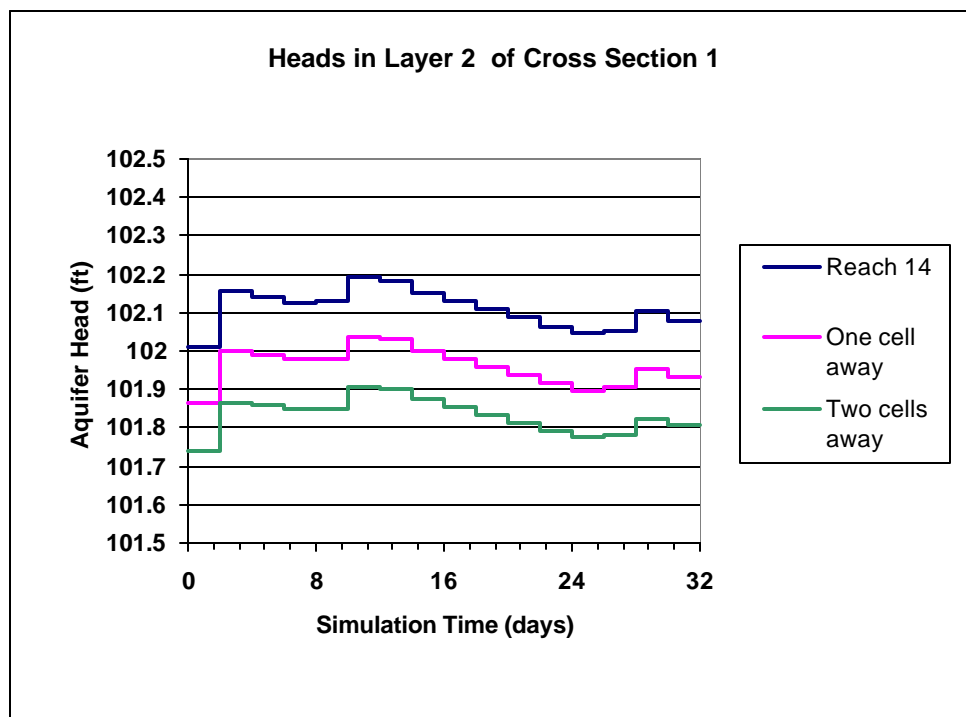


Figure 6.7 Aquifer Heads in Layer 2 of Cross Section 1 Using a 2-Day Time-Step

## **6.5 River Leakage Rates**

The river leakage rates for Reach 14 and the segment of the Colorado River in the modeling domain are presented in Figures 6.8 and 6.9. As seen in the figures, there is a positive correlation between river discharge and river leakage rate. The peak discharges correspond to the peak river leakage rates. This is evident from Darcy's Law in which higher river hydraulic heads produce higher leakage rates. The peak discharge values were significant enough to change the segment of the river being modeled from a gaining stream to a losing stream. The figures are presented in units of  $\text{m}^3/\text{s}$  to provide a comparison of the leakage rates and the river discharge. Therefore, for a  $1033 \text{ m}^3/\text{s}$  river discharge, the leakage rate for the 74.4 km stretch of the Colorado River was less than  $0.50 \text{ m}^3/\text{s}$ . These results are based on the initial head in the aquifer, the hydraulic conductivity of both the riverbed and Layer 1, as well as other factors.

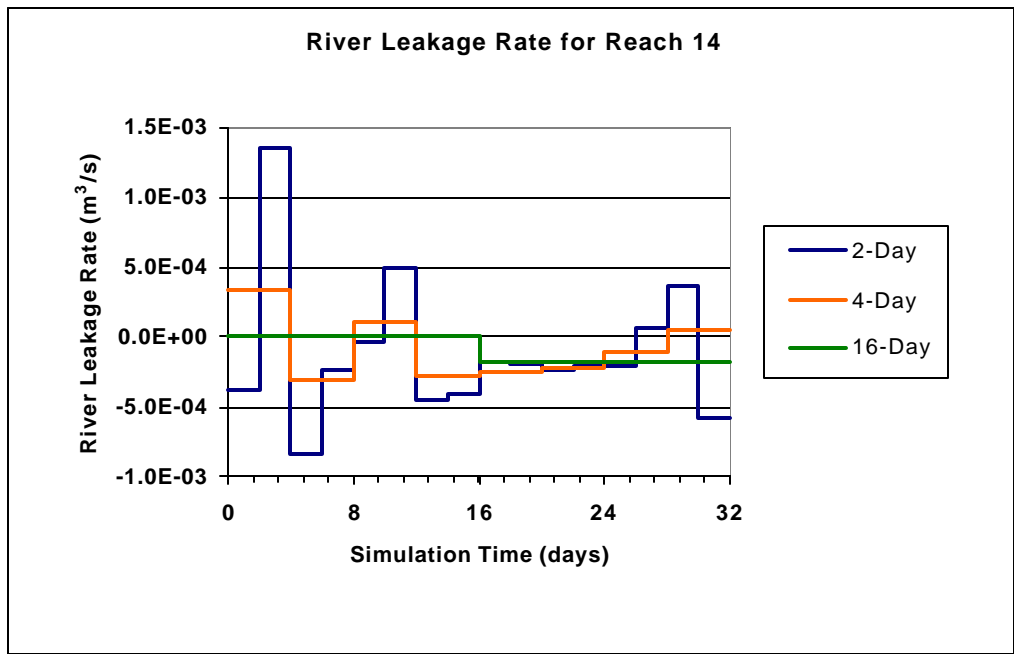


Figure 6.8 River Leakage Rate in Reach 14 Using Three Different Time-Steps

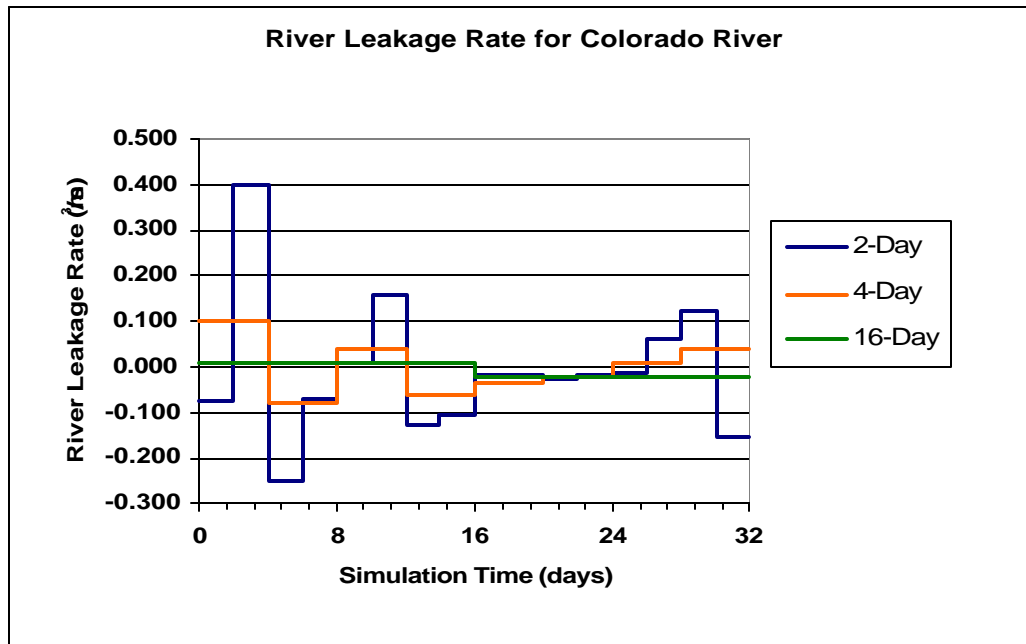


Figure 6.9 Sum of River Leakage Rates for All 35 Reaches Using Three Different Time-Steps

Interestingly, the minimum river leakage rate did not result from the lowest river discharge. In fact, the 2-day and 4-day time-step simulations, show the lowest river leakage rates (i.e. the highest amount of baseflow to the river) occurred right after the peak discharges. Figure 6.10 shows the aquifer head change across Cross Section 1 in Layer 1 as a result of the flood wave. The x-axis of the figure is the distance in miles from Reach 14. Negative distances denote that the cells are located west of the river reach (or left in Figure 6.3). The cell containing Reach 14 is therefore at the intersection of the two axes. The head gradient under the initial condition shows that groundwater is typically recharging the Colorado River. During the first peak discharge (during days 2-4) the head gradient is inverted, causing the Reach 14 to change from a gaining stream to a losing stream. However, once the first wave had passed, (during days 4-6) the piezometric head profile resumed its original gradient towards the river. The negative river leakage rates following the peak discharge indicate that the water that was leaked from the river during the peak discharge returned to the river as baseflow due to the return of the piezometric head surface to its original profile.



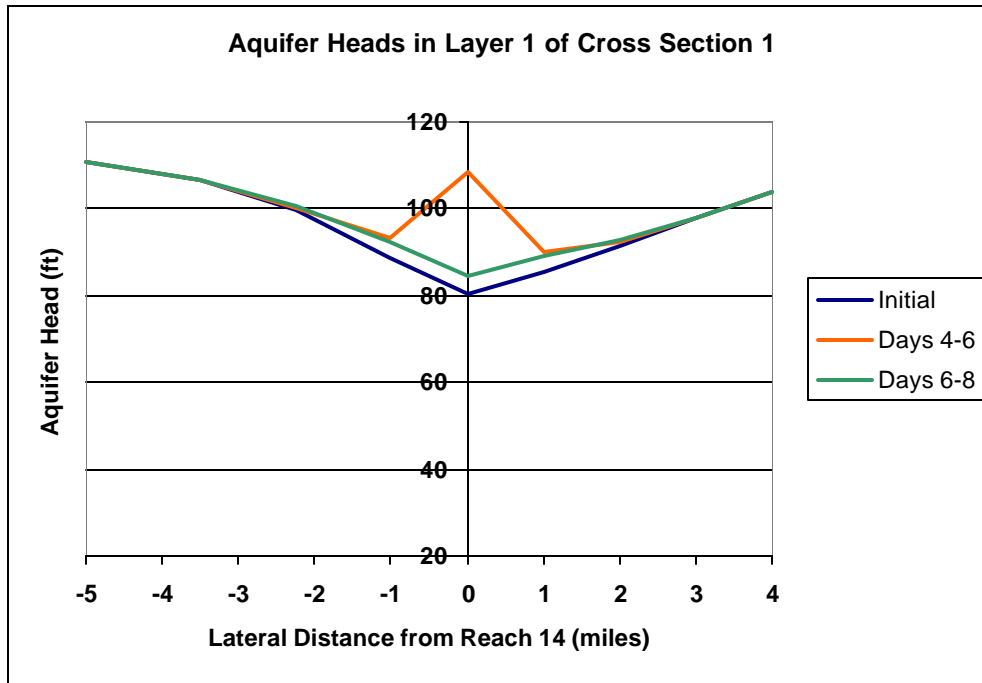


Figure 6.10 Aquifer Heads in Layer 1 of Cross Section 1

The total volume of surface water lost to the aquifer as leakage during the 32-day simulations is presented in Table 6.1. These values were calculated by summing the river leakage rates, as determined by MODFLOW, over the 32-day total simulation time. The amount of water exchanged was examined for three segments of the Colorado River: Reach 14, Reach 27 and the entire segment of Colorado River being modeled in this study. The table presents values for the volume of water exchanged between the two systems based on 2, 4, 8 and 16-day time-steps. The volume exchanged is reported in the same units used by the revised BEG MODFLOW model, namely cubic feet.

Initially, it appeared as if for each simulation and averaging method, the minimum gain to the river occurred using a time-step of 4 days. This trend was

difficult to decipher. On further investigation, it became apparent that the third peak occurred right before the end of the 32-day simulation. Therefore, for time-steps greater than 2 days, it was possible that the response of the aquifer to the third peak was not able to be determined because the simulation came to an end. To rectify the possibility of the end of the simulation affecting the results, the sum of the river leakage rates for the 35 reaches was examined over the first 8, 16, 24 days of the simulations, before the occurrence of the third flood wave peak. These values are presented in Table 6.2 along with the results of the 32-day simulation.

**Table 6.1 Volume of Groundwater Flow Entering into the Colorado River over the 32-Day Total Simulation Time**

Time-Step (days)	Volume of River Leakage (ft <sup>3</sup> )		
	Reach 14	Reach 27	Total
2	-10115	-3617	-691848
4	-7770	1011	-181978
8	-8016	64.5	-404740
16	-8368	-905	-576911

A comparison of the different values in Table 6.2 indicates that a pattern may exist between time-step and the volume of water exchanged between the river and aquifer. Although seemingly anti-intuitive, the results show that baseflow to the river increases (or river leakage rate decreases) with a decreasing time-step. Prior to obtaining these results, it had been hypothesized that the smaller time-steps would capture higher peak flows and therefore would result in an increase in river leakage. Assuming that the results accurately model what occurs in the aquifer, these results point toward the importance of the initial piezometric heads of the aquifer in affecting the river leakage. As described above, there is a large influx of groundwater into the river in the time-step after the peak discharge. The high baseflows that occur after the peak discharges,

which are the most evident during the 2-day time-step simulation, may be the factor that causes the trend in the volume of water leaked. Therefore, along with other parameters, the initial piezometric head profile may be worth investigating. If the initial head gradient was away from the river, possibly due to well pumping, water leaked from the river under high river discharge will most likely not return to the river. Therefore, the trend observed in the volume of water exchanged between the two systems under a losing stream scenario, may be different than what was observed in the gaining stream scenario presented here.

**Table 6.2 Volume of Water Leaked from River During the First 8, 16, 24 and 32 Days of Simulation**

	<b>Volume of Leakage from 35 Reaches</b>			
	<b>(ft<sup>3</sup>)</b>			
	Simulation Time (days)			
Time-Step (days)	8	16	24	32
2	45652	-351852	-813655	-691848
4	119198	-48947	-765617	-181978
8	713439	328280	-657081	-404740
16	--	461068	--	-678925

However, due to the preliminary nature of these results, it is important to determine whether what is being modeled is actually what is occurring in aquifers under similar stresses. One possible explanation of the results may be that there is either an error or inaccuracy in the modeling systems. This could be an error in

how the two models are linked, in which case the output of another coupled modeling system (such as MODFLOW-SURFACT or MIKE-SHE) would need to be provided for comparison. Another possibility is that the models are working properly, however, basic assumptions in either the MODFLOW or surface water model create an inaccuracy. This inaccuracy may be compounded by the number of model runs or may be exacerbated by high river discharge. Two possible assumptions that could be the cause of the inaccuracies are the use of Darcy's Law in modeling the river and aquifer interaction and the riverbed slopes used in Manning's Equation. Both of these assumptions fall in the latter category of becoming increasingly inaccurate with higher surface water flowrates. To determine if these assumptions are creating inaccurate results, these results would need to be compared to observational data gathered from wells near the river during a similar flood wave.

Therefore, before the results are assumed correct, the dynamically linked models must be validated.

## **6.6 Approximation of the Saint-Venant Equations**

Future investigations of the aquifer river interaction in this study area may wish to include simulations that are not influenced by flood waves. In Chapter 2, the criteria presented by Vieira (1983) in determining the appropriate approximation to the Saint-Venant equations when modeling lateral inflow were discussed. In order to determine the correct wave routing method under a non-flood wave condition, the two governing parameters of the criteria,  $\mathbf{k}$  and  $\mathbf{F}_0$  were

calculated for the dynamically linked models used in this study. The equations pertaining to the two parameters are presented in Equations 2.3.1 and 2.3.2 and again here as 6.6.1 and 6.6.2. Equation 6.6.3 defines the Chezy coefficient in terms of Manning's roughness coefficient.

$$k = \left( \frac{g^3 L \sin \boldsymbol{q}}{C^4 q^2} \right)^{1/3} \quad (6.6.1)$$

$$F_o = C \left( \frac{\tan \boldsymbol{q}}{g} \right)^{1/2} \quad (6.6.2)$$

$$C = \frac{R^{1/6}}{n} \quad (6.6.3)$$

where,

k = kinematic wave number

g = gravitational acceleration [L<sup>2</sup>/T]

L = length of river reach [L]

θ = constant angle of the slope

R = hydraulic radius [L]

q = lateral runoff [L/T]

n = Manning's equation

F<sub>o</sub> = Froude number

The initial conditions of the river, resulting from the coupled model calibration, were used in calculating the two governing parameters. Furthermore,

the 35 separate reaches were modeled as one unit. Therefore, the average initial stage in the river was used in calculating the hydraulic radius,  $R$ . The slope was determined by calculating the elevation drop between the upstream and downstream ends of the river, and by dividing by the river length. Due to the order of magnitude difference between the aquifer lateral inflow ( $q_a$ ) and the runoff lateral inflow terms ( $q_r$ ),  $q_a$  was neglected when calculating both  $k$  and  $F_o$ .

The resulting  $F_o$  and  $k$  values were 0.090 and 22.9, respectively. The flow in the river is therefore subcritical flow. According to the criteria published by Vieira, these values indicate that lateral inflow into a river under non-flood conditions, should be modeled using the diffusive approximation. Therefore, the diffusive wave equation will be required for any further studies of the aquifer and river interaction in the study area under a steady-state upper boundary condition.

## **CHAPTER 7: CONCLUSIONS**

### **7.1 Introduction**

This chapter presents a summary of the results of the dynamic linkage of a groundwater and surface water model. Section 7.2 discusses the methodology used to meet the research objectives outlined in Chapter 1. Section 7.3 presents a discussion on the different software issues that became evident in linking the two models. A summary of the results of the time-step simulations is presented in Section 7.4, while recommendations for future research are presented in Section 7.5.

### **7.2 Objectives**

The following methodologies were used to meet the three research objectives discussed in Chapter 1:

- The first objective was to create a physically distributed surface water model of the Colorado River. The model consisted of 13 Excel worksheets and used the kinematic wave equation and Manning's equation in succession to determine the change in hydraulic river head caused by lateral inflow and a transient upper boundary condition. The worksheets in the model include worksheets containing input inlet river discharges,



river parameters, kinematic wave and Manning's equation calculations as well as worksheets to store the output of the dynamically linked models.

- The second objective was to design the code for the interface that dynamically linked the models. In this project, the interface was written in the Visual Basic Language in the Excel Visual Basic editor. The interface was able to elicit input from the user regarding the time-step, run the surface water and groundwater models in an alternating fashion as well as write the output to worksheets in the Excel surface water model. Due to a lack of a Lahey FORTRAN compiler, the running of the MODFLOW model was not fully automated in this research.
- The effect of time-step in modeling the interaction between the groundwater and surface water systems was analyzed by simulating a flood wave through the Colorado River. The results of the simulation, however, are preliminary and need to be verified by a comparison with results produced by another surface water/ groundwater modeling system and with observed data in stream gages and aquifer wells located near the Colorado River. The preliminary results of the simulations are presented in Section 7.5.

## **7.3 Software**

In creating the dynamic linkage between the two models, there were observations made regarding the role and potential role for software in facilitating the dynamic linkage. Obstacles caused by using incompatible software were also encountered. These observations are discussed in the following subsections.

### **7.3.1 THE ROLE OF GIS**

A Geographic Information System (GIS) was used to assemble data for input into the surface water model, and can be useful in providing the data for MODFLOW's input files. Equally as important, the GIS provided a geographically referenced framework in which the surface and groundwater modeling domains could overlap. In this way, river reaches were created specifically to overlie MODFLOW's River Package cells. A GIS, therefore, allowed the interaction between the two physically distributed models to be location specific.

There were still some aspects of a GIS that can enhance the linkage of the two models, which were not fully utilized in this study. As a powerful visualization tool, a GIS can be used to present the results of the MODFLOW model. Although results from the MODFLOW simulations were not transferred into a GIS, future research can help determine the best way to view MODFLOW's results, by either grid (raster) or vector (polygon) coverages. In addition, new GIS software, such as Arc/Info 8.0, is Visual Basic compatible and would therefore be able to interact directly with the surface water and groundwater models. Consequently, the potential exists to automate some of the

processes that were accomplished manually for this project. These processes include determining river reach lengths, as well as the initial river discharge in the surface water model.

### **7.3.2 FORTRAN COMPILER**

This project also pointed to the importance of consistently using the same FORTRAN compiler if changes to the MODFLOW code are needed. Because of the possible incompatibility of the MODFLOW input files that would result by using a different FORTRAN compiler, the process of running MODFLOW was not fully automated.

## **7.4 Preliminary Results**

The results of the preliminary investigation into the effect of time-step in modeling groundwater and surface water interaction are presented in this section.

As expected the smaller time-steps were able to capture the large changes in surface water discharge with more accuracy. Therefore, the fluctuations in the river and aquifer systems were larger when using a small time-step.

The aquifer's responses to the flood wave in Layers 1 and 2 were different. In Layer 1, aquifer heads responded more slowly to the flood wave with greater distance from the river. Furthermore, the fluctuations in the aquifer head farther from the river diminished in size. Aquifer heads in Layer 2, however, did not display either a reduction in fluctuations or a lag time in responding to the flood wave as a function of distance from the river. Also, aquifer head fluctuations in Layer 2 were much smaller than those in Layer 1.

A possible trend was discerned between the amount of water exchanged and time-step when examining the first 8, 16 and 24 days of the simulation. The smallest time-steps showed the smallest amount of river leakage into the aquifer. However, the dynamically linked models need to be validated. Furthermore, with the limited number of short simulations that were conducted, it is difficult to determine whether this trend can be applicable over a longer period of time and for other flood scenarios.

Finally, an analysis of the lateral inflow and river characteristics indicated that the diffusive wave equation should be used in simulations that do not include the influence of a flood wave. Therefore, any future research may wish to change the surface water model to accommodate more diverse simulations.

## **7.5 Recommendations**

Future research of the Colorado River and the Carrizo-Wilcox aquifer may wish to consider the following recommendations:

- Modifying MODFLOW's FORTRAN code and compiling using a Lahey compiler to fully automate the dynamic linkage
- Conducting a sensitivity analysis of the results to the riverbed conductance used in MODFLOW's River Package and to the riverbed slopes used in Manning's equation
- Conducting simulations that exceed 32 days to assess whether the observed trend in river leakage rate is generally applicable

- Considering a losing stream initial condition in which the river leakage caused by a flood wave would not return to the river as baseflow in the time-step following the peak discharge
- Introducing a well field near the river to assess the possible decrease in streamflow caused by well pumpage
- Using the diffusive wave approximation because of its applicability under non-flood scenarios

## **Appendix A: Surface Water Model Data**

**Table A1. River Discharge in Nodes Resulting from GIS Analysis and Model Calibration**

Node	River Discharge (m <sup>3</sup> /s)		
	GIS Analysis	Surface Water Model Calibration	Dynamically Linked Model Calibration
0	65.70	77.30	77.30
1	65.75	77.35	77.35
2	65.82	77.42	77.42
3	65.86	77.46	77.46
4	66.38	77.98	77.98
5	66.39	77.99	77.99
6	66.41	78.01	78.01
7	66.46	78.06	78.06
8	66.58	78.18	78.18
9	66.59	78.19	78.19
10	66.61	78.21	78.21
11	66.62	78.22	78.22
12	66.63	78.23	78.23
13	66.64	78.24	78.24
14	66.79	78.39	78.40
15	66.80	78.40	78.40
16	67.16	78.76	78.76
17	67.31	78.91	78.91
18	67.35	78.95	78.95
19	68.01	79.61	79.61
20	68.04	79.64	79.65
21	68.38	79.98	79.99
22	68.41	80.01	80.01
23	68.47	80.07	80.07
24	68.49	80.09	80.09
25	68.53	80.13	80.14
26	68.54	80.14	80.14
27	68.61	80.21	80.22
28	68.64	80.24	80.25
29	69.77	81.37	81.37
30	69.79	81.39	81.39
31	69.89	81.49	81.49
32	70.02	81.62	81.62
33	70.03	81.63	81.64
34	70.05	81.65	81.66
35	71.88	83.48	83.49

Table A2. River Parameters in *Par* Worksheet

Node	Reach Length (m)	Distance from Inlet (m)	Reach Width (m)	Slope	<b>a</b>
0	0	0	76.2	1.71E-04	11.06
1	1120	1120	76.2	1.71E-04	11.06
2	2665	3785	76.2	1.19E-04	12.34
3	2445	6230	76.2	6.31E-05	14.93
4	3280	9510	76.2	1.28E-04	12.08
5	1890	11400	76.2	7.39E-05	14.24
6	1720	13120	76.2	7.76E-05	14.03
7	2260	15380	76.2	1.26E-04	12.12
8	2010	17390	76.2	6.95E-05	14.50
9	1990	19380	76.2	1.69E-04	11.10
10	1820	21200	76.2	3.84E-05	17.33
11	890	22090	76.2	7.84E-05	13.98
12	1120	23210	76.2	1.25E-04	12.17
13	1920	25130	76.2	1.03E-04	12.89
14	2550	27680	76.2	5.47E-05	15.58
15	710	28390	76.2	1.97E-04	10.61
16	1440	29830	76.2	9.70E-05	13.12
17	1860	31690	76.2	1.50E-04	11.51
18	1810	33500	76.2	1.54E-04	11.42
19	2540	36040	76.2	5.50E-05	15.56
20	1860	37900	76.2	7.51E-05	14.17
21	2490	40390	76.2	5.61E-05	15.47
22	1040	41430	76.2	1.34E-04	11.90
23	2450	43880	76.2	3.21E-05	18.29
24	1730	45610	76.2	4.54E-05	16.48
25	2600	48210	76.2	1.41E-04	11.72
26	970	49180	76.2	1.80E-04	10.90
27	2150	51330	76.2	6.50E-05	14.80
28	1930	53260	76.2	1.72E-04	11.05
29	3100	56360	76.2	8.12E-05	13.84
30	1870	58230	76.2	2.24E-04	10.21
31	6090	64320	76.2	6.31E-05	14.93
32	2210	66530	76.2	6.32E-05	14.92
33	1740	68270	76.2	8.03E-05	13.89
34	1640	69910	76.2	1.70E-04	11.08
35	4470	74380	76.2	6.25E-05	14.97



**Table A3. Initial Conditions for Simulations**

Nodes	River Discharge (m <sup>3</sup> /s)	River Heads (ft)	River Leakage Rates	
			(ft <sup>3</sup> /d)	(m <sup>3</sup> /s)
0	77.30	86.26	0	0
1	77.35	86.07	-628.76	-2.06E-04
2	77.42	86.19	-497.97	-1.63E-04
3	77.46	86.67	-450.86	-1.48E-04
4	77.98	84.53	-449.87	-1.47E-04
5	77.99	84.42	-366.33	-1.20E-04
6	78.01	83.84	-377.56	-1.24E-04
7	78.06	82.28	-483.69	-1.59E-04
8	78.18	82.76	-402.72	-1.32E-04
9	78.19	80.29	-544.30	-1.78E-04
10	78.21	82.86	-439.58	-1.44E-04
11	78.22	80.66	-457.05	-1.50E-04
12	78.23	79.36	-380.79	-1.25E-04
13	78.24	79.33	-466.57	-1.53E-04
14	78.40	80.28	-375.20	-1.23E-04
15	78.40	76.89	-284.21	-9.31E-05
16	78.76	77.93	-536.52	-1.76E-04
17	78.91	76.53	-706.95	-2.32E-04
18	78.95	75.56	-323.84	-1.06E-04
19	79.61	77.14	-351.18	-1.15E-04
20	79.65	75.86	-445.48	-1.46E-04
21	79.99	76.20	-364.60	-1.19E-04
22	80.01	73.61	-716.33	-2.35E-04
23	80.07	76.97	88.16	2.89E-05
24	80.09	75.63	-511.04	-1.67E-04
25	80.14	72.54	-354.88	-1.16E-04
26	80.14	70.84	-758.11	-2.48E-04
27	80.22	72.60	-174.69	-5.73E-05
28	80.25	69.91	-821.38	-2.69E-04
29	81.37	70.56	-1179.61	-3.87E-04
30	81.39	67.54	-798.66	-2.62E-04
31	81.49	69.02	-750.85	-2.46E-04
32	81.62	67.76	-1414.47	-4.64E-04
33	81.64	66.68	-277.97	-9.11E-05
34	81.66	64.53	-1349.15	-4.42E-04
35	83.49	66.08	-2863.41	-9.38E-04

Table A4. Nodes and Corresponding River Package Cells in MODFLOW

Nodes	River Package Cells		
	Layer	Row	Column
0	-	-	-
1	1	21	5
2	1	21	6
3	1	22	7
4	1	22	8
5	1	23	8
6	1	24	8
7	1	25	8
8	1	26	9
9	1	26	10
10	1	27	11
11	1	28	11
12	1	28	10
13	1	29	10
14	1	30	9
15	1	31	9
16	1	31	8
17	1	32	8
18	1	32	9
19	1	32	10
20	1	33	10
21	1	34	10
22	1	35	10
23	1	35	11
24	1	35	12
25	1	36	12
26	1	36	11
27	1	37	12
28	1	37	13
29	1	38	14
30	1	39	13
31	1	39	11,12*
32	1	40	13
33	1	40	12
34	1	40	11
35	1	41	11

\* Two River Package cells were modeled as one reach in the surface water model

**Table A5. Inlet River Discharge for Various Time-Steps**

<b>Simulation Day</b>	<b>Date</b>	<b>1-Day*</b>	<b>2-Day</b>	<b>4-Day</b>	<b>8-Day</b>	<b>16-Day</b>
0	1/8/1991	11.19	14.17	412.01	266.39	227.05
1	1/9/1991	17.16	14.17	412.01	266.39	227.05
2	1/10/1991	586.15	809.85	412.01	266.39	227.05
3	1/11/1991	1033.56	809.85	412.01	266.39	227.05
4	1/12/1991	223.13	146.82	120.77	266.39	227.05
5	1/13/1991	70.51	146.82	120.77	266.39	227.05
6	1/14/1991	51.25	94.72	120.77	266.39	227.05
7	1/15/1991	138.18	94.72	120.77	266.39	227.05
8	1/16/1991	171.88	125.73	275.66	187.70	227.05
9	1/17/1991	79.57	125.73	275.66	187.70	227.05
10	1/18/1991	267.87	425.60	275.66	187.70	227.05
11	1/19/1991	583.32	425.60	275.66	187.70	227.05
12	1/20/1991	230.78	153.05	99.75	187.70	227.05
13	1/21/1991	75.32	153.05	99.75	187.70	227.05
14	1/22/1991	52.10	46.44	99.75	187.70	227.05
15	1/23/1991	40.78	46.44	99.75	187.70	227.05
16	1/24/1991	43.61	49.13	46.72	36.66	73.76
17	1/25/1991	54.65	49.13	46.72	36.66	73.76
18	1/26/1991	52.39	44.32	46.72	36.66	73.76
19	1/27/1991	36.25	44.32	46.72	36.66	73.76
20	1/28/1991	30.02	29.17	26.60	36.66	73.76
21	1/29/1991	28.32	29.17	26.60	36.66	73.76
22	1/30/1991	24.98	24.04	26.60	36.66	73.76
23	1/31/1991	23.11	24.04	26.60	36.66	73.76
24	2/1/1991	21.95	21.68	54.42	110.85	73.76
25	2/2/1991	21.41	21.68	54.42	110.85	73.76
26	2/3/1991	19.99	87.16	54.42	110.85	73.76
27	2/4/1991	154.33	87.16	54.42	110.85	73.76
28	2/5/1991	427.58	286.85	167.28	110.85	73.76
29	2/6/1991	146.11	286.85	167.28	110.85	73.76
30	2/7/1991	56.63	47.71	167.28	110.85	73.76
31	2/8/1991	38.79	47.71	167.28	110.85	73.76

\* 1-day average is equivalent to the original data provided by USGS gage 8160400

## **Appendix B: Interface Visual Basic Code**

**Procedure cmdExit\_Click**

```
Private Sub cmdExit_Click()
```

```
'Function: Exits the model
```

```
'Procedure runs when user click Exit button on frmInput form
```

```
End
```

```
End Sub
```

**Procedure cmdOK\_Click**

```
Private Sub cmdOK_Click()
```

```
'Function: Performs dynamic linkage of MODFLOW and surface water models
```

```
'Procedure runs when user clicks OK on frmInput form
```

```
Dim iTimestep As Integer
```

```
Dim sPath As String
```

```
Dim iLoopcount As Integer
```

```
Dim iTotTime As Double
```

```
Dim dMultiFactor As Double
```

```
Dim iTime As Integer
```

```
Application.DisplayAlerts = False
```

```
iLoopcount = 0
```

```
iTotTime = txtTotTime.Text
```

```
iTimestep = txtTimestep.Text
```

```
sPath = txtPathname.Text
```

```
iTime = 0
```

```
Initialize sPath, iLoopcount
```

```
Do
```

```
    iLoopcount = iLoopcount + 1
```

```
    iTime = iTime + iTimestep
```

```
    Outputsheet iTimestep, iTime, iLoopcount
```

```
    Rename sPath, iLoopcount
```

```
    Open_Bas iTimestep, sPath, iLoopcount
```

```
    Open_Riv sPath
```

```
    Run_MODFLOW sPath
```

```
    Output_qa sPath, iLoopcount
```

```
Loop Until iTime >= iTotTime
```

```
Application.DisplayAlerts = True
```

```
End
```

```
End Sub
```

### Sub-Procedure Initialize

'Function: Initializes surface water model and the three output worksheets for new simulation

Sub Initialize(sPath As String, iLoopcount As Integer)

'Copies initial leakage rates from *Par* worksheet to *qa,h\_fix* worksheet

```
Sheets("Par").Select
Range("A28:AJ28").Select
Selection.Copy
Sheets("qa,h_fix").Select
Range("D5").Select
Selection.PasteSpecial Paste:=xlValues, Operation:=xlNone, SkipBlanks:= _
False, Transpose:=True
```

'Copies initial flowrate from *Par* worksheet to *Q* worksheet

```
Sheets("Par").Select
Range("A16:AJ16").Select
Selection.Copy
Sheets("Q").Select
Range("D3").Select
ActiveSheet.Paste
Windows("kinematic8").Activate
```

'Clears *flowrate* worksheet of any results from previous simulation

```
Sheets("flowrate").Select
Rows("4:100").Select
Selection.ClearContents
```

'Clears *riv\_head* worksheet of any results from previous simulation

```
Sheets("riv_head").Select
Rows("4:100").Select
Selection.ClearContents
```

'Clears *aq\_head* worksheet of any results from previous simulation

```
Sheets("aq_head").Select
Rows("4:100").Select
Selection.ClearContents
```

### **Sub-Procedure Surface\_Run**

'Function: Sets new inlet river discharges as the upper boundary condition for a 'one-day simulation

```
Private Sub Surface_Run(n As Integer, iTime As Integer, iTimestep As Integer)
Dim iDay As Integer
```

```
iDay = n + iTime - iTimestep
```

```
  If iTimestep = 2 Then
```

```
    Sheets("inlet2").Select
```

```
  ElseIf iTimestep = 4 Then
```

```
    Sheets("inlet4").Select
```

```
  ElseIf iTimestep = 8 Then
```

```
    Sheets("inlet8").Select
```

```
  ElseIf iTimestep = 16 Then
```

```
    Sheets("inlet16").Select
```

```
  End If
```

```
  Range(Cells(3, iDay + 4), Cells(483, iDay + 4)).Select
```

```
  Selection.Copy
```

```
  Sheets("Q").Select
```

```
  Range("D3").Select
```

```
  Selection.PasteSpecial Paste:=xlValues, Operation:=xlNone, SkipBlanks:= _
```

```
    False, Transpose:=False
```

```
End Sub
```

### Sub-Procedure Outputsheet

'Function: Runs Surface\_Run for the number of days in the interface time-step (iTimestep). Also copies the river heads and discharge resulting from the simulation into the *flowrate* and *riv\_head* worksheets, respectively.

```
Private Sub Outputsheet (iTimestep As Integer, iTime As Integer, iLoopcount As Integer)
Dim n As Integer
Dim yo As Double
Dim iCol As Integer
```

'Initialize parameters

```
n = 0
Do

    If iTimestep = 2 Or iTimestep = 4 Or iTimestep = 8 Or iTimestep = 16 Then
        Surface_Run n, iTime, iTimestep
    End If
    Sheets("Q").Select
    Range("D483:AN483").Select
    Selection.Copy
    ActiveWindow.LargeScroll Down:=-10
    Range("D3").Select
    Selection.PasteSpecial Paste:=xlValues, Operation:=xlNone, SkipBlanks:= _
        False, Transpose:=False
    n = n + 1
Loop Until n >= iTimestep
```

'Copies river flowrate resulting from simulation from the *Q* worksheet to the *flowrate* sheet

```
Range("D482:AM482").Copy
Sheets("flowrate").Select
Cells(iLoopcount + 3, 3).Select
Selection.PasteSpecial Paste:=xlValues, Operation:=xlNone, SkipBlanks:= _
    False, Transpose:=False
```

'Copies river heads resulting from simulation from the *h* worksheet into *qa,h\_fix* worksheet

```
Sheets("h").Select
Range("E482:AM482").Copy
yo = Cells(482, 4).Value
Sheets("qa,h_fix").Select
Range("M5").Select
Selection.PasteSpecial Paste:=xlValues, Operation:=xlNone, SkipBlanks:= _
    False, Transpose:=True
```

'Copies river heads for nodes 1-36 from sheet *qa,h\_fix*, and pastes in *riv\_head* sheet

```
Sheets("qa,h_fix").Select
Range("P5:P39").Select
Selection.Copy
Sheets("riv_head").Select
Range(Cells(iLoopcount + 3, 4), Cells(iLoopcount + 3, 38)).Select
Selection.PasteSpecial Paste:=xlValues, Operation:=xlNone, SkipBlanks:= _
    False, Transpose:=True
```



### Sub-Procedure Outputsheet cont'd

'Writes the river hydraulic head for reach 0 in the river head reach 0 column of *riv\_head* sheet

```
Cells(iLoopcount + 3, 3).Value = yo * 3.281 + 79.8
```

'Writes the time total simulation time in the second column of *flowrate* the sheet

```
Sheets("flowrate").Select
```

```
Cells(iLoopcount + 3, 2).Value = iTime
```

'Writes the loop index number in the first column of *flowrate* sheet

```
Cells(iLoopcount + 3, 1).Value = iLoopcount
```

'Writes the total simulation time in the second column of the *riv\_head* sheet

```
Sheets("riv_head").Select
```

```
Cells(iLoopcount + 3, 2).Value = iTime
```

'Writes the loop index number in the first column of *riv\_head* sheet

```
Cells(iLoopcount + 3, 1).Value = iLoopcount
```

'Writes the total simulation time 'in the second column of the *aq\_head* sheet

```
Sheets("aq_head").Select
```

```
Cells(iLoopcount + 3, 2).Value = iTime
```

'Writes the loop index number in the first column of *aq\_head* sheet

```
Cells(iLoopcount + 3, 1).Value = iLoopcount
```

End Sub

**Sub-Procedure Rename**

'Function: Initializes the starting heads for the first MODFLOW run (i.e. iLoopcount = 1). Also, 'renames \*.hed file at the end of MODFLOW run to the \*.shd (starting head file). The \*.shd file 'contains the starting heads used in the beginning of the next MODFLOW run.

```
Private Sub Rename(sPath As String, iLoopcount As Integer)

If iLoopcount = 1 Then

    FileCopy sPath & "\modflow\initial.bas", sPath & "\modflow\Cw409_s2.bas"
    FileCopy sPath & "\modflow\initial.nam", sPath & "\modflow\Cw409_s2.nam"

ElseIf iLoopcount = 2 Then

    FileCopy sPath & "\modflow\standard.bas", sPath & "\modflow\Cw409_s2.bas"
    FileCopy sPath & "\modflow\standard.nam", sPath & "\modflow\Cw409_s2.nam"
    FileCopy sPath & "\modflow\Cw409_s2.hed", sPath & "\modflow\Cw409_s2.shd"

ElseIf iLoopcount > 2 Then

    FileCopy sPath & "\modflow\Cw409_s2.hed", sPath & "\modflow\Cw409_s2.shd"
End If

End Sub
```

### **Sub-Procedure Open\_Bas**

Sub Open\_Bas(iTimestep As Integer, sPath As String, iLoopcount As Integer)

' Function: Enters the time-step for the MODFLOW run into the Basic Package  
'It's important that the Basic Package initially be saved as a \*.csv (comma delimited) file

```
Workbooks.OpenText Filename:=sPath & "\modflow\CW409_S2.BAS", Origin _  
:=xlWindows, StartRow:=1, DataType:=xlDelimited, TextQualifier:= _  
xlDoubleQuote, ConsecutiveDelimiter:=True, Tab:=False, Semicolon:=False, _  
Comma:=True, Space:=False, Other:=False, FieldInfo:=Array(Array(1, 1), _  
Array(2, 1), Array(3, 1), Array(4, 1), Array(5, 1), Array(6, 1), Array(7, 1), Array(8, 1), _  
Array(9, 1))
```

'Sets MODFLOW variable NPER (number of stress periods) = 1

```
Range("E3").Select  
ActiveCell.FormulaR1C1 = "1"
```

'Sets MODFLOW variable PERLEN (length of stress period) equal to user specified time-step

```
If iLoopcount = 1 Then  
Range("A437").Select  
ActiveCell.Value = iTimestep  
Else  
Range("A227").Select  
ActiveCell.Value = iTimestep  
End If
```

'Saves and closes Basic Package

```
ActiveWorkbook.SaveAs Filename:=sPath & "\modflow\CW409_S2.BAS", _  
FileFormat:=xlCSV, CreateBackup:=False  
ActiveWorkbook.Close  
End Sub
```

### **Sub-Procedure Open\_Riv**

'Funtion: Opens River Package and inserts new river heads from sheet *qa,h\_fix*  
'River Package (\*.riv) must be saved as a csv (comma delimited) file

Sub Open\_Riv(sPath As String)

```
Workbooks.OpenText Filename:=sPath & "\modflow\Cw409_S2.riv", Origin:= _  
xlWindows, StartRow:=1, DataType:=xlDelimited, TextQualifier:= _  
xlDoubleQuote, ConsecutiveDelimiter:=True, Tab:=False, Semicolon:=False, _  
Comma:=True, Space:=False, Other:=False, FieldInfo:=Array(Array(1, 1), _  
Array(2, 1), Array(3, 1), Array(4, 1), Array(5, 1), Array(6, 1), Array(7, 1))  
Windows("kinematic8.xls").Activate  
Sheets("qa,h_fix").Select
```

'Copies cells which contain the new river heads from *qa,h\_fix* worksheet

```
Range("T5:T40").Select  
Selection.Copy  
Windows("CW409_S2.RIV").Activate
```

'Pastes onto cell D67 of the River Package

```
Range("D67").Select  
Selection.PasteSpecial Paste:=xlValues, Operation:=xlNone, SkipBlanks:= _  
False, Transpose:=False  
Range("D67:D108").Select  
Selection.NumberFormat = "0.00"
```

'Saves as a .csv file and closes

```
ActiveWorkbook.SaveAs Filename:=sPath & "\modflow\CW409_S2.RIV", FileFormat _  
:=xlCSV, CreateBackup:=False
```

```
ActiveWorkbook.Close
```

```
End Sub
```

### **Sub-Procedure Run\_MODFLOW**

'Function: Runs MODFLOW. This sub-procedure is not fully automated and requires user to  
'enter in the MODFLOW Name file (cw409\_S2.nam).

```
Private Sub Run_MODFLOW(sPath As String)
```

```
Dim Start As Double
```

```
Dim ID As Integer
```

```
ID = Shell(sPath & "\modflow\Modflw96.exe")
```

```
MsgBox ("RUN MODFLOW")
```

```
End Sub
```

### Sub-Procedure Output\_qa

'Function: Transfers river leakage rates from MODFLOW listing file (\*.out) to *qa,h\_fix* sheet  
'Also transfers aquifer heads in Cross Sections 1 and 2 to *aq\_head* sheet

Private Sub Output\_qa(sPath As String, iLoopcount As Integer)

Dim iRow As Integer

Dim iCount As Integer

Dim iRowaqhead As Integer

Dim lay1 As Boolean

'initialize iRow

iRow = 0

'Opens listing file (.out)

Workbooks.OpenText Filename:= \_

sPath & "\modflow\Cw409\_s2.out", Origin:=xlWindows, \_

StartRow:=1, DataType:=xlDelimited, TextQualifier:=xlDoubleQuote, \_

ConsecutiveDelimiter:=True, Tab:=False, Semicolon:=False, Comma:=False, \_

Space:=True, Other:=False, FieldInfo:=Array(Array(1, 1), Array(2, 1), Array(3, \_

1), Array(4, 1), Array(5, 1), Array(6, 1), Array(7, 1), Array(8, 1))

'Uses Excel's Find command to locate Reach 1 (or REACH 65 in revised BEG model) and copies river leakage rates. Searches for the word "leakage" in column C and assigns that row as iRow

Columns("C:C").Select

iRow = Selection.Find(What:="leakage", After:=ActiveCell, LookIn:=xlFormulas, \_

LookAt:=xlPart, SearchOrder:=xlByRows, SearchDirection:=xlNext, \_

MatchCase:=False).Row

Range(Cells(iRow + 65, 11), Cells(iRow + 100, 11)).Select

Selection.Copy

Windows("kinematic8.xls").Activate

' Pastes river leakage rates into sheet *qa,h\_fix*

Sheets("qa,h\_fix").Select

Range("D5").Select

ActiveSheet.Paste

' Copies river leakage rates for reaches 14, 27, 28 and for the all of the 35 reaches being modeled and pastes into *aq\_head* sheet

'Reach 14

Sheets("qa,h\_fix").Select

Range("D16").Select

Selection.Copy

Sheets("aq\_head").Select

' Range("AO3").Select

Cells(iLoopcount + 3, 41).Select

Selection.PasteSpecial Paste:=xlValues, Operation:=xlNone, SkipBlanks:= \_

False, Transpose:=False

'Reach 27

Sheets("qa,h\_fix").Select

Range("D34").Select

```

Selection.Copy
Sheets("aq_head").Select
'Range("AQ3").Select
Cells(iLoopcount + 3, 42).Select
ActiveSheet.Paste

```

#### 'Reach 28

```

Sheets("qa,h_fix").Select
Range("D39").Select
Selection.Copy
Sheets("aq_head").Select
' Range("AR3").Select
Cells(iLoopcount + 3, 43).Select
Selection.PasteSpecial Paste:=xlValues, Operation:=xlNone, SkipBlanks:= _
    False, Transpose:=False

```

#### 'All 35 reaches

```

Sheets("qa,h_fix").Select
Range("D41").Select
Selection.Copy
Sheets("aq_head").Select
' Range("AR3").Select
Cells(iLoopcount + 3, 44).Select
Selection.PasteSpecial Paste:=xlValues, Operation:=xlNone, SkipBlanks:= _
    False, Transpose:=False

```

' Locates the final aquifer heads in Layer 1 resulting from the simulation in the Listing file.

'Designates iRow as the row where "end" appears in Column G.

```

Windows("Cw409_s2.out").Activate
iRow = 0
Columns("G:G").Select

iRow = Selection.Find(What:="END", After:=ActiveCell, LookIn:=xlFormulas, _
LookAt:=xlPart, SearchOrder:=xlByRows, SearchDirection:=xlNext, _
MatchCase:=False).Row
iRowaqhead = iRow + 193

```

' Locates aquifer heads in Cross Sections 1 and 2 by referencing iRow

```

lay1 = True
makegrid iRowaqhead, iLoopcount
outputhead iRowaqhead, iLoopcount, lay1
iRowaqhead = iRowaqhead + 216
    lay1 = False
makegrid iRowaqhead, iLoopcount
outputhead iRowaqhead, iLoopcount, lay1

```

'Closes listing file

```

Windows("CW409_S2.OUT").Activate
ActiveWorkbook.Close

```

End Sub

### **Sub-Procedure Makegrid**

Function: Reformats aquifer heads in the MODFLOW listing file to resemble the domain grid.

```
Private Sub makegrid(iRowaqhead As Integer, iLoopcount As Integer)
```

```
Dim iRow2 As Integer  
Dim Count As Integer  
Dim iFinish As Integer  
Dim sFile As String
```

```
    If iLoopcount = 0 Then  
        sFile = "initial.out"  
    Else  
        sFile = "Cw409_s2.out"  
    End If
```

```
    Windows(sFile).Activate  
    iRow2 = iRowaqhead  
    iFinish = iRow2 + 22
```

```
    Do  
        Range(Cells(iRow2 + 1, 2), Cells(iRow2 + 1, 10)).Select  
        Selection.Cut  
        Cells(iRow2, 12).Select  
        ActiveSheet.Paste  
        Range(Cells(iRow2 + 2, 2), Cells(iRow2 + 2, 10)).Select  
        Selection.Cut  
        Cells(iRow2, 21).Select  
        ActiveSheet.Paste  
        Range(Cells(iRow2 + 3, 2), Cells(iRow2 + 3, 10)).Select  
        Selection.Cut  
        Cells(iRow2, 30).Select  
        ActiveSheet.Paste  
        Range(Cells(iRow2 + 4, 2), Cells(iRow2 + 4, 10)).Select  
        Selection.Cut  
        Cells(iRow2, 39).Select  
        ActiveSheet.Paste  
        Range(Cells(iRow2 + 5, 2), Cells(iRow2 + 5, 10)).Select  
        Selection.Cut  
        Cells(iRow2, 48).Select  
        ActiveSheet.Paste  
        Range(Cells(iRow2 + 6, 2), Cells(iRow2 + 6, 10)).Select  
        Selection.Cut  
        Cells(iRow2, 57).Select  
        ActiveSheet.Paste  
        Range(Cells(iRow2 + 7, 2), Cells(iRow2 + 7, 10)).Select  
        Selection.Cut  
        Cells(iRow2, 66).Select  
        ActiveSheet.Paste  
        Range(Cells(iRow2 + 8, 2), Cells(iRow2 + 8, 10)).Select
```

### **Sub-Procedure Makegrid cont'd**

```
Selection.Cut
Cells(iRow2, 75).Select
ActiveSheet.Paste
Count = 0
Do
    Count = Count + 1
    Rows(iRow2 + 1).Delete
Loop Until (Count = 8)
iRow2 = iRow2 + 1
Loop Until iRow2 = iFinish
End Sub
```



### **Sub-Procedure Outputhead**

'Function: Extracts aquifer heads from Cross Section 1 and 2 from the MODFLOW listing file

```
Sub outputhead(iRow As Integer, iLoopcount As Integer, lay1 As Boolean)
Dim sFile As String
Dim iRow2 As Integer
```

```
iRow2 = iRow
sFile = "Cw409_s2.out"
```

#### 'Cross Section 1

```
Windows(sFile).Activate
Range(Cells(iRow2 + 9, 7), Cells(iRow2 + 9, 15)).Select
Selection.Copy
Windows("kinematic8.xls").Activate
Sheets("aq_head").Select
If lay1 = True Then
    Cells(iLoopcount + 3, 3).Select
Else
    Cells(iLoopcount + 3, 12).Select
End If
```

```
ActiveSheet.Paste
```

#### 'Cross Section 2

```
Windows(sFile).Activate
Range(Cells(iRow2 + 16, 10), Cells(iRow2 + 16, 19)).Select
Selection.Copy
Windows("kinematic8.xls").Activate
If lay1 = True Then
    Cells(iLoopcount + 3, 21).Select
Else
    Cells(iLoopcount + 3, 31).Select
End If
ActiveSheet.Paste
End Sub
```

## **Appendix C: Simulation Results**

Table C1. Cross Section 1 Aquifer Heads in Layer 1 from 2-Day Time-Step Simulation

Time (days)	Aquifer Heads (ft) in Cross Section 1, Layer 1								
	-4	-3	-2	-1*	Reach 14	1	2	3	4
0	110.628	106.773	99.929	88.751	80.288	85.421	91.612	97.677	103.902
2	110.627	106.762	99.813	87.728	74.555	84.360	91.415	97.643	103.896
4	110.633	106.806	100.340	93.106	108.324	89.893	92.310	97.777	103.917
6	110.643	106.865	100.623	92.312	84.573	89.256	92.783	97.945	103.957
8	110.654	106.919	100.720	91.307	81.475	88.293	92.932	98.083	104.005
10	110.667	106.964	100.767	91.028	83.353	88.011	92.995	98.190	104.056
12	110.683	107.029	101.055	93.200	96.448	90.254	93.466	98.348	104.118
14	110.702	107.091	101.193	92.540	84.889	89.648	93.677	98.495	104.185
16	110.719	107.132	101.116	90.902	77.926	87.971	93.523	98.572	104.244
18	110.733	107.150	100.957	89.900	78.141	86.879	93.234	98.582	104.288
20	110.744	107.148	100.767	89.171	77.722	86.052	92.896	98.538	104.314
22	110.751	107.129	100.549	88.427	76.295	85.210	92.518	98.450	104.322
24	110.754	107.094	100.324	87.827	75.743	84.518	92.136	98.330	104.311
26	110.753	107.048	100.106	87.366	75.473	83.976	91.774	98.189	104.284
28	110.750	107.007	100.019	88.021	80.946	84.600	91.637	98.073	104.250
30	110.748	106.994	100.199	90.235	91.117	86.889	91.957	98.049	104.225
32	110.746	106.984	100.217	89.313	78.027	86.016	91.997	98.034	104.206

\*Negative values indicate the distance in MODFLOW cells from Reach 14 in the southwestern direction. Positive values indicate the distance in MODFLOW cells from Reach 14 in the northeastern direction.

Table C2. Cross Section 1 Aquifer Heads in Layer 2 from 2-Day Time-Step Simulation

Time (days)	Aquifer Heads (ft) in Cross Section 1, Layer 2								
	-4	-3	-2	-1*	Reach 14	1	2	3	4
0	101.547	101.651	101.765	101.890	102.039	102.170	102.238	102.256	102.355
2	101.527	101.630	101.742	101.866	102.012	102.144	102.213	102.232	102.334
4	101.635	101.745	101.864	101.999	102.156	102.284	102.349	102.360	102.450
6	101.635	101.743	101.859	101.988	102.139	102.270	102.336	102.352	102.445
8	101.627	101.734	101.849	101.977	102.126	102.258	102.325	102.341	102.436
10	101.628	101.735	101.851	101.979	102.129	102.260	102.327	102.343	102.438
12	101.678	101.787	101.906	102.039	102.193	102.323	102.389	102.401	102.491
14	101.676	101.784	101.901	102.031	102.182	102.313	102.380	102.394	102.487
16	101.651	101.757	101.873	102.000	102.149	102.281	102.349	102.365	102.460
18	101.632	101.738	101.853	101.980	102.128	102.260	102.328	102.345	102.442
20	101.614	101.720	101.834	101.960	102.109	102.241	102.309	102.327	102.424
22	101.594	101.699	101.813	101.938	102.086	102.218	102.286	102.305	102.404
24	101.575	101.679	101.792	101.917	102.064	102.196	102.265	102.284	102.384
26	101.557	101.661	101.774	101.898	102.045	102.177	102.245	102.265	102.366
28	101.561	101.666	101.779	101.905	102.054	102.185	102.253	102.272	102.372
30	101.600	101.707	101.823	101.952	102.104	102.234	102.301	102.317	102.413
32	101.586	101.691	101.805	101.931	102.079	102.211	102.279	102.297	102.396

\*Negative values indicate the distance in MODFLOW cells from Reach 14 in the southwestern direction. Positive values indicate the distance in MODFLOW cells from Reach 14 in the northeastern direction.

Table C3. Cross Section 2 Aquifer Heads in Layer 1 from 2-Day Time-Step Simulation

Time (days)	Aquifer Heads (ft) in Cross Section 2, Layer 1									
	-4	-3	-2	-1*	Reach 27	Reach 28	1	2	3	4
0	95.616	90.014	83.018	76.919	72.604	69.927	79.385	87.997	94.995	100.670
2	95.612	89.992	82.882	76.094	67.298	65.952	78.659	87.888	94.980	100.668
4	95.624	90.077	83.505	80.444	99.063	89.691	82.507	88.393	95.040	100.675
6	95.651	90.197	83.880	80.062	76.715	72.993	82.124	88.691	95.124	100.692
8	95.688	90.310	84.042	79.383	73.740	70.771	81.494	88.813	95.202	100.714
10	95.730	90.408	84.140	79.207	75.503	72.081	81.324	88.883	95.269	100.739
12	95.783	90.543	84.520	81.021	87.861	81.319	82.915	89.183	95.362	100.770
14	95.844	90.678	84.735	80.637	76.987	73.200	82.547	89.347	95.454	100.806
16	95.903	90.772	84.694	79.379	70.424	68.289	81.419	89.303	95.518	100.841
18	95.956	90.820	84.538	78.532	70.598	68.422	80.671	89.170	95.549	100.872
20	95.997	90.827	84.327	77.866	70.211	68.133	80.093	88.996	95.552	100.896
22	96.024	90.796	84.069	77.172	68.877	67.137	79.496	88.788	95.529	100.912
24	96.037	90.734	83.789	76.579	68.373	66.763	78.994	88.565	95.485	100.920
26	96.034	90.647	83.508	76.094	68.121	66.572	78.587	88.344	95.425	100.920
28	96.022	90.566	83.373	76.513	73.216	70.376	78.978	88.242	95.369	100.913
30	96.011	90.538	83.561	78.276	82.810	77.551	80.547	88.401	95.352	100.908
32	96.001	90.519	83.575	77.609	70.531	68.378	79.949	88.417	95.341	100.904

\*Negative values indicate the distance in MODFLOW cells from Reach 27 in the southwestern direction. Positive values indicate the distance in MODFLOW cells from Reach 28 in the northeastern direction.

Table C4. Cross Section 2 Aquifer Heads in Layer 2 from 2-Day Time-Step Simulation

Time (days)	Aquifer Heads (ft) in Cross Section 2, Layer 1									
	-4	-3	-2	-1*	Reach 27	Reach 28	1	2	3	4
0	98.268	98.074	97.901	97.677	97.583	97.596	97.676	97.789	97.873	97.978
2	98.246	98.050	97.874	97.648	97.552	97.572	97.659	97.779	97.865	97.971
4	98.365	98.182	98.024	97.816	97.730	97.714	97.761	97.844	97.915	98.018
6	98.350	98.159	97.990	97.767	97.665	97.665	97.731	97.830	97.906	98.010
8	98.335	98.141	97.969	97.743	97.641	97.645	97.717	97.821	97.900	98.004
10	98.336	98.142	97.971	97.745	97.644	97.648	97.718	97.822	97.900	98.005
12	98.389	98.201	98.036	97.817	97.719	97.708	97.762	97.851	97.923	98.026
14	98.379	98.187	98.017	97.790	97.685	97.682	97.746	97.842	97.917	98.021
16	98.349	98.154	97.979	97.748	97.642	97.647	97.721	97.827	97.906	98.010
18	98.332	98.136	97.961	97.731	97.627	97.635	97.711	97.819	97.900	98.004
20	98.318	98.121	97.946	97.716	97.614	97.624	97.702	97.813	97.895	97.999
22	98.300	98.104	97.928	97.698	97.597	97.610	97.691	97.805	97.888	97.993
24	98.285	98.088	97.911	97.682	97.583	97.599	97.682	97.798	97.883	97.988
26	98.271	98.073	97.897	97.668	97.571	97.589	97.674	97.792	97.878	97.983
28	98.280	98.085	97.912	97.686	97.592	97.605	97.684	97.798	97.882	97.987
30	98.323	98.133	97.965	97.746	97.653	97.654	97.720	97.821	97.899	98.003
32	98.302	98.106	97.932	97.705	97.605	97.617	97.696	97.807	97.890	97.995

\*Negative values indicate the distance in MODFLOW cells from Reach 27 in the southwestern direction. Positive values indicate the distance in MODFLOW cells from Reach 28 in the northeastern direction.

Table C5. Leakage Rates from 2-Day Time-Step Simulation

Leakage Rate (ft <sup>3</sup> /d)				
Time (days)	Reach14	Reach 27	Reach 28	Total
0	-375.20	-174.69	-821.38	-21216.42
2	-1182.82	-1842.06	-2028.62	-237321.32
4	4145.75	9477.00	6198.37	1224020.27
6	-2549.99	-5508.15	-4947.08	-757116.01
8	-722.14	-966.11	-1506.98	-206757.09
10	-137.39	339.90	-527.27	28122.22
12	1537.29	3797.98	1964.95	478992.32
14	-1393.40	-2724.72	-2871.44	-388353.93
16	-1263.92	-2114.46	-2349.31	-317512.74
18	-527.87	-402.69	-1030.72	-49928.88
20	-576.54	-529.55	-1099.28	-45093.05
22	-714.59	-822.76	-1289.16	-82071.65
24	-633.40	-621.18	-1114.81	-53807.83
26	-599.79	-546.89	-1044.50	-40479.20
28	212.32	1142.19	187.53	177597.38
30	1109.75	2897.35	1408.93	383904.14
32	-1760.59	-3384.36	-3237.97	-460118.96

Table C6a. River Discharge at Finite Difference Nodes for a 2-Day Time-Step Simulation

<i>River Discharge (m<sup>3</sup>/s)</i>									
<b>Time (days)</b>	<b>0</b>	<b>1</b>	<b>2</b>	<b>3</b>	<b>4</b>	<b>5</b>	<b>6</b>	<b>7</b>	<b>8</b>
0	77.300	77.348	77.416	77.456	77.982	77.991	78.008	78.062	78.181
2	14.172	14.221	14.289	14.329	14.856	14.864	14.881	14.935	15.054
4	809.854	809.908	809.982	810.033	810.568	810.589	810.618	810.673	810.794
6	146.821	146.836	146.875	146.848	147.329	147.268	147.213	147.261	147.372
8	94.719	94.788	94.875	94.954	95.508	95.556	95.614	95.672	95.797
10	125.726	125.779	125.851	125.902	126.436	126.457	126.487	126.542	126.661
12	425.598	425.645	425.712	425.749	426.274	426.281	426.296	426.349	426.468
14	153.051	153.086	153.143	153.155	153.664	153.645	153.633	153.684	153.800
16	46.439	46.498	46.575	46.635	47.175	47.204	47.242	47.298	47.420
18	49.129	49.185	49.260	49.317	49.855	49.881	49.917	49.972	50.092
20	44.315	44.364	44.433	44.474	45.002	45.013	45.032	45.086	45.205
22	29.166	29.215	29.283	29.324	29.852	29.862	29.880	29.934	30.053
24	24.041	24.091	24.160	24.203	24.732	24.744	24.764	24.818	24.938
26	21.676	21.725	21.794	21.836	22.363	22.374	22.393	22.447	22.566
28	87.158	87.207	87.276	87.316	87.844	87.853	87.871	87.925	88.044
30	286.847	286.890	286.953	286.982	287.501	287.499	287.504	287.557	287.675
32	47.713	47.751	47.810	47.827	48.339	48.325	48.318	48.370	48.487



Table C6b. River Discharge at Finite Difference Nodes for a 2-Day Time-Step Simulation

<i>River Discharge (m<sup>3</sup>/s)</i>									
<b>Time (days)</b>	<b>9</b>	<b>10</b>	<b>11</b>	<b>12</b>	<b>13</b>	<b>14</b>	<b>15</b>	<b>16</b>	<b>17</b>
0	78.192	78.206	78.220	78.226	78.240	78.393	78.396	78.761	78.908
2	15.066	15.080	15.094	15.101	15.116	15.269	15.272	15.637	15.785
4	810.806	810.821	810.835	810.844	810.858	811.012	811.015	811.380	811.528
6	147.377	147.390	147.403	147.402	147.415	147.567	147.569	147.933	148.079
8	95.813	95.827	95.842	95.854	95.869	96.023	96.026	96.392	96.540
10	126.674	126.688	126.702	126.710	126.724	126.878	126.881	127.246	127.394
12	426.479	426.493	426.507	426.514	426.528	426.681	426.684	427.049	427.197
14	153.809	153.823	153.837	153.840	153.854	154.007	154.009	154.374	154.521
16	47.433	47.448	47.462	47.471	47.486	47.639	47.643	48.008	48.156
18	50.105	50.120	50.134	50.143	50.158	50.311	50.314	50.680	50.827
20	45.217	45.231	45.245	45.253	45.267	45.420	45.423	45.788	45.936
22	30.065	30.079	30.094	30.101	30.115	30.268	30.271	30.637	30.784
24	24.950	24.964	24.978	24.986	25.000	25.153	25.156	25.522	25.670
26	22.578	22.592	22.606	22.614	22.628	22.781	22.784	23.149	23.297
28	88.056	88.070	88.085	88.092	88.106	88.259	88.262	88.628	88.775
30	287.685	287.699	287.713	287.719	287.733	287.886	287.889	288.254	288.401
32	48.496	48.510	48.524	48.528	48.542	48.695	48.698	49.063	49.210

Table C6c. River Discharge at Finite Difference Nodes for a 2-Day Time-Step Simulation

<i>River Discharge (m<sup>3</sup>/s)</i>									
<b>Time (days)</b>	<b>18</b>	<b>19</b>	<b>20</b>	<b>21</b>	<b>22</b>	<b>23</b>	<b>24</b>	<b>25</b>	<b>26</b>
0	78.945	79.611	79.642	79.982	80.010	80.069	80.089	80.134	80.137
2	15.821	16.487	16.518	16.859	16.887	16.948	16.969	17.018	17.022
4	811.565	812.231	812.263	812.603	812.632	812.692	812.712	812.759	812.762
6	148.115	148.779	148.808	149.146	149.173	149.229	149.248	149.289	149.290
8	96.578	97.245	97.277	97.618	97.647	97.709	97.730	97.779	97.782
10	127.431	128.096	128.128	128.468	128.497	128.557	128.577	128.623	128.626
12	427.234	427.899	427.930	428.270	428.299	428.358	428.378	428.424	428.427
14	154.557	155.222	155.253	155.592	155.620	155.678	155.698	155.742	155.744
16	48.194	48.859	48.891	49.232	49.261	49.321	49.342	49.389	49.392
18	50.865	51.530	51.562	51.902	51.931	51.992	52.012	52.059	52.062
20	45.973	46.638	46.670	47.010	47.038	47.098	47.118	47.164	47.167
22	30.821	31.487	31.518	31.858	31.887	31.947	31.967	32.013	32.016
24	25.707	26.372	26.404	26.744	26.772	26.832	26.852	26.898	26.901
26	23.334	24.000	24.031	24.371	24.400	24.459	24.479	24.526	24.528
28	88.812	89.478	89.509	89.849	89.878	89.938	89.957	90.004	90.006
30	288.438	289.104	289.135	289.474	289.503	289.562	289.582	289.627	289.629
32	49.246	49.911	49.942	50.281	50.309	50.368	50.387	50.432	50.434

Table C6d. River Discharge at Finite Difference Nodes for a 2-Day Time-Step Simulation

<i>River Discharge (m<sup>3</sup>/s)</i>									
<b>Time (days)</b>	<b>27</b>	<b>28</b>	<b>29</b>	<b>30</b>	<b>31</b>	<b>32</b>	<b>33</b>	<b>34</b>	<b>35</b>
0	80.211	80.242	81.366	81.386	81.485	81.615	81.632	81.647	83.479
2	17.101	17.138	18.284	18.317	18.644	18.883	18.997	19.095	21.414
4	812.836	812.868	813.994	814.014	814.117	814.248	814.266	814.281	816.113
6	149.362	149.391	150.511	150.528	150.611	150.741	150.754	150.766	152.598
8	97.858	97.891	99.018	99.040	99.150	99.281	99.301	99.317	101.149
10	128.700	128.732	129.857	129.877	129.979	130.109	130.127	130.142	131.974
12	428.500	428.532	429.656	429.676	429.775	429.906	429.923	429.937	431.769
14	155.817	155.847	156.970	156.989	157.082	157.212	157.228	157.241	159.073
16	49.467	49.499	50.625	50.646	50.751	50.882	50.901	50.916	52.751
18	52.137	52.169	53.294	53.315	53.418	53.549	53.567	53.582	55.414
20	47.241	47.273	48.397	48.417	48.518	48.648	48.666	48.680	50.513
22	32.090	32.121	33.246	33.266	33.370	33.502	33.521	33.537	35.384
24	26.976	27.007	28.132	28.152	28.258	28.390	28.410	28.427	30.277
26	24.603	24.634	25.759	25.779	25.884	26.016	26.036	26.052	27.899
28	90.080	90.112	91.237	91.257	91.358	91.488	91.505	91.520	93.352
30	289.703	289.734	290.858	290.877	290.975	291.106	291.122	291.137	292.969
32	50.507	50.538	51.661	51.680	51.775	51.906	51.922	51.936	53.770

Table C7a. River Hydraulic Heads at Finite Difference Nodes for a 2-Day Time-Step Simulation

<i>River Head (ft)</i>									
<b>Time (days)</b>	<b>0</b>	<b>1</b>	<b>2</b>	<b>3</b>	<b>4</b>	<b>5</b>	<b>6</b>	<b>7</b>	<b>8</b>
0	86.262	86.070	86.194	86.670	84.526	84.420	83.838	82.284	82.756
2	82.137	81.942	81.591	81.105	80.050	79.145	78.643	77.797	77.395
4	106.278	106.079	108.520	113.670	106.361	110.153	109.190	104.192	108.961
6	89.304	89.105	89.578	90.759	87.827	88.306	87.664	85.589	86.708
8	87.106	86.909	87.131	87.806	85.445	85.505	84.910	83.210	83.863
10	88.459	88.262	88.639	89.627	86.915	87.236	86.613	84.681	85.623
12	97.798	97.600	99.058	102.227	97.103	99.241	98.440	94.902	97.847
14	89.544	89.345	89.847	91.086	88.093	88.622	87.977	85.860	87.032
16	84.564	84.368	84.296	84.376	82.677	82.242	81.695	80.432	80.543
18	84.728	84.531	84.478	84.596	82.854	82.451	81.900	80.609	80.754
20	84.432	84.235	84.147	84.195	82.530	82.068	81.522	80.283	80.364
22	83.404	83.207	83.001	82.810	81.416	80.755	80.228	79.165	79.028
24	83.009	82.813	82.562	82.279	80.989	80.253	79.734	78.738	78.519
26	82.816	82.620	82.347	82.018	80.781	80.006	79.491	78.529	78.268
28	86.751	86.553	86.733	87.321	85.052	85.040	84.449	82.812	83.387
30	94.004	93.806	94.825	97.107	92.961	94.360	93.630	90.745	92.875
32	84.642	84.444	84.380	84.474	82.754	82.330	81.778	80.504	80.628

Table C7b. River Hydraulic Heads at Finite Difference Nodes for a 2-Day Time-Step Simulation

<i>River Head (ft)</i>									
<b>Time (days)</b>	<b>9</b>	<b>10</b>	<b>11</b>	<b>12</b>	<b>13</b>	<b>14</b>	<b>15</b>	<b>16</b>	<b>17</b>
0	80.294	82.859	80.659	79.361	79.329	80.275	76.890	77.932	76.528
2	76.192	76.454	75.492	74.866	74.568	74.531	72.976	73.113	72.308
4	100.350	114.174	105.925	101.347	102.619	108.415	96.062	101.620	97.300
6	83.318	87.580	84.469	82.676	82.840	84.515	79.779	81.499	79.654
8	81.142	84.182	81.727	80.291	80.314	81.464	77.700	78.932	77.404
10	82.488	86.284	83.423	81.766	81.877	83.352	78.986	80.520	78.796
12	91.844	100.892	95.209	92.022	92.741	96.478	87.929	91.569	88.485
14	83.567	87.968	84.781	82.948	83.129	84.864	80.016	81.792	79.912
16	78.601	80.215	78.526	77.505	77.363	77.902	75.273	75.938	74.780
18	78.763	80.467	78.730	77.683	77.551	78.128	75.427	76.128	74.947
20	78.464	80.001	78.353	77.355	77.204	77.709	75.142	75.776	74.639
22	77.442	78.405	77.066	76.235	76.018	76.278	74.167	74.576	73.587
24	77.052	77.797	76.575	75.808	75.565	75.733	73.795	74.118	73.187
26	76.860	77.497	76.334	75.598	75.343	75.465	73.612	73.894	72.991
28	80.777	83.613	81.267	79.891	79.890	80.952	77.351	78.501	77.027
30	88.039	94.951	90.416	87.851	88.322	91.139	84.292	87.074	84.543
32	78.666	80.316	78.608	77.576	77.438	77.992	75.334	76.013	74.846

Table C7c. River Hydraulic Heads at Finite Difference Nodes for a 2-Day Time-Step Simulation

<i>River Head (ft)</i>									
<b>Time (days)</b>	<b>18</b>	<b>19</b>	<b>20</b>	<b>21</b>	<b>22</b>	<b>23</b>	<b>24</b>	<b>25</b>	<b>26</b>
0	75.558	77.141	75.858	76.196	73.612	76.972	75.633	72.538	70.842
2	71.374	71.481	70.705	70.592	69.301	70.351	69.670	68.298	66.899
4	96.160	105.193	101.403	104.065	95.056	109.926	105.320	93.655	90.480
6	78.659	81.357	79.697	80.380	76.832	81.919	80.090	75.707	73.789
8	76.427	78.322	76.934	77.368	74.514	78.358	76.882	73.426	71.668
10	77.808	80.200	78.643	79.231	75.947	80.561	78.866	74.837	72.980
12	87.417	93.281	90.556	92.227	85.948	95.928	92.709	84.684	82.138
14	78.914	81.704	80.013	80.725	77.097	82.327	80.457	75.969	74.033
16	73.825	74.790	73.717	73.864	71.818	74.216	73.151	70.772	69.200
18	73.990	75.014	73.922	74.086	71.989	74.479	73.387	70.940	69.357
20	73.685	74.600	73.544	73.675	71.673	73.994	72.950	70.629	69.067
22	72.642	73.189	72.260	72.278	70.598	72.343	71.463	69.572	68.084
24	72.246	72.653	71.772	71.749	70.190	71.717	70.900	69.172	67.712
26	72.051	72.391	71.533	71.489	69.991	71.411	70.624	68.975	67.530
28	76.053	77.814	76.471	76.863	74.125	77.761	76.344	73.043	71.312
30	83.507	87.957	85.707	86.936	81.876	89.671	87.073	80.675	78.409
32	73.891	74.879	73.798	73.952	71.885	74.320	73.244	70.838	69.262

Table C7d. River Hydraulic Heads at Finite Difference Nodes for a 2-Day Time-Step Simulation

<i>River Head (ft)</i>									
<b>Time (days)</b>	<b>27</b>	<b>28</b>	<b>29</b>	<b>30</b>	<b>31</b>	<b>32</b>	<b>33</b>	<b>34</b>	<b>35</b>
0	72.603	69.907	70.555	67.540	69.021	67.764	66.683	64.530	66.085
2	67.256	65.915	65.617	63.899	63.728	62.495	61.790	60.633	60.969
4	99.260	89.816	95.443	85.894	95.865	94.588	91.647	84.452	92.922
6	76.603	72.894	74.280	70.287	73.037	71.776	70.416	67.509	70.082
8	73.724	70.744	71.598	68.309	70.146	68.888	67.729	65.365	67.204
10	75.505	72.074	73.257	69.532	71.934	70.675	69.391	66.692	68.984
12	87.936	81.358	84.859	78.089	84.449	83.179	81.029	75.979	81.490
14	76.934	73.141	74.588	70.514	73.370	72.108	70.726	67.756	70.415
16	70.376	68.244	68.487	66.015	66.792	65.538	64.611	62.878	63.877
18	70.588	68.402	68.684	66.160	67.004	65.750	64.808	63.034	64.086
20	70.195	68.109	68.320	65.891	66.611	65.358	64.443	62.743	63.699
22	68.862	67.113	67.087	64.982	65.283	64.033	63.210	61.760	62.394
24	68.357	66.736	66.622	64.639	64.782	63.533	62.745	61.389	61.905
26	68.109	66.552	66.395	64.472	64.538	63.289	62.518	61.207	61.666
28	73.241	70.383	71.148	67.977	69.660	68.403	67.277	65.005	66.720
30	82.874	77.578	80.132	74.603	79.349	78.083	76.286	72.194	76.389
32	70.459	68.306	68.564	66.071	66.874	65.620	64.687	62.938	63.958

Table C8. Cross Section 1 Aquifer Heads in Layer 1 from 4-Day Time-Step Simulation

Time (days)	Aquifer Heads (ft) in Cross Section 1, Layer 1								
	-4	-3	-2	-1*	Reach 14	1	2	3	4
0	110.628	106.773	99.929	88.751	80.288	85.421	91.612	97.677	103.902
4	110.650	106.890	100.671	92.922	95.969	89.857	92.854	98.002	103.985
8	110.677	106.992	100.867	91.573	83.070	88.583	93.153	98.249	104.088
12	110.714	107.120	101.254	92.999	90.663	90.114	93.767	98.550	104.221
16	110.748	107.195	101.207	91.375	81.787	88.444	93.648	98.688	104.331
20	110.770	107.198	100.881	89.583	77.935	86.497	93.070	98.627	104.381
24	110.777	107.139	100.451	88.179	76.024	84.917	92.339	98.419	104.365
28	110.773	107.065	100.189	88.120	78.567	84.763	91.909	98.206	104.312
32	110.771	107.046	100.344	89.917	85.616	86.636	92.190	98.167	104.279

\*Negative values indicate the distance in MODFLOW cells from Reach 14 in the southwestern direction. Positive values indicate the distance in MODFLOW cells from Reach 14 in the northeastern direction.



Table C9. Cross Section 1 Aquifer Heads in Layer 2 from 4-Day Time-Step Simulation

Time (days)	Aquifer Heads (ft) in Cross Section 1, Layer 2								
	-4	-3	-2	-1*	Reach 14	1	2	3	4
0	101.547	101.651	101.765	101.890	102.039	102.170	102.238	102.256	102.355
4	101.650	101.759	101.877	102.009	102.163	102.292	102.358	102.371	102.462
8	101.642	101.749	101.865	101.993	102.143	102.274	102.342	102.357	102.452
12	101.688	101.797	101.916	102.047	102.200	102.330	102.397	102.410	102.501
16	101.666	101.774	101.890	102.019	102.169	102.300	102.368	102.383	102.477
20	101.626	101.732	101.847	101.973	102.122	102.254	102.322	102.340	102.437
24	101.585	101.690	101.803	101.928	102.075	102.207	102.276	102.295	102.395
28	101.573	101.677	101.791	101.916	102.064	102.196	102.264	102.283	102.383
32	101.604	101.711	101.826	101.954	102.104	102.235	102.303	102.320	102.417

\*Negative values indicate the distance in MODFLOW cells from Reach 14 in the southwestern direction. Positive values indicate the distance in MODFLOW cells from Reach 14 in the northeastern direction.

Table C10. Cross Section 2 Aquifer Heads in Layer 1 from 4-Day Time-Step Simulation

Time (days)	Aquifer Heads (ft) in Cross Section 2, Layer 1									
	-4	-3	-2	-1*	Reach 27	Reach 28	1	2	3	4
0	95.616	90.014	83.018	76.919	72.604	69.927	79.385	87.997	94.995	100.670
4	95.675	90.250	83.953	80.534	87.416	80.988	82.539	88.744	95.159	100.706
8	95.764	90.467	84.273	79.680	75.254	71.902	81.736	88.986	95.309	100.758
12	95.885	90.740	84.827	81.018	82.405	77.249	82.881	89.417	95.496	100.830
16	96.002	90.916	84.856	79.797	74.037	70.996	81.779	89.424	95.615	100.899
20	96.083	90.943	84.505	78.259	70.409	68.289	80.432	89.134	95.631	100.948
24	96.110	90.839	83.980	76.937	68.635	66.955	79.299	88.716	95.559	100.965
28	96.098	90.699	83.623	76.708	70.990	68.714	79.132	88.439	95.463	100.961
32	96.086	90.661	83.778	78.143	77.630	73.681	80.411	88.575	95.441	100.957

\*Negative values indicate the distance in MODFLOW cells from Reach 27 in the southwestern direction. Positive values indicate the distance in MODFLOW cells from Reach 28 in the northeastern direction.

Table C11. Cross Section 2 Aquifer Heads in Layer 2 from 4-Day Time-Step Simulation

Time (days)	Aquifer Heads (ft) in Cross Section 2, Layer 2									
	-4	-3	-2	-1*	Reach 27	Reach 28	1	2	3	4
0	98.268	98.074	97.901	97.677	97.583	97.596	97.676	97.789	97.873	97.978
4	98.368	98.180	98.016	97.799	97.703	97.694	97.750	97.840	97.914	98.017
8	98.348	98.155	97.984	97.758	97.655	97.657	97.726	97.827	97.905	98.009
12	98.392	98.202	98.034	97.811	97.707	97.700	97.758	97.850	97.923	98.026
16	98.366	98.172	97.999	97.769	97.663	97.665	97.734	97.835	97.912	98.016
20	98.329	98.133	97.957	97.727	97.623	97.632	97.709	97.817	97.898	98.003
24	98.294	98.097	97.921	97.691	97.591	97.605	97.687	97.802	97.886	97.991
28	98.287	98.091	97.916	97.689	97.592	97.605	97.686	97.801	97.884	97.989
32	98.321	98.129	97.958	97.735	97.638	97.642	97.713	97.818	97.898	98.002

\*Negative values indicate the distance in MODFLOW cells from Reach 27 in the southwestern direction. Positive values indicate the distance in MODFLOW cells from Reach 28 in the northeastern direction.

Table C12. Leakage Rates from 4-Day Time-Step Simulation

Leakage Rate (ft <sup>3</sup> /d)				
Time (days)	Reach14	Reach 27	Reach 28	Total
0	-375.201	-174.686	-821.384	-21216.420
4	1029.300	2587.630	1069.640	299930.497
8	-964.381	-1627.310	-2014.150	-250130.969
12	351.587	1215.300	50.630	123104.650
16	-836.333	-1273.370	-1739.830	-185140.890
20	-726.143	-886.831	-1379.340	-109646.680
24	-672.762	-715.988	-1201.160	-69520.910
28	-319.623	-5.775	-670.439	22445.224
32	195.845	959.140	-22.168	123464.396

Table C13a. River Discharge at Finite Difference Nodes for a 4-Day Time-Step Simulation

<i>River Discharge (m<sup>3</sup>/s)</i>									
<b>Time (days)</b>	<b>0</b>	<b>1</b>	<b>2</b>	<b>3</b>	<b>4</b>	<b>5</b>	<b>6</b>	<b>7</b>	<b>8</b>
0	77.300	77.348	77.416	77.456	77.982	77.991	78.008	78.062	78.181
4	412.013	412.062	412.130	412.170	412.696	412.705	412.722	412.776	412.895
8	120.770	120.810	120.871	120.894	121.409	121.400	121.398	121.451	121.568
12	275.662	275.717	275.790	275.843	276.378	276.400	276.431	276.486	276.606
16	99.745	99.790	99.854	99.887	100.409	100.410	100.419	100.472	100.590
20	46.722	46.775	46.847	46.896	47.429	47.447	47.474	47.529	47.649
24	26.603	26.654	26.724	26.769	27.299	27.312	27.335	27.389	27.509
28	54.417	54.467	54.536	54.578	55.107	55.118	55.138	55.192	55.311
32	167.280	167.327	167.394	167.432	167.957	167.963	167.977	168.031	168.149

Table C13b. River Discharge at Finite Difference Nodes for a 4-Day Time-Step Simulation

<i>River Discharge (m<sup>3</sup>/s)</i>									
<b>Time (days)</b>	<b>9</b>	<b>10</b>	<b>11</b>	<b>12</b>	<b>13</b>	<b>14</b>	<b>15</b>	<b>16</b>	<b>17</b>
0	78.192	78.206	78.220	78.226	78.240	78.393	78.396	78.761	78.908
4	412.907	412.921	412.935	412.942	412.956	413.110	413.112	413.478	413.625
8	121.578	121.592	121.606	121.610	121.624	121.777	121.779	122.145	122.292
12	276.619	276.633	276.648	276.656	276.671	276.824	276.827	277.193	277.340
16	100.601	100.615	100.629	100.635	100.649	100.802	100.805	101.170	101.317
20	47.661	47.675	47.690	47.698	47.712	47.865	47.868	48.234	48.382
24	27.521	27.535	27.550	27.557	27.571	27.725	27.728	28.093	28.241
28	55.323	55.337	55.352	55.359	55.373	55.527	55.530	55.895	56.043
32	168.161	168.175	168.189	168.196	168.210	168.363	168.366	168.732	168.879

Table C13c. River Discharge at Finite Difference Nodes for a 4-Day Time-Step Simulation

<i>River Discharge (m<sup>3</sup>/s)</i>									
<b>Time (days)</b>	<b>18</b>	<b>19</b>	<b>20</b>	<b>21</b>	<b>22</b>	<b>23</b>	<b>24</b>	<b>25</b>	<b>26</b>
0	78.945	79.611	79.642	79.982	80.010	80.069	80.089	80.134	80.137
4	413.662	414.328	414.359	414.699	414.728	414.787	414.807	414.853	414.856
8	122.328	122.993	123.024	123.363	123.392	123.450	123.470	123.515	123.517
12	277.377	278.043	278.075	278.415	278.444	278.504	278.524	278.571	278.574
16	101.354	102.019	102.050	102.390	102.418	102.477	102.497	102.543	102.545
20	48.419	49.084	49.116	49.456	49.485	49.545	49.565	49.612	49.615
24	28.278	28.943	28.975	29.315	29.344	29.403	29.423	29.470	29.473
28	56.080	56.745	56.777	57.117	57.145	57.205	57.225	57.271	57.274
32	168.916	169.582	169.613	169.953	169.981	170.041	170.061	170.107	170.109

Table C13d. River Discharge at Finite Difference Nodes for a 4-Day Time-Step Simulation

<i>River Discharge (m<sup>3</sup>/s)</i>									
<b>Time (days)</b>	<b>27</b>	<b>28</b>	<b>29</b>	<b>30</b>	<b>31</b>	<b>32</b>	<b>33</b>	<b>34</b>	<b>35</b>
0	80.211	80.242	81.366	81.386	81.485	81.615	81.632	81.647	83.479
4	414.930	414.961	416.086	416.106	416.206	416.336	416.354	416.368	418.201
8	123.590	123.621	124.744	124.764	124.859	124.989	125.006	125.019	126.851
12	278.648	278.680	279.806	279.826	279.929	280.059	280.078	280.093	281.925
16	102.619	102.650	103.774	103.794	103.891	104.022	104.039	104.053	105.885
20	49.689	49.721	50.846	50.866	50.968	51.099	51.117	51.132	52.964
24	29.547	29.578	30.703	30.723	30.825	30.955	30.973	30.988	32.820
28	57.348	57.380	58.505	58.525	58.626	58.756	58.774	58.789	60.621
32	170.183	170.215	171.339	171.359	171.459	171.589	171.607	171.621	173.453



Table C14a. River Hydraulic Head at Finite Difference Nodes for a 4-Day Time-Step Simulation

<i>River Head (ft)</i>									
<b>Time (days)</b>	<b>0</b>	<b>1</b>	<b>2</b>	<b>3</b>	<b>4</b>	<b>5</b>	<b>6</b>	<b>7</b>	<b>8</b>
0	86.262	86.070	86.194	86.670	84.526	84.420	83.838	82.284	82.756
4	97.451	97.253	98.671	101.759	96.724	98.795	98.000	94.522	97.393
8	88.253	88.055	88.408	89.346	86.687	86.965	86.345	84.449	85.345
12	93.669	93.471	94.452	96.656	92.598	93.932	93.210	90.382	92.441
16	87.336	87.139	87.386	88.110	85.689	85.790	85.188	83.450	84.150
20	84.581	84.385	84.314	84.398	82.694	82.262	81.713	80.448	80.561
24	83.210	83.014	82.786	82.550	81.207	80.509	79.987	78.957	78.779
28	85.039	84.842	84.824	85.014	83.190	82.846	82.288	80.945	81.155
32	90.078	89.880	90.444	91.809	88.678	89.313	88.658	86.449	87.736

Table C14b. River Hydraulic Head at Finite Difference Nodes for a 4-Day Time-Step Simulation

<i>River Head (ft)</i>									
<b>Time (days)</b>	<b>9</b>	<b>10</b>	<b>11</b>	<b>12</b>	<b>13</b>	<b>14</b>	<b>15</b>	<b>16</b>	<b>17</b>
0	80.294	82.859	80.659	79.361	79.329	80.275	76.890	77.932	76.528
4	91.496	100.350	94.771	91.641	92.337	95.990	87.597	91.158	88.125
8	82.276	85.953	83.155	81.533	81.630	83.054	78.783	80.269	78.576
12	87.707	94.432	89.997	87.487	87.937	90.673	83.974	86.681	84.199
16	81.361	84.524	82.003	80.531	80.568	81.771	77.909	79.190	77.630
20	78.615	80.236	78.544	77.521	77.379	77.921	75.286	75.954	74.794
24	77.251	78.108	76.827	76.027	75.797	76.012	73.985	74.352	73.392
28	79.069	80.946	79.116	78.019	77.907	78.558	75.720	76.489	75.263
32	84.106	88.810	85.461	83.540	83.755	85.621	80.532	82.429	80.470

Table C14c. River Hydraulic Head at Finite Difference Nodes for a 4-Day Time-Step Simulation

<i>River Head (ft)</i>									
<b>Time (days)</b>	<b>18</b>	<b>19</b>	<b>20</b>	<b>21</b>	<b>22</b>	<b>23</b>	<b>24</b>	<b>25</b>	<b>26</b>
0	75.558	77.141	75.858	76.196	73.612	76.972	75.633	72.538	70.842
4	87.060	92.795	90.113	91.744	85.576	95.356	92.194	84.318	81.797
8	77.589	79.903	78.373	78.937	75.721	80.212	78.552	74.613	72.772
12	83.166	87.492	85.284	86.475	81.521	89.126	86.582	80.325	78.084
16	76.651	78.627	77.211	77.670	74.746	78.715	77.203	73.654	71.880
20	73.839	74.809	73.735	73.883	71.832	74.239	73.171	70.786	69.213
24	72.449	72.927	72.022	72.020	70.399	72.037	71.188	69.376	67.902
28	74.304	75.439	74.308	74.507	72.312	74.976	73.835	71.259	69.653
32	79.468	82.458	80.700	81.474	77.673	83.213	81.255	76.536	74.560

Table C14d. River Hydraulic Head at Finite Difference Nodes for a 4-Day Time-Step Simulation

<i>River Head (ft)</i>									
<b>Time (days)</b>	<b>27</b>	<b>28</b>	<b>29</b>	<b>30</b>	<b>31</b>	<b>32</b>	<b>33</b>	<b>34</b>	<b>35</b>
0	72.603	69.907	70.555	67.540	69.021	67.764	66.683	64.530	66.085
4	87.473	81.012	84.428	77.770	83.983	82.713	80.596	75.633	81.024
8	75.223	71.864	72.994	69.338	71.650	70.391	69.127	66.481	68.701
12	82.433	77.248	79.720	74.299	78.905	77.640	75.874	71.865	75.945
16	74.013	70.959	71.866	68.507	70.434	69.176	67.997	65.579	67.490
20	70.394	68.257	68.504	66.027	66.809	65.556	64.627	62.890	63.894
24	68.615	66.929	66.860	64.815	65.038	63.788	62.982	61.578	62.153
28	70.990	68.702	69.056	66.434	67.405	66.151	65.181	63.332	64.483
32	77.650	73.676	75.256	71.007	74.090	72.829	71.396	68.291	71.134

Table C15. Cross Section 1 Aquifer Heads in Layer 1 from 8-Day Time-Step Simulation

Time (days)	Aquifer Heads (ft) in Cross Section 1, Layer 1								
	-4	-3	-2	-1*	Reach 14	1	2	3	4
0	110.628	106.773	99.929	88.751	80.288	85.421	91.612	97.677	103.902
8	110.679	106.983	100.840	92.322	90.265	89.304	93.106	98.214	104.088
16	110.748	107.180	101.249	92.312	86.656	89.400	93.727	98.649	104.313
24	110.770	107.134	100.601	88.943	77.037	85.758	92.607	98.437	104.339
32	110.780	107.106	100.530	89.714	82.474	86.501	92.491	98.335	104.328

Table C16. Cross Section 1 Aquifer Heads in Layer 2 from 8-Day Time-Step Simulation

Time (days)	Aquifer Heads (ft) in Cross Section 1, Layer 2								
	-4	-3	-2	-1*	Reach 14	1	2	3	4
0	101.547	101.651	101.765	101.890	102.039	102.170	102.238	102.256	101.547
8	101.652	101.760	101.878	102.008	102.160	102.291	102.357	102.372	101.652
16	101.681	101.790	101.907	102.037	102.189	102.320	102.387	102.401	101.681
24	101.603	101.708	101.822	101.948	102.096	102.228	102.296	102.314	101.603
32	101.613	101.719	101.834	101.962	102.112	102.243	102.311	102.328	101.613

\*Negative values indicate the distance in MODFLOW cells from Reach 14 in the southwestern direction. Positive values indicate the distance in MODFLOW cells from Reach 14 in the northeastern direction

Table C17. Cross Section 2 Aquifer Heads in Layer 1 from 8-Day Time-Step Simulation

Time (days)	Aquifer Heads (ft) in Cross Section 2, Layer 1									
	-4	-3	-2	-1*	Reach 27	Reach 28	1	2	3	4
0	95.616	90.014	83.018	76.919	72.604	69.927	79.385	87.997	94.995	100.670
8	95.773	90.452	84.234	80.216	82.030	76.973	82.224	88.956	95.298	100.763
16	95.998	90.886	84.889	80.522	78.633	74.429	82.429	89.456	95.595	100.898
24	96.082	90.826	84.141	77.598	69.571	67.660	79.879	88.852	95.553	100.951
32	96.116	90.784	84.040	78.119	74.665	71.462	80.362	88.779	95.527	100.976

Table C18. Cross Section 2 Aquifer Heads in Layer 2 from 8-Day Time-Step Simulation

Time (days)	Aquifer Heads (ft) in Cross Section 2, Layer 2									
	-4	-3	-2	-1*	Reach 27	Reach 28	1	2	3	4
0	98.268	98.074	97.901	97.677	97.583	97.596	97.676	97.789	97.873	97.978
8	98.364	98.174	98.006	97.784	97.685	97.681	97.742	97.837	97.912	98.016
16	98.384	98.192	98.022	97.795	97.690	97.686	97.749	97.844	97.919	98.023
24	98.310	98.113	97.938	97.708	97.606	97.618	97.697	97.809	97.891	97.996
32	98.324	98.130	97.957	97.731	97.631	97.638	97.711	97.818	97.898	98.003

\*Negative values indicate the distance in MODFLOW cells from Reach 27 in the southwestern direction. Positive values indicate the distance in MODFLOW cells from Reach 28 in the northeastern direction.

Table C19. Leakage Rates from 8-Day Time-Step Simulation

Leakage Rate (ft <sup>3</sup> /d)				
Time (days)	Reach14	Reach 27	Reach 28	Total
0	-375.201	-174.686	-821.384	-21216.420
8	239.400	941.619	-129.422	89179.734
16	-279.300	-135.934	-930.565	-48144.746
24	-789.873	-1019.400	-1455.530	-123170.194
32	-172.230	221.782	-563.729	31542.606

Table C20a. River Discharge at Finite Difference Nodes for 8-Day Time-Step Simulation

<i>River Discharge (m<sup>3</sup>/s)</i>									
<b>Time (days)</b>	<b>0</b>	<b>1</b>	<b>2</b>	<b>3</b>	<b>4</b>	<b>5</b>	<b>6</b>	<b>7</b>	<b>8</b>
0	77.300	77.348	77.416	77.456	77.982	77.991	78.008	78.062	78.181
8	266.392	266.440	266.508	266.548	267.075	267.083	267.101	267.155	267.274
16	187.704	187.749	187.815	187.849	188.372	188.375	188.385	188.439	188.557
24	36.663	36.712	36.781	36.822	37.350	37.361	37.380	37.434	37.553
32	110.849	110.900	110.970	111.015	111.546	111.560	111.584	111.638	111.758

Table C20b. River Discharge at Finite Difference Nodes for 8-Day Time-Step Simulation

<i>River Discharge (m<sup>3</sup>/s)</i>									
<b>Time (days)</b>	<b>9</b>	<b>10</b>	<b>11</b>	<b>12</b>	<b>13</b>	<b>14</b>	<b>15</b>	<b>16</b>	<b>17</b>
0	78.192	78.206	78.220	78.226	78.240	78.393	78.396	78.761	78.908
8	267.285	267.299	267.314	267.321	267.335	267.488	267.491	267.856	268.004
16	188.568	188.582	188.597	188.602	188.617	188.769	188.772	189.138	189.285
24	37.565	37.579	37.593	37.600	37.615	37.768	37.771	38.136	38.283
32	111.770	111.784	111.798	111.806	111.820	111.974	111.977	112.342	112.490



Table C20c. River Discharge at Finite Difference Nodes for 8-Day Time-Step Simulation

<i>River Discharge (m<sup>3</sup>/s)</i>									
<b>Time (days)</b>	<b>18</b>	<b>19</b>	<b>20</b>	<b>21</b>	<b>22</b>	<b>23</b>	<b>24</b>	<b>25</b>	<b>26</b>
0	78.945	79.611	79.642	79.982	80.010	80.069	80.089	80.134	80.137
8	268.041	268.706	268.738	269.078	269.106	269.166	269.186	269.232	269.234
16	189.322	189.987	190.018	190.358	190.386	190.446	190.465	190.511	190.514
24	38.320	38.986	39.017	39.357	39.386	39.445	39.465	39.511	39.514
32	112.527	113.192	113.224	113.564	113.593	113.653	113.673	113.719	113.722

Table C20d. River Discharge at Finite Difference Nodes for 8-Day Time-Step Simulation

<i>River Discharge (m<sup>3</sup>/s)</i>									
<b>Time (days)</b>	<b>27</b>	<b>28</b>	<b>29</b>	<b>30</b>	<b>31</b>	<b>32</b>	<b>33</b>	<b>34</b>	<b>35</b>
0	80.211	80.242	81.366	81.386	81.485	81.615	81.632	81.647	83.479
8	269.308	269.340	270.464	270.484	270.585	270.715	270.732	270.747	272.579
16	190.587	190.618	191.743	191.762	191.861	191.991	192.008	192.022	193.854
24	39.588	39.620	40.744	40.764	40.865	40.995	41.012	41.027	42.859
32	113.796	113.828	114.953	114.973	115.075	115.205	115.223	115.238	117.070

Table C21a. River Hydraulic Head at Finite Difference Nodes for 8-Day Time-Step Simulation

<i>River Head (ft)</i>									
<b>Time (days)</b>	<b>0</b>	<b>1</b>	<b>2</b>	<b>3</b>	<b>4</b>	<b>5</b>	<b>6</b>	<b>7</b>	<b>8</b>
0	86.262	86.070	86.194	86.670	84.526	84.420	83.838	82.284	82.756
8	93.388	93.189	94.137	96.275	92.289	93.568	92.851	90.072	92.070
16	90.813	90.615	91.264	92.801	89.480	90.257	89.589	87.253	88.698
24	83.934	83.737	83.592	83.524	81.990	81.432	80.895	79.741	79.716
32	87.829	87.631	87.936	88.776	86.227	86.425	85.814	83.991	84.797

Table C21b. River Hydraulic Head at Finite Difference Nodes for 8-Day Time-Step Simulation

<i>River Head (ft)</i>									
<b>Time (days)</b>	<b>9</b>	<b>10</b>	<b>11</b>	<b>12</b>	<b>13</b>	<b>14</b>	<b>15</b>	<b>16</b>	<b>17</b>
0	80.294	82.859	80.659	79.361	79.329	80.275	76.890	77.932	76.528
8	87.422	93.988	89.639	87.175	87.606	90.274	83.702	86.346	83.904
16	84.842	89.959	86.388	84.346	84.610	86.653	81.235	83.298	81.232
24	77.968	79.227	77.730	76.812	76.629	77.016	74.669	75.194	74.129
32	81.857	85.298	82.627	81.074	81.143	82.466	78.383	79.775	78.143

Table C21c. River Hydraulic Head at Finite Difference Nodes for 8-Day Time-Step Simulation

<i>River Head (ft)</i>									
<b>Time (days)</b>	<b>18</b>	<b>19</b>	<b>20</b>	<b>21</b>	<b>22</b>	<b>23</b>	<b>24</b>	<b>25</b>	<b>26</b>
0	75.558	77.141	75.858	76.196	73.612	76.972	75.633	72.538	70.842
8	82.874	87.094	84.922	86.080	81.217	88.658	86.160	80.026	77.806
16	80.223	83.486	81.636	82.495	78.459	84.420	82.343	77.310	75.280
24	73.179	73.915	72.921	72.997	71.151	73.192	72.228	70.116	68.590
32	77.160	79.319	77.841	78.357	75.274	79.527	77.934	74.174	72.364

Table C21d. River Hydraulic Head at Finite Difference Nodes for 8-Day Time-Step Simulation

<i>River Head (ft)</i>									
<b>Time (days)</b>	<b>27</b>	<b>28</b>	<b>29</b>	<b>30</b>	<b>31</b>	<b>32</b>	<b>33</b>	<b>34</b>	<b>35</b>
0	72.603	69.907	70.555	67.540	69.021	67.764	66.683	64.530	66.085
8	82.055	76.966	79.367	74.038	78.524	77.259	75.519	71.582	75.564
16	78.627	74.405	76.168	71.679	75.073	73.810	72.310	69.021	72.115
24	69.547	67.625	67.720	65.449	65.965	64.713	63.843	62.264	63.062
32	74.669	71.450	72.478	68.958	71.094	69.835	68.610	66.068	68.147

Table C22. Cross Section 1 Aquifer Heads in Layer 1 from 16-Day Time-Step Simulation

	<b>Aquifer Heads (ft) in Cross Section 1, Layer 1</b>								
<b>Time (days)</b>	<b>-4</b>	<b>-3</b>	<b>-2</b>	<b>-1*</b>	<b>Reach 14</b>	<b>1</b>	<b>2</b>	<b>3</b>	<b>4</b>
0	110.628	106.773	99.929	88.751	80.288	85.421	91.612	97.677	103.902
16	110.747	107.148	101.139	92.377	88.530	89.423	93.546	98.555	104.290
32	110.777	107.112	100.580	89.517	80.031	86.332	92.579	98.366	104.322

Table C23. Cross Section 1 Aquifer Heads in Layer 2 from 16-Day Time-Step Simulation

	<b>Aquifer Heads (ft) in Cross Section 1, Layer 2</b>								
<b>Time (days)</b>	<b>-4</b>	<b>-3</b>	<b>-2</b>	<b>-1*</b>	<b>Reach 14</b>	<b>1</b>	<b>2</b>	<b>3</b>	<b>4</b>
0	101.547	101.651	101.765	101.89	102.039	102.17	102.238	102.256	102.355
16	101.677	101.785	101.903	102.033	102.185	102.316	102.383	102.397	102.489
32	101.612	101.718	101.832	101.959	102.108	102.239	102.307	102.325	102.423

\*Negative values indicate the distance in MODFLOW cells from Reach 14 in the southwestern direction. Positive values indicate the distance in MODFLOW cells from Reach 14 in the northeastern direction.

Table C24. Cross Section 2 Aquifer Heads in Layer 1 from 16-Day Time-Step Simulation

Time (days)	Aquifer Heads (ft) in Cross Section 2, Layer 1									
	-4	-3	-2	-1*	Reach 27	Reach 28	1	2	3	4
0	95.616	90.014	83.018	76.919	72.604	69.927	79.385	87.997	94.995	100.670
16	95.996	90.826	84.738	80.492	80.391	75.740	82.418	89.339	95.555	100.898
32	96.105	90.793	84.101	78.005	72.381	69.753	80.251	88.828	95.536	100.972

Table C25. Cross Section 2 Aquifer Heads in Layer 1 from 16-Day Time-Step Simulation

Time (days)	Aquifer Heads (ft) in Cross Section 2, Layer 1									
	-4	-3	-2	-1*	Reach 27	Reach 28	1	2	3	4
0	98.268	98.074	97.901	97.677	97.583	97.596	97.676	97.789	97.873	97.978
16	98.382	98.191	98.022	97.797	97.693	97.689	97.750	97.845	97.919	98.023
32	98.321	98.126	97.952	97.724	97.623	97.631	97.707	97.816	97.897	98.002

\*Negative values indicate the distance in MODFLOW cells from Reach 27 in the southwestern direction. Positive values indicate the distance in MODFLOW cells from Reach 28 in the northeastern direction.

Table C26. Leakage Rates from 16-Day Time-Step Simulation

Leakage Rate (ft <sup>3</sup> /d)				
Time (days)	Reach14	Reach 27	Reach 28	Total
0	-375.201	-174.686	-821.384	-21216.420
16	2.850	453.130	-495.138	28816.784
32	-525.836	-509.674	-1100.140	-64873.732

Table C27a. River Discharge at Finite Difference Nodes for 16-Day Time-Step Simulation

<i>River Discharge (m<sup>3</sup>/s)</i>									
<b>Time (days)</b>	<b>0</b>	<b>1</b>	<b>2</b>	<b>3</b>	<b>4</b>	<b>5</b>	<b>6</b>	<b>7</b>	<b>8</b>
0	77.300	77.348	77.416	77.456	77.982	77.991	78.008	78.062	78.181
16	227.048	227.096	227.164	227.204	227.731	227.739	227.756	227.810	227.929
32	73.756	73.803	73.870	73.907	74.433	74.439	74.453	74.507	74.626

Table C27b. River Discharge at Finite Difference Nodes for 16-Day Time-Step Simulation

<i>River Discharge (m<sup>3</sup>/s)</i>									
<b>Time (days)</b>	<b>9</b>	<b>10</b>	<b>11</b>	<b>12</b>	<b>13</b>	<b>14</b>	<b>15</b>	<b>16</b>	<b>17</b>
0	78.192	78.206	78.220	78.226	78.240	78.393	78.396	78.761	78.908
16	227.941	227.955	227.970	227.977	227.991	228.144	228.147	228.512	228.660
32	74.637	74.651	74.665	74.672	74.686	74.839	74.842	75.207	75.354

Table C27c. River Discharge at Finite Difference Nodes for 16-Day Time-Step Simulation

<i>River Discharge (m<sup>3</sup>/s)</i>									
<b>Time (days)</b>	<b>18</b>	<b>19</b>	<b>20</b>	<b>21</b>	<b>22</b>	<b>23</b>	<b>24</b>	<b>25</b>	<b>26</b>
0	78.945	79.611	79.642	79.982	80.010	80.069	80.089	80.134	80.137
16	228.697	229.362	229.393	229.733	229.762	229.822	229.842	229.888	229.890
32	75.391	76.057	76.088	76.428	76.456	76.516	76.536	76.581	76.584

Table C27d. River Discharge at Finite Difference Nodes for 16-Day Time-Step Simulation

<i>River Discharge (m<sup>3</sup>/s)</i>									
<b>Time (days)</b>	<b>27</b>	<b>28</b>	<b>29</b>	<b>30</b>	<b>31</b>	<b>32</b>	<b>33</b>	<b>34</b>	<b>35</b>
0	80.211	80.242	81.366	81.386	81.485	81.615	81.632	81.647	83.479
16	229.964	229.996	231.120	231.140	231.241	231.371	231.388	231.403	233.235
32	76.658	76.689	77.814	77.833	77.933	78.063	78.080	78.095	79.927



Table C28a. River Hydraulic Head at Finite Difference Nodes for 16-Day Time-Step Simulation

<i>River Head (ft)</i>									
<b>Time (days)</b>	<b>0</b>	<b>1</b>	<b>2</b>	<b>3</b>	<b>4</b>	<b>5</b>	<b>6</b>	<b>7</b>	<b>8</b>
0	86.262	86.070	86.194	86.670	84.526	84.420	83.838	82.284	82.756
16	92.145	91.947	92.751	94.599	90.933	91.971	91.277	88.712	90.443
32	86.088	85.890	85.993	86.427	84.330	84.189	83.611	82.087	82.520

Table C28b. River Hydraulic Head at Finite Difference Nodes for 16-Day Time-Step Simulation

<i>River Head (ft)</i>									
<b>Time (days)</b>	<b>9</b>	<b>10</b>	<b>11</b>	<b>12</b>	<b>13</b>	<b>14</b>	<b>15</b>	<b>16</b>	<b>17</b>
0	80.294	82.859	80.659	79.361	79.329	80.275	76.890	77.932	76.528
16	86.177	92.045	88.071	85.811	86.161	88.527	82.512	84.875	82.615
32	80.114	82.578	80.432	79.164	79.120	80.023	76.718	77.720	76.342

Table C28c. River Hydraulic Head at Finite Difference Nodes for 16-Day Time-Step Simulation

<i>River Head (ft)</i>									
<b>Time (days)</b>	<b>18</b>	<b>19</b>	<b>20</b>	<b>21</b>	<b>22</b>	<b>23</b>	<b>24</b>	<b>25</b>	<b>26</b>
0	75.558	77.141	75.858	76.196	73.612	76.972	75.633	72.538	70.842
16	81.595	85.353	83.336	84.350	79.886	86.613	84.318	78.715	76.587
32	75.373	76.891	75.630	75.947	73.421	76.679	75.369	72.349	70.667

Table C28d. River Hydraulic Head at Finite Difference Nodes for 16-Day Time-Step Simulation

<i>River Head (ft)</i>									
<b>Time (days)</b>	<b>27</b>	<b>28</b>	<b>29</b>	<b>30</b>	<b>31</b>	<b>32</b>	<b>33</b>	<b>34</b>	<b>35</b>
0	72.603	69.907	70.555	67.540	69.021	67.764	66.683	64.530	66.085
16	80.400	75.730	77.823	72.899	76.859	75.594	73.970	70.346	73.899
32	72.366	69.730	70.334	67.377	68.783	67.526	66.461	64.354	65.848

## References

- Abbott, M. B., J. C. Bathurst, J.A. Cunge, P.E. O'Connell and J. Rasmussen. "An Introduction to the European Hydrological System- Systeme Hydrologique Europeen, 'SHE', 1: History and Philosophy of a physically-based , distributed modeling system." *Journal of Hydrology*. 87 (1986): 45-59.
- Bathurst, J.C. "Sensitivity Analysis of the Systeme Hydrologique Europeen for an Updated Catchment." *Journal of Hydrology*. 87 (1986): 103-123.
- Charbeneau, R. *Groundwater Hydraulics and Pollutant Transport*. Upper Saddle River: Prentice Hall, 2000.
- Chow, V. T., D. R. Maidment, and L. W. Mays. *Applied Hydrology*. New York: McGraw Hill, 1988.
- Danish Hydraulic Institute. "MIKE-11 - A Modeling System for Rivers and Channels" Online. Available: <http://www.dhi.dk/mike11/index.htm>. Accessed April 2, 2000.
- Danish Hydraulic Institute. "MIKE-SHE - An Integrated Hydrological Modeling System." Online. Available: <http://www.dhi.dk/mikeshe/index.htm>. Accessed April 2, 2000.
- Dutton, A. R. *Groundwater Availability in the Carrizo-Wilcox Aquifer in Central Texas- Numerical Simulations of 2000 through 2050 Withdrawal Projections*. Report No. 256. Austin, Tex: Bureau of Economic Geology, 1999.
- Hinaman, K. C. "Use of a Geographic Information System to Assemble Input-Data Sets for a Finite Difference Model of Groundwater Flow" *Water Resource Bulletin, American Water Resources Association*. 29 (1993) :401-406.
- Hubert, M. and B. Bullock. "Senate Bill 1, The First Big and Bold Step Toward Meeting Texas's Future Water Needs" 30, *Texas Technical Law Review*. 53 (1999).
- HydroGeologic, Inc. "MODFLOW-SURFACT Volume III: Surface Water Flow Modules." Herndon, VA. (Software Documentation)

- Lighthill, M. J., and G.B. Whitham. "On Kinematic Waves, I: Flood Movement in Long Rivers." *Proc. R. Soc. London A.* 229 (1955):281-316.
- Lusk, Stephanie E. Hayes "Texas Groundwater: Reconciling the Rule of Capture with the Environmental and Community Demands," 30 *St. Mary's Law Journal* 305, 1998.
- Mace, R. E., and Mullican, W. F., III, 2000, The past, present, and future of groundwater availability modeling in Texas: Southwest Focus Ground Water Conference, National Ground Water Association, p. 35-36.
- Mueller, F. A. and J. W. Male. "A Management Model for Specification of Groundwater Withdrawal Permits." *Water Resources Research.* 29 (1993): 1359-1368.
- Olivera, Francisco. "Calculation of Hydrologic Parameters using CRWR PrePro." Presented in October 1998 at the CE394-K3 GIS in Water Resources class at the University of Texas at Austin. Austin, Texas. Online. Available: <http://www.ce.utexas.edu/prof/olivera/prepro/prepro.htm>. Accessed October 13, 1999.
- Orzol, L. L. and T. S. McGrath. "Summary of Modifications of the U.S. Geological Survey Modular Finite Difference, Groundwater Flow Model to Read and Write Geographic Information System Files." *Water Resources Bulletin, American Water Resources Association.* 29 (1993):843-846.
- Perkins, S. P. and M. Sophocleous. "Development of a Comprehensive Watershed Model Applied to Study Stream Yield under Drought Conditions." *Ground Water.* 37 (1999): 418-426.
- Richards, C. J., h. Roaza and R. M. Roaza. "Integrating Geographic Information system and MODFLOW for Ground Water Resources Assessments." *Water Resources Bulletin, American Water Resources Association.* 29 (1993): 847-853.
- Refsgaard, J. C. "Parameterization, Calibration and Validation of Distributed Hydrological Models." *Journal of Hydrology.* 198 (1997): 69-97.
- Refsgaard, J. C. and J. Knudsen "Operational validation and intercomparison of different types of hydrological models" *Water Resources Research.* 32 (1996):2189-2202.

- Romanek, Andrew "Surface Water Modeling at Marcus Hook." Presented on April 23, 1998. Online. Available: <http://www.ce.utexas.edu/prof/maidment/grad/romanek/gisproject/gis/sld001.htm>. Accessed March 17, 2000.
- Sophocleous, M. "Evaluation of Simplified Stream Aquifer Depletion Models for Water Rights Administration." *Ground Water*. 33 (1995): 579-588.
- Texas Water Code 16.012, 75<sup>th</sup> Legislature (1997). Online. Available: <http://capitol.tlc.state.tx.us/statutes/codes/WA000010.html>. Accessed April 14, 2000.
- Texas Water Code 36.311, 75<sup>th</sup> Legislature (1997). Online. Available: <http://capitol.tlc.state.tx.us/statutes/codes/WA000025.html>. Accessed April 14, 2000.
- Vance, Benjamin R. "Total Aquifer Management: A New Approach to Groundwater Protection." 30, *University of San Francisco Law Review*. 803 (1996).
- Vieira, J. H. "Conditions governing the use of the approximations for the Saint-Venant Equations for Shallow Surface Water Flow." *Journal of Hydrology*. 60 (1983): 43-58.

## Vita

Shiva Niazi was born in Mashad, Iran on September 21, 1975. She moved to Berkeley, CA in August of 1979 following the Revolution in Iran and has resided in America ever since. She is the youngest of four children. Her parents, Mansour and Fereshteh Niazi, sister Jaleh, and brother Kaveh still live in the San Francisco Bay Area. Her third sibling, Kayvan is currently living in Los Angeles, CA.

Shiva attended Berkeley High School from 1989 through 1993. She went on to receive her B.S. in Environmental Engineering Science in 1997 from the University of California at Berkeley. Following her undergraduate work, she worked for an environmental consultant, SOMA Engineering, Inc. for six months before beginning her graduate work at the University of Texas at Austin in August 1998.

Permanent address: 925 Hilldale Ave.  
Berkeley, CA 94708

This thesis was typed by the author.